JAERI-Tech
95-022

HEAT TRANSFER EXPERIMENTS ON THE COOLING TUBES FOR DIVERTOR PLATES UNDER ONE-SIDED HEATING CONDITIONS

March 1995

Masanori ARAKI, Masuro OGAWA
Tomoaki KUNUGI, Shuichi IKEDA*
Kazuyoshi SATOH, Satoshi SUZUKI
Yoshihiko NISHINO, Masayuki DAIRAKU
Kazuyuki NAKAMURA, Kenji YOKOYAMA
and Masato AKIBA

日本原子力研究所
Japan Atomic Energy Research Institute

本レポートは，日本原子力研究所が不定期に公刊している研究報告書です。
入手の問合わせは，日本原子力研究所技術情報部情報資料課（〒319－11 茨城県那珂郡東海村）あて，お申し越しください。なお，このほかに財団法人原子力弘済会資料センター（〒319－11 茨城県那珂郡東海村日本原子力研究所内）で複写による実費頒布をおこなっております。

This report is issued irregularly.
Inquiries about availability of the reports should be addressed to Information Division, Department of Technical Information, Japan Atomic Energy Research Institute, Tokai-mura, Naka-gun, Ibaraki-ken 319-11, Japan.

編集兼発行　日本原子力研究所
印　　刷　日立高速印刷株式会社

Heat Transfer Experiments on the Cooling Tubes for Divertor Plates under One-sided Heating Conditions

Masanori ARAKI, Masuro OGAWA[+], Tomoaki KUNUGI[++], Shuichi IKEDA*
Kazuyoshi SATOH, Satoshi SUZUKI, Yoshihiko NISHINO, Masayuki DAIRAKU
Kazuyuki NAKAMURA, Kenji YOKOYAMA and Masato AKIBA

Department of Fusion Engineering Research
Naka Fusion Research Establishment
Japan Atomic Energy Research Institute
Naka-machi, Naka-gun, Ibaraki-ken

(Received February 10, 1995)

No literatures and experimental results have been published so far prediction of heat transfer coefficients under one-sided heating conditions. It is a recent concern whether or not existing correlations developed for uniform heating conditions, i. e., Thom and/of Shah(Jens-Lottes)correlations, are applicable to one-sided heating conditions. Furthermore, they predict differet values as large as twece even if the identical calculation condition is applied. This reason is attributable mainly to lack of database and wide extrapolation at high superheat region.

In the cooling channel of the divertor plates, partial nucleate boiling will be expected due to high heat flux, resulting in the diffeculty on the design such as the evaluation of the surface temperature of plasma facing components. Therefore, JAERI has carried out heat trasfer experiments on two different test samples to systematically evaluate heat transfer phenomena under one-sided heating conditions. In the experiments, temperature profile along the

---

[+] Office of Planning
[++] Department of High Temperature Engineering
* On leave from Science University of Tokyo

circumference of the test sample were measured at a condition for the inlet water temprerature from 20 to 80℃, the local water pressure from 0.5 to 1.5 Mpa, the flow velocity from 4 to 16m/s, and the peak surface heat flux ranged from 2 MW/m^2 to burnout. Simple copmparisons between the experimental data and the existing heat transfer correlations were also done to investigate the applicability of use of the existing correlation to one-sided heating conditions. As a result of the comparison, the existing correlations are applicable to one-sided heating conditions at non-boiling region, but can not predict to the experimental results at partial nucleate boiling region with high superheat. As a first step to determine heat tranfer correlations, an inverse analysis code of heat conduction problems was developed.

Keywords : Divertor Plate, High Heat Flux, One-sided Heating Conditions, Nucleate Boiling, Superheat, Heat Transfer.

各融合炉ダイバータ板用冷却管の片面加熱条件下における熱伝達実験

日本原子力研究所那珂研究所核融合工学部
荒木　政則・小川　益郎[+]・功刀　資彰[++]・池田　秀一[*]
佐藤　和義・鈴木　　哲・西野　好彦・大楽　正幸
中村　和幸・横山　堅二・秋場　真人

（1995年2月10日受理）

片面加熱条件下における熱伝達特性を予測する相関式は存在しない。例えばThomやShahの提案するような一様加熱条件での熱伝達相関式が片面加熱条件に適用できるか否かについては未だ検討されていないのが現状である。さらに，これら既存の熱伝達相関式において，同一計算条件の元で得られる熱伝達率には2倍もの相違が認められる。この主な理由としては，実験データの不足や高過熱度域への過大な外挿等があげられる。

一方，核融合炉ダイバータ板用冷却管では，高い表面熱流束のため部分的核沸騰が予想され，プラズマ対向機器を設計する上で重要なアーマ表面温度の予測に支障をきたしている。そこで，片面加熱条件下における熱伝達現象を系統的に評価するために，2種類の冷却管構造に対する熱伝達実験を実施した。本報告では，冷却水入口温度20～80℃，冷却水入口圧力0.5～1.5MPa，流速4～16m／sの冷却条件及び表面熱流束2MW／m^2～バーンアウトに至る加熱条件のもとでの温度及び分布測定結果について示すと共に，実験結果と既存の熱伝達相関式からの予測結果の比較を実験して，既存の熱伝達相関式の片面加熱条件下への適用性を調べた。この結果，既存相関式は非沸騰域においては実験結果とよく一致したが，高過熱度を伴った部分沸騰域においては実験結果を予測できないことが明らかとなった。このため，新たな熱伝達相関式を開発する第1段階として定常熱伝導逆問題解法コードを開発した。

那珂研究所：〒311-01　茨城県那珂郡那珂町大字向山801-1
＋企画室
＋＋高温工学部
＊特別研究生，東京理科大学

Contents

目　　次

1. INTRODUCTION

The plasma facing component is exposed to severe heat loads on its plasma facing side. In particular, the surface heat flux to the divertor plate was expected to be 15 to 30 MW/m^2 in ITER-CDA [1]. To reduce the surface heat flux on the divertor plate, some ideas have been proposed [2-4]. In ITER-EDA, a dynamic gas target concept is considered [4]. When this concept effectively works, the heat flux on the divertor plate can be reduced down to around 5 MW/m^2. However feasibility of this concept is still uncertain, we have to develop the divertor plate which withstands steady state heat flux more than 15 MW/m^2.

To design the divertor plate for ITER, it is important to evaluate heat transfer coefficients under one-sided heating conditions. Up to now, studies on heat transfer evaluation at uniform heating conditions have been done in the world [5 - 10]. Based on the existing heat transfer correlation, Schlosser et al [11] proposed a heat transfer correlation under one-sided heating conditions. However, he also informed that further efforts for developing the precise heat transfer correlation should be neccessary due to lack of data bases for his correlation. Therefore, heat transfer experiments of smooth circular tube and swirl tube have been performed under one sided heating conditions at JAERI ion beam test facility. The experimental data have been compared with the existing heat transfer correlations to investigate the applicability of their correlations to one-sided heating conditions. In this report, experimental set-up describes in section 2. Experiments and experimental results are presented in section 3 and 4, respectively.

2. EXPERIMENTAL SET-UP

In the experiments, Particle Beam Engineering Test Facility [12], namely PBEF, was used. PBEF, which consists of vacuum chambers, an ion source, high voltage power supply system, cooling water system, vacuum pumping system, control system, and data acquisition system as shown in Fig. 2-1, can deliver an intense hydrogen ion beams up to 5 MW for durations from 0.01 to 10 s.

2.1 Vacuum Chamber

Figure 2-2 shows a schematic of the PBEF vacuum chamber. This chamber made of stainless steel has many ports for installing the measuring equipment and data acquisition system. Major dimensions of the vacuum chamber are 1.5 m diameter and 5.0 m high. At the top of the chamber, a multi-pole magnetic cusp

1. INTRODUCTION

The plasma facing component is exposed to severe heat loads on its plasma facing side. In particular, the surface heat flux to the divertor plate was expected to be 15 to 30 MW/m^2 in ITER-CDA [1]. To reduce the surface heat flux on the divertor plate, some ideas have been proposed [2-4]. In ITER-EDA, a dynamic gas target concept is considered [4]. When this concept effectively works, the heat flux on the divertor plate can be reduced down to around 5 MW/m^2. However feasibility of this concept is still uncertain, we have to develop the divertor plate which withstands steady state heat flux more than 15 MW/m^2.

To design the divertor plate for ITER, it is important to evaluate heat transfer coefficients under one-sided heating conditions. Up to now, studies on heat transfer evaluation at uniform heating conditions have been done in the world [5 - 10]. Based on the existing heat transfer correlation, Schlosser et al [11] proposed a heat transfer correlation under one-sided heating conditions. However, he also informed that further efforts for developing the precise heat transfer correlation should be neccessary due to lack of data bases for his correlation. Therefore, heat transfer experiments of smooth circular tube and swirl tube have been performed under one sided heating conditions at JAERI ion beam test facility. The experimental data have been compared with the existing heat transfer correlations to investigate the applicability of their correlations to one-sided heating conditions. In this report, experimental set-up describes in section 2. Experiments and experimental results are presented in section 3 and 4, respectively.

2. EXPERIMENTAL SET-UP

In the experiments, Particle Beam Engineering Test Facility [12], namely PBEF, was used. PBEF, which consists of vacuum chambers, an ion source, high voltage power supply system, cooling water system, vacuum pumping system, control system, and data acquisition system as shown in Fig. 2-1, can deliver an intense hydrogen ion beams up to 5 MW for durations from 0.01 to 10 s.

2.1 Vacuum Chamber

Figure 2-2 shows a schematic of the PBEF vacuum chamber. This chamber made of stainless steel has many ports for installing the measuring equipment and data acquisition system. Major dimensions of the vacuum chamber are 1.5 m diameter and 5.0 m high. At the top of the chamber, a multi-pole magnetic cusp

ion source is mounted. In the chamber, there are three test sections, i. e., two test sections with forced cooling lines and one test bed with a remotely handled system. At the bottom of the chamber, a passively cooled ion dump which consists of many array of copper blocks with cooling tubes is installed to stop whole particle beams. In the heat transfer experiments, an additional ion dump, an actively cooled ion dump which consists of 16 array of swirl tubes with an external fin, is also installed from the side port of the chamber as shown in Fig. 2-2 in order to handle steady state intense hydrogen ion beams because an area of the intense ion beams is much wide compared with the test sample size.

2.2 Ion Source

This ion source have originally been developed for neutral beam injectors of JT-60. As seen in Fig. 2-3, the ion source consists of a source plasma generator and acceleration grid system. At the plasma generator which is multipole magnetic cusp bucket source, hydrogen source plasma is produced by arc discharge process using hair-pin-shaped tungsten filaments. Only hydrogen ions are extracted by the acceleration grid system, which has four grids, i. e., a plasma grid, a gradient grid, an electron suppression grid and an exit grid (ground grid). A transparency efficiency of the acceleration grid system is around 40 %. This ion source can stably be extracted the intense hydrogen ion beams at a beam energy from 30 to 100 keV with current up to 50 A which corresponds to a current density of up to 400 mA/cm^2 for durations from 0.01 to 10 s. Other feature of the ion source is high proton yield around 90 %. Major performances of the ion source are as follows;

- Acceleration Voltage, kV ; 30 to 100
- Acceleration Current, A ; up to 50
- Arc Power Supply System ; 30 to 120V, up to 2000 A x 2
- Filament ; 5 to 12 V, up to 400 A x 2
- Hydrogen Gas Feed, Pa·l/s ; up to 2700
- Beam Divergence, degree ; 0.9 to 1.2
- Operating Gas Pressure, Pa ; 0.05
- Area of the Acceleration Grid, mm ; 120 x 270
- Transparency, % ; 40
- Heated Area at the Test Sample (e-folding width) ; 160 x 200 mm
- Duration ; up to 10 s

2.3 High Voltage Power Supply System

The overall description of the PBEF facility can be found elsewhere. Figure 2-4 and Table 2-1 are a schematic diagram and fundamental specifications of the power supply system, respectively. In the following subsections, the accel power supply, the plasma generator and suppresser grid power supplies, and the time sequence are described.

2.3-1 The accel power supply [13]

In order to supply gradient grid voltage, a tube-resistor divider was selected because it affords to feed the high current required in the beam initiation phase and thus is capable of voltage control even during purveyance mismatched beam initiation from the underdense side. The beam initiation from the underdense side makes laborious adjustments of timing or waveforms unnecessary and, as a result, permits the use of a GTO (gate turn-off) valve. Furthermore, the tube-resistor divider also has the ability to change the ratio of gradient grid voltage to accel voltage during the pulse.

The GTO valve is composed of GTAS and GTAR. A 100 series element GTO stack (GTAS) is dedicated to switch on and off the DC current only, while a 20 series element stack, each provided with a parallel non-linear resistor (GTAR) serves the role of holding the overcharged voltage and each GTO independently becomes conducting as the voltage decreases when the beam initiates. The limiting voltage of each non-linear resistor used in GTAR is about 1 kV. The specifications of the GTO's used are listed in Table 2-2. The voltage safety factor based on the maximum rated voltage of 100 kV is 2.5. The regulator/switch tube has been replaced by a set of the GTO valve and a L-R-Diode element connected to the output side of the GTO valve (see Fig. 2-4), while a crowbar switch to protect the tube was eliminated. The function of the L-R-Diode element is to limit the surge current during source breakdowns. The accel voltage is roughly set by a transformer with tap-changer. Fine control of the accel voltage is made by phase-control of the AC thyrister switch, QSWA, which has a hybrid feedback loop of both the DC output voltage and the DC output current to achieve fast regulation.

Since stray capacitance and its countermeasure have a definite role of the performance in PBEF power supply system, the accel voltage is supplied to the plasma grid through an air insulated cable duct with the electrical power to the plasma generator. The gradient grid voltage is fed through a coaxial cable whose outer conductor is connected to the accel voltage. In this system, stray capacitance can be grouped into two sets. One, which is charged up to the accel

voltage, is the sum of the stray capacitance in the isolation transformer of the plasma generators and the distributed capacitance of the cable duct. This is estimated to be as much as 24,000 pF. The other, which is charged up to the accel voltage minus the gradient grid voltage, is distributed in the gradient grid's coaxial cable, and is about 7,000 pF. A ferrite core of 30 mH, +0.02 - 0.02 Vs with a resistor of 12.5 W in the secondary winding is present for surge protection. Although the original function of the diode D1 is to suppress the back swing of the accel voltage after source breakdown, the resistor located at the anode of the diode also absorbs the surge energy. It should be noted that stray capacitance affects the initiation characteristics of the accel and gradient grid voltages.

2.3-2 The power supplies for the plasma generators and the suppresser grids

A 5 parallel element GTO stack is also used in each arc power supply. The GTO stacks were first connected in parallel to the loads and the arc currents were snubbed for a short time just before the accel voltage was supplied. In this case, the current rise of the arc after the snub was too fast to keep the accel voltage constant and overshoot of the arc current was inevitable. These two effects made the source condition overdense and in turn were apt to cause an electrical instability characterized by a sudden transition to a sate in which the gradient grid voltage is almost equal to the accel voltage. The GTO stacks were then connected in series to the loads as sown in Fig. 2-4 and the beam initiation from the underdense side was adopted, eliminating this instability. The GTO valves in the arc power supplies also have the function of cutting off the output currents to the filament when filament arcing is detected. Arcing is detected by monitoring the unbalance of arc currents flowing through each filament.

Each filament power supply is composed of 8 sets of DC output, one for each filament. The negative arc terminal is connected to each positive terminal of the filament power supply in order to reduce inequality of the total current over each filament. A vacuum tube is used as a regulator/switch valve in the suppresser grid power supply.

2.4 Water Cooling System

PBEF water cooling system consists of deionized water cooling loops at a pressure of up to 1.5 MPa and a heat exhausting loop. As shown in Fig. 2-1, one

deionized water cooling loop is for cooling all beamline components such as the ion source, ion dumps and test sections and the other loop is for cooling the power supply system. In the cooling loop for the beamline, deionized water is pumped up at a pressure up to 1.5 MPa with a circulating pump and cools the beamline components. In particular, high pressurized water up to 2.0 MPa at the pump out put point is available for the actively cooled ion dump and the test sections using an additional pump unit. Deionized water is produced with an ion purification system to keep its electric resistance more than 1 MΩ•cm. To supply low temperature water to the beamline components, deionized water is also cooled with a heat exchanger unit as shown in Fig. 2-1. Deionized water with temperatures up to 100 °C is also temporarily possible to be supplied in the test sample in order to evaluate an effect of heat transfer on different subcoolings. In this case, inlet water pressure was limited to be up to 1 MPa due to adding temporal cooling system.

At the inlet point of the test sample, maximum pressure and flow rate (flow velocity) were 1.6 MPa and 75 l/min (up to 16 m/s), respectively, because of high pressure drop in the cooling system. Major performance of the cooling system is as follows;

(1)Water Circulating Pump

•Type	RPK 150 - 400
•Permissible Flow Rate	250 m^3/h
•Head	150 mm

(2)High Pressurizing Pump

•Type	RPK 80 - 315
•Permissible Flow Rate	60 m^3/h
•Head	100 mm

(3)Water Storage Tank

•Volume	6 m^3

(4)Heat Exchanger

•Type	Plate, UX - 426 - HP - 100
•Capacity	3.8 TW/°C
•Flow Rate	250 m^3/h

2.5 Vacuum Pumping System

PBEF vacuum pumping system consists of three turbo molecular pump units, four mechanical booster pump units with oil cold trappings, and four rotary pump units as shown in Fig. 2-1. One mechanical booster pump and rotary pump unit are used for vacuum pumping at back of the turbo molecular pump. One set, a mechanical booster pump unit and a rotary pump unit, is used for vacuum pumping from the atmospheric pressure to around 10-1 Pa. During the operation, the chamber can be kept a pressure around 0.05 Pa for steady state gas feed. Major performances are as follows;

(1)Rotary Pump

•Type	OV - K1500 III
•Pumping Speed	1500 l/min
•Number	4

(2)Mechanical Booster Pump

•Type	OV-RD600
•Pumping Speed	600 m^3/hr
•Number	4

(3)Turbo Molecular Pump

•Type	TPH 2001
•Pumping Speed	2000 l/sec for hydrogen gas
•Number	3

2.6 Control System

Control system mainly controls high voltage power supply system. In this section, time sequence describes. A typical timing chart of the PBEF facility is shown in figure 2-5. The most notable point is the relation between the initiation of the are and accel power supply outputs. Perveance matched beam initiation has long been understand to be an ideal way of avoiding breakdown during beam initiation phase. This initiation method requires fine timing adjustments and also accurate control of the arc power and accel voltage waveforms and, practically, operating without manual adjustment does not seem achievable for various operating conditions. Judging from our experience of both perveance matched and mismatched beam initiations, however, we believe that source plasma build up in the presence of a constant accel voltage induces less frequent breakdowns. In this mode of operation, the accel voltage is applied first and after it reaches a steady state, the arc current is switched on with a comparatively slow rise time.

With this method, a fraction of the ion beam hits the accelerator grids and hardens the periphery of extraction apertures. We believe this process contributes to the elimination of breakdowns at high voltages and at deviated conditions. This may be true in circular hole accelerator like our sources but not in slot-type aperture accelerators because slots form stronger electrostatic lenses than circular holes do and it seems that at the beam initiation phase too much beam strikes the electrodes to avoid producing breakdowns.

2.7 Data Acquisition System

PBEF has many data acquisition systems. For heat transfer experiments, data logging system which has a sampling speed as fast as 1.0 ms/32 channel, and an infrared camera which has a sampling speed of 30 ms/image were mainly used as shown in Figs. 2-1 and 2-2. In particular, the data logging system consists of two parts, i. e., a data logging part with 32-channel high speed amplifiers for various types of the thermocouples, strain gages, signals with a voltage from + 10 V - 10 V and data analyzing part. In the data analyzing equipments, all data are recorded in its hard disk memory and are analyzed using original software developed for this experiment.

3. EXPERIMENTS

Heat transfer experiments for two different test samples have been carried out at JAERI particle beam engineering facility. This section describes test samples, experimental conditions, and surface heat flux measurements.

3.1 Test Samples

To investigate heat transfer under one-sided heating conditions, it is essential to measure surface and inside wall temperature distributions along the circumference of the tube. For measurement of the surface temperature with the infrared camera, this method would be applicable to only measure temperature at the top flat region of the test sample, however it has less accuracy to determine the temperature distribution because of the circular shape and different emissivities. It is also difficult to attach thermocouples along the circumference of the tube wall. Therefore, we determined that temperature distribution at the selected points along the circumference in the tube are measured instead of the temperature measurements on the surface and the wall of the tube. Based on

With this method, a fraction of the ion beam hits the accelerator grids and hardens the periphery of extraction apertures. We believe this process contributes to the elimination of breakdowns at high voltages and at deviated conditions. This may be true in circular hole accelerator like our sources but not in slot-type aperture accelerators because slots form stronger electrostatic lenses than circular holes do and it seems that at the beam initiation phase too much beam strikes the electrodes to avoid producing breakdowns.

2.7 Data Acquisition System

PBEF has many data acquisition systems. For heat transfer experiments, data logging system which has a sampling speed as fast as 1.0 ms/32 channel, and an infrared camera which has a sampling speed of 30 ms/image were mainly used as shown in Figs. 2-1 and 2-2. In particular, the data logging system consists of two parts, i. e., a data logging part with 32-channel high speed amplifiers for various types of the thermocouples, strain gages, signals with a voltage from + 10 V - 10 V and data analyzing part. In the data analyzing equipments, all data are recorded in its hard disk memory and are analyzed using original software developed for this experiment.

3. EXPERIMENTS

Heat transfer experiments for two different test samples have been carried out at JAERI particle beam engineering facility. This section describes test samples, experimental conditions, and surface heat flux measurements.

3.1 Test Samples

To investigate heat transfer under one-sided heating conditions, it is essential to measure surface and inside wall temperature distributions along the circumference of the tube. For measurement of the surface temperature with the infrared camera, this method would be applicable to only measure temperature at the top flat region of the test sample, however it has less accuracy to determine the temperature distribution because of the circular shape and different emissivities. It is also difficult to attach thermocouples along the circumference of the tube wall. Therefore, we determined that temperature distribution at the selected points along the circumference in the tube are measured instead of the temperature measurements on the surface and the wall of the tube. Based on

temperature distributions at the selected points for different surface heat fluxes measured, wall temperatures and their distributions can be analyzed by applying the inverse analysis of heat conduction problems.

Figures 3-1 and 3-2 show a schematic of the test samples, i. e., circular smooth and circular swirl tubes. Major dimensions of the test samples are as follows;

Outer diameter	: 15 mm
Inner diameter	: 10 mm
Length	: 474 mm
test section	: 400 mm
Thermocouple position	: 13.0 mm, pitch circle diameter
Number of thermocouples:	
at top surface	: 5 in-line
along the circumference	: 13

Many thermocouples are brazed in the tube along the flow direction and the circumferential direction, respectively. The specification of each thermocouple is high quality class K-type sheathed with outer diameter of 0.5 mm made of stainless steel (SS316L), which has a response time of several ms and accuracy of 0.4 % for full scale. For the purpose of this experiment, the accuracy is the most important matter and the response time is enough fast for the temperature measurement even if burnout would occur. However permissible maximum temperature of this thermocouple at steady sate is limited to be around 500 °C, transient temperature measurements up to 700 °C is possible.

Since heat transfer experiments on their test samples are carried out at a hydrogen ion beam test facility in JAERI which can not extract flat beams, measurement of heat flux profile at the test sample position is very important. Five thermocouples positioned along the flow direction are used for monitoring them during the experiment. On the other hand, thermocouple position for temperature measurement along the circumference of the test sample was determined from the results on the previous critical heat flux experiments [9]. From zero to 180 ° from the top of the test sample, thermocouples are bonded into the test sample with every angle of 22.5 ° as shown in Fig. 3-3. On the other side, thermocouples are also bonded into the test sample with every 22.5 ° from 11.25 ° to 78.75 ° in order to interpolate temperature data at heating side.

The test samples were made of oxygen free high conductivity copper (OFHC-Cu) because its thermal and mechanical properties are well-known. Table 3.1 shows major properties of OFHC-Cu used. A silver brazing filler metal with a melting temperature around 720 °C which consists of 44 - 46 % silver, 29 - 31 %

copper and 23 - 27 % zinc was used in order to match the thermal properties of OFHC-Cu bulk material.

Since these test samples are exposed to high heat loads from single side, large thermal deformations would be expected. If the test sample would be deformed due to one-sided heating conditions, water flow direction has different angles from the original direction according the heat flux level, resulting different heat transfer phenomenon. To minimize the thermal deformation during heating, a plate made of OFHC-Cu with thickness of 4.8 mm and depth of 15 mm was brazed to the test sample at rear side (bottom of the tube) as shown in Figs. 3-1 and 3-2.

For swirl tube, a thin tape with a thickness of 0.5 mm made of Inconnel-625 was twisted, and then this twisted tape was inserted and fixed to a smooth tube inner wall made of OFHC-Cu by cold working process. A tape twist ratio is defined as a number of internal diameters for 180° of twist. In this experiment, a tape twist ratio of 3.0 was selected from the previous results of critical heat flux experiments [8]. In the swirl tube, the binding force between a twisted tape and an inside wall of the tube, which is amount of the tensile force divided by the tape insertion length, was more than 600 N/m at temperatures in the range 20 to 400 °C. This value is enough to be fit for a water pressure of up to 4 MPa. Furthermore, even if the binding force is reduced, sleeves which protrude from the inside wall at both ends of the tube will prevent the twisted tape from slipping off. After fabricating the swirl tube, 0.5 mm diameter thermocouples were bonded at the identical positions as the smooth tube.

Since heat transfer experiments of the test samples described above under one-sided heating conditions was planned to carry out at a hydrogen ion beam test facility at JAERI, easy mechanical joints between the test sample and a connections for pressurized water supply line in the vacuum chamber were used in order to turnaround the experiment. This mechanical joint, CAJON Joint, which is made of stainless steel 316, has performances that water leakage rate is as low as less than 1 x10-9 cc/s at a water pressure of up to 15 MPa and that permissible maximum temperature is around 200 °C because of o-ring seal.

It is also very important to measure inlet and outlet water pressures for the determination of the subcooling and pressure drop. Figure 3-4 shows a test sample manifold with pressure measurement ports. This manifold set at both ends of the test sample. For the measurement of the water pressure, sensors with a diaphragm were used. This sensor has specifications that permissible measurable pressure and temperature ranges are from 0 to 5 MPa within an error of 3 % with respect to the full scale and from 0 to 200 °C, respectively.

Test sample was set in the vacuum chamber as shown in Fig. 2-2 to form a horizontal flow configuration. All thermocouples were connected to the data logging system through a vacuum multi-junction terminal.

3.2 Experimental Conditions

Two experimental conditions are basically selected. One is to determine heat transfer coefficients in non-boiling to nucleate boiling regions under one-sided heating conditions, and the other is to evaluate an effect of heat transfer on different subcoolings. These experimental conditions are summarized as follows;

Condition 1 :

- Flow velocity, m/s ; 4.2 to 16
- Local pressure, MPa ; 0.5 to 1.3
- Surface heat flux, MW/m^2 ; 2.0 to burnout
- Inlet water temperature, °C ; up to 30
- Beam duration, s ; up to 2.0

Condition 2 :

- Flow velocity, m/s ; 5.5
- Local pressure, MPa ; 0.6
- Surface heat flux, MW/m^2 ; 2.0 to 10
- Inlet water temperature, °C ; 20 to 80
- Beam duration, s ; up to 2.0

The experimental procedure is as follows; at first, flow velocity and local pressure were adjusted by inlet and outlet slot valves. Keeping these flow conditions, hydrogen ion beams were exposed to the test sample till all thermocouples bonded in the test sample were reached to steady state condition. Subsequently, surface heat flux increases with a small step around 2 MW/m^2 up to burnout. As the preliminary experiment, it was confirmed that beam duration up to 1.0 s was enough to obtain steady state condition. Detail will be discussed in the next section. Therefore, the duration was fixed to 1.0 s.

Comparing cooling conditions between this experiment and the design value in ITER, there are some differences, in particular inlet water temperature and local water pressure. From thermal-hydraulic point of view, we believe that influences of the pressure and/or inlet water temperature on heat transfer should be simulated by changing the subcooling and by monitoring the local

water temperature due to relatively wide beam heating in this experiment compared with the ITER relevant heating conditions.

3.3 Surface Heat Flux Measurements [14]

For measuring surface heat flux at the test sample position, two different calorimetries are applied. One is a multi-channel calorimeter, and the other is a water calorimetry. Figure 3-5 shows a schematic of a multi-channel calorimeter which consists of 11 cylindrical copper chips with each surface area of 2 cm^2 for volume of 1 cm^3. One high grade K-type thermocouple with a sheath diameter of 1.0 mm is bonded to each copper chip in the rear side with a depth of 2.0 mm. To obtain almost adiabatic temperature rise of the cylindrical copper chip during heating, each copper chip is fixed by a small cylindrical stud bolt made of stainless steel with a diameter of 3 mm. Therefore, heat loss through the bolt can be minimized due to its low thermal conductivity compared with copper and be expected to be several percents (up to 3 %) of the total deposited power. From adiabatic temperature rises of 11 copper chips in line, surface heat fluxes and a beam profile can be calculated by the following equation;

$$q_{BEAM,\,i} = \frac{V}{S \cdot (t_{2,\,i} - t_{1,\,i})} \left\{ \rho(T_{2,\,i}) \cdot C_p(T_{2,\,i}) - \rho(T_{1,\,i}) \cdot C_p(T_{1,\,i}) \right\}, \quad (i = 1, 2, \cdots, 11) \quad \cdots\cdots (3\text{-}1)$$

where,

q_{BEAM} ; Surface heat flux, W/m^2

V ; Volume of calorimeter chip, (= 1 cm^3)

S ; Heated surface area, (= 2 cm^2)

ρ ; Density, kg/m^3

C_p ; Specific Heat, J/kg/K

t_1, t_2 ; Heating duration, s

T_1, T_2 ; Average temperature ascending of calorimeter chip at t_1 and t_2, °C

i ; Number of calorimeter chip, (= 11)

Figure 3-6 shows typical surface heat flux distributions measured with the multi-channel calorimeter for different beam conditions. The abscissa is the position along the flow direction where position zero corresponds to the center of the test sample. Each symbol ,○, □, ◇, △, + and × in the figure shows surface heat flux at different beam conditions. Heat flux profile in the flow direction is almost Gaussian with a full width at half maximum of around 160 mm for all beam extraction conditions because of purveyance matching operation. On the other

hand, deposited heat flux distributions in the cross sectional direction of the test sample have been measured and confirmed to be almost flat within a width of ±20 mm where is much wider than the width of the test sample. In the experiment, surface heat flux distribution along the circumference of the test sample is assumed to be cosine profile because of its circular surface and of few reflection loss (up to 2 %).

The other calorimetry, water calorimetry, has been carried out in order to make a cross checking for multi-channel calorimetry described above. From the water calorimetry, only total deposited power into the water is measured. Since surface heat flux distribution is already obtained by the multi-channel calorimetry, total deposited power into water should be given as a sum of the deposited heat fluxes in the test sample. Therefore, surface heat flux can be predicted by the following equation;

$$D \cdot \int q_{BEAM} dL = C_p \cdot \rho \cdot V \cdot \Delta T \qquad \cdots\cdots\cdots\cdots\cdots\cdots \quad (3\text{-}2)$$

where,

q_{BEAM} ; Surface Heat Flux, W/m^2

D ; Outer Diameter of the Test Sample, m

L ; Length in the Flow Direction, m

C_p ; Specific Heat of Water, J/kg/K

ρ ; Density of Water, kg/m^3

V ; Flow Rate, m^3/s

ΔT ; Temperature Rise, K.

Surface heat fluxes measured by water calorimetry are compared with those measured by multi-channel calorimetry. As seen in Fig. 3-7, their relationship shows linear dependence, resulting the promising heat flux measurement in the experiment.

4. EXPERIMENTAL RESULTS

4.1 Pressure Drop

Figure 4-1 shows pressure drop of each test sample. In the smooth tube test sample, pressure drop can be predicted by the following equation;

hand, deposited heat flux distributions in the cross sectional direction of the test sample have been measured and confirmed to be almost flat within a width of ±20 mm where is much wider than the width of the test sample. In the experiment, surface heat flux distribution along the circumference of the test sample is assumed to be cosine profile because of its circular surface and of few reflection loss (up to 2 %).

The other calorimetry, water calorimetry, has been carried out in order to make a cross checking for multi-channel calorimetry described above. From the water calorimetry, only total deposited power into the water is measured. Since surface heat flux distribution is already obtained by the multi-channel calorimetry, total deposited power into water should be given as a sum of the deposited heat fluxes in the test sample. Therefore, surface heat flux can be predicted by the following equation;

$$D \cdot \int q_{BEAM} dL = C_p \cdot \rho \cdot V \cdot \Delta T \qquad \cdots\cdots\cdots\cdots\cdots\cdots \quad (3\text{-}2)$$

where,

q_{BEAM} ; Surface Heat Flux, W/m^2

D ; Outer Diameter of the Test Sample, m

L ; Length in the Flow Direction, m

C_p ; Specific Heat of Water, J/kg/K

ρ ; Density of Water, kg/m^3

V ; Flow Rate, m^3/s

ΔT ; Temperature Rise, K.

Surface heat fluxes measured by water calorimetry are compared with those measured by multi-channel calorimetry. As seen in Fig. 3-7, their relationship shows linear dependence, resulting the promising heat flux measurement in the experiment.

4. EXPERIMENTAL RESULTS

4.1 Pressure Drop

Figure 4-1 shows pressure drop of each test sample. In the smooth tube test sample, pressure drop can be predicted by the following equation;

$$\Delta P = A\frac{\lambda \cdot \rho \cdot V_a^2}{2g} \cdot \frac{L}{D_i}, \qquad \cdots\cdots\cdots\cdots\cdots\cdots \quad (4\text{-}1)$$

where,

- ΔP ; Pressure Drop, MPa
- λ ; Friction Factor
- ρ ; Bulk Coolant Density, kg/m^3
- V_a ; Superficial Axial coolant Velocity, m/s
- L ; Axial Tube Length, m
- D_i ; Inside Diameter, m
- A ; Conversion Factor, (=1.0197 x 10^{-3} MPa/kg/m^2)
- g ; Gravitational Acceleration, m/s^2

On the other hand, it is also confirmed that pressure drop of the swirl tube test sample can roughly be predicted by the existing pressure drop correlation proposed by Gambill correlation as follows;

$$\Delta P = A_c \cdot f_a \frac{\rho \cdot V_a^2}{2g} \cdot \frac{L}{D_i}, \qquad \cdots\cdots\cdots\cdots\cdots\cdots \quad (4\text{-}2)$$

$$f_a = 0.0037 \cdot y^{-0.6} \cdot D_i^{-1.2} \qquad \cdots\cdots\cdots\cdots\cdots\cdots \quad (4\text{-}3)$$

where,

- y ; Tape Twist Ratio, Internal Diameters/180-deg Twist Length.
- Ac ; Conversion Factor, (= 6.895 x 10^{-3} MPa/psi).

4.2 Experimental Data

To accelerate turnaround the experiments, pulse heating experiments have been done. A pulse duration of 1 s was selected to reach steady state heating condition. Figure 4-2 shows a typical temperature responses measured with thermocouples bonded in the test sample. From Fig. 4-2(a), it is clearly seen that all temperature signals from the thermocouples reach to steady state temperatures at a pulse duration of up to 1.0 s. A temperature distribution along the circumference of the test sample after 1.0 s beam on is shown in Fig. 4-2(b). At the surface heat flux of 12.8 MW/m^2, which nucleate boiling is formed in a region from top around ± 60 °, temperature difference between the top and the bottom of the smooth tube test sample reaches to about 200 K.

Figure 4-3 shows the temperature distribution in the flow direction measured with thermocouples bonded in the test sample at the identical heating and cooling conditions in Fig. 4-2. The abscissa is thermocouple position in the flow direction. It is confirmed that a fraction of heat deposited in the test sample at a position of TP4 where 13 thermocouples are bonded along the circumference slightly move to flow direction. However this fraction of the deposited heat is much smaller than 3.5 % compared with heat conduction to the circumference. Therefore, the fraction of heat loss in the flow direction is not considered in the analyses described in next section.

Experimental data for both of the test samples are listed in appendix as Tables 4-1 and 4-2. In the table, Q, V, and P are a coolant flow rate in l/min, a coolant axial velocity in m/s, and a coolant pressure at center of the test sample (local pressure) in MPa, respectively.

5. HEAT TRANSFER EVALUATIONS

Since temperature distributions are obtained from the experiments, heat transfer coefficients should be estimated from them. Figure 5-1 shows the evaluation procedure for the prediction of heat transfer coefficients under one sided heating conditions. It is two parts as follows; 1) finite element thermal analyses using the existing heat transfer correlations are performed under the experimental conditions. From the analyses, temperatures in the test sample and inside heat flux and heat transfer coefficient can be obtained. Subsequently, temperature distribution at the thermocouple position is compared with the experimental results to evaluate the applicability on the existing correlations to one side heating conditions. 2) based on the experimental data, inverse analyses in thermal conduction problems are done to predict inside distributions in heat flux, temperature, and in heat transfer coefficient, since all boundary conditions such as the surface heat flux distribution and the temperature distribution at the thermocouple position are given.

5.1 Comparison Between the Existing Correlations and the Experimental Data [11]

In general, the following existing heat transfer correlations which were obtained under uniform heating condition are used,

(1) at non-boiling,

Figure 4-3 shows the temperature distribution in the flow direction measured with thermocouples bonded in the test sample at the identical heating and cooling conditions in Fig. 4-2. The abscissa is thermocouple position in the flow direction. It is confirmed that a fraction of heat deposited in the test sample at a position of TP4 where 13 thermocouples are bonded along the circumference slightly move to flow direction. However this fraction of the deposited heat is much smaller than 3.5 % compared with heat conduction to the circumference. Therefore, the fraction of heat loss in the flow direction is not considered in the analyses described in next section.

Experimental data for both of the test samples are listed in appendix as Tables 4-1 and 4-2. In the table, Q, V, and P are a coolant flow rate in l/min, a coolant axial velocity in m/s, and a coolant pressure at center of the test sample (local pressure) in MPa, respectively.

5. HEAT TRANSFER EVALUATIONS

Since temperature distributions are obtained from the experiments, heat transfer coefficients should be estimated from them. Figure 5-1 shows the evaluation procedure for the prediction of heat transfer coefficients under one sided heating conditions. It is two parts as follows; 1) finite element thermal analyses using the existing heat transfer correlations are performed under the experimental conditions. From the analyses, temperatures in the test sample and inside heat flux and heat transfer coefficient can be obtained. Subsequently, temperature distribution at the thermocouple position is compared with the experimental results to evaluate the applicability on the existing correlations to one side heating conditions. 2) based on the experimental data, inverse analyses in thermal conduction problems are done to predict inside distributions in heat flux, temperature, and in heat transfer coefficient, since all boundary conditions such as the surface heat flux distribution and the temperature distribution at the thermocouple position are given.

5.1 Comparison Between the Existing Correlations and the Experimental Data [11]

In general, the following existing heat transfer correlations which were obtained under uniform heating condition are used,

(1) at non-boiling,

$Nua = 0.023 \cdot Re^{0.8} \cdot Pr^{0.4}$ Dittus-Boelter equation ·····(5-1)

$Nu_W = Nu_a \cdot (\mu/\mu_W)^{0.14}$ ·····(5-2)

for swirl flow, the following additional heat transfer enhancement factor introduced by Gambill is applied,

$Nu_S = 2.18 \cdot Nu_a / y^{0.09}$ Gambill equation ·····(5-3)

$Nu_{SW} = Nu_S \cdot (\mu/\mu_W)^{0.14}$ ·····(5-4)

(2) at transient to nucleate boiling,

$$\frac{q}{q_{con}} = \left[1 + \left\{\frac{q_{boil}}{q_{con}}\left(1 - \frac{q_{bi}}{q_{boil}}\right)\right\}^2\right]^{1/2},$$ Bergles-Rohsenow equation ·····(5-5)

(3) at nucleate boiling,

the following three heat transfer correlations are available,

$T_{wall} - T_{sat} = 0.022 \cdot q^{1/2} / \exp(p/8.6)$ Thom correlation ·····(5-6)

$T_{wall} - T_{sat} = 0.79 \cdot q^{1/4} / \exp(p/6.2)$, Jens-Lottes equation ·····(5-7)

$T_W = \{(\psi - 1.0) \cdot (T_{SAT} - T_L) + (q/h_L)\}/\psi + T_L$, Shah correlation ·····(5-8)

$\psi = 230.0 \cdot (q/(G \cdot H_g))^{0.5}$.

where,

Nu : Nusselt number (-),

Nu_s : Nusselt Number for swirl flow (-),

Re : Reynolds Number (-),

Pr : Prandtl Number (-),

μ : Dynamic viscosity of liquid (Pa•s),

μ_w : Dynamic viscosity of liquid at wall temperature (Pa•s),

y : Tape twist ratio (=L180/D_i),

q : Total heat flux ($MW \cdot m^{-2}$),

q_{con} : Heat flux predicted at forced convection flow ($MW \cdot m^{-2}$),

q_{boil} : Heat flux for boiling ($MW \cdot m^{-2}$),

q_{bi} : Fully developed boiling heat flux at incipient boiling ($MW \cdot m^{-2}$),

T_{wall} : Wall temperature (K),

T_{sat} : Saturation temperature (K),

p : Local water pressure (MPa),

T_L : Mixed-mean temperature of liquid (K),
h_L : Heat transfer coefficient at non-boiling region ($W \cdot m^{-2} \cdot K^{-1}$),
G : Mass flow rate ($kg \cdot s^{-1}$),
H_g : Latent heat of vaporization ($J \cdot K^{-1}$).

At the first step, 2-dimensional finite element analysis using ADINA has been performed applying the experimental conditions to predict the temperature distributions at the thermocouple positions and has been compared with the experiments. Typical results in the tube without a twisted tape are shown in Figs. 5-2, 5-3 and 5-4. Figure 5-2 shows an example of temperature distributions at the thermocouple positions for different surface heat fluxes ranged from non boiling to nucleate boiling close to burnout. The abscissa shows the angle from the top of the tube. This figure also shows analytical results predicted by Thom and Shah correlations. At forced convection cooling (none boiling) region, analytical results show relatively good agreement with the experimental results. On the other hand, at transition to boiling and partial nucleate boiling regions it is found that experimental data have positioned among lines predicted by their correlations within an error of -10 % to + 30 % as shown in Fig. 5-2, where Thom correlation overpredicts the temperatures, while Shah correlation underpredicts. It means that experimental data can roughly be predicted within a band between their predicted lines. Based on these results, temperature distributions at the tube inner wall and heat transfer coefficients are analyzed as shown in Figs. 5-3 and 5-4, respectively. In particular the calculated heat transfer coefficients for both predictions are deviated, resulting the difficulty of the applications for the prediction of heat transfer coefficients under one-sided heating conditions. To determine the actual heat transfer coefficients, further evaluations such as inverse analyses of heat conduction are necessary.

For the tube with a twisted tape inserted, similar evaluation procedure has been applied to predict heat transfer coefficients under one-sided heating conditions. In this case, large heat transfer enhancement is expected due to vortex flow. At the first step for the evaluations, Gambill correlation [4] for heat transfer enhancement factor at non boiling region has simply been applied for all regions. Figure 5-5 shows a comparison of experimental and analytical temperature distributions at the thermocouple positions for different incident heat fluxes. Experimental data have also roughly positioned among the predicted lines as the similar to the results of the tube without a twisted tape, leading us to similar results to the smooth tube.

However existing heat transfer correlations would be available for predicting heat transfer coefficients under one-sided heating conditions within an accuracy

of ± 30%, new correlation under one side heating would be required to perform the promising design of the ITER plasma facing components.

5.2 Inverse Analyses of Heat Conduction Problems

To determine heat transfer coefficient under one-sided heating conditions, 2-dimensional inverse analyses of heat conduction problems have been done using the experimental data. Analytical procedure and model are shown in figures 5-6 and 5-7, respectively. From the analyses, inside heat flux and temperature are calculated.

5.2.1 Integral equation for inverse problems of heat conduction

Figure 5-8 shows a conceptual diagram of inverse analysis of heat conduction problems. To analyze inverse problems of heat conduction, boundary element method (BEM) was applied [12]. This analytical method is to solve linear integral equations obtained by the following process; 1) at first, a partial differential equation of the boundary problem which has solution is translated into integral equation on the boundary applying Green theorem, 2) the boundary is divided to boundary elements which are defined by linear equations.

In x-y plane, a temperature at a finite region D where are closed with each smoothen simple closed curve can be assumed to be obtained as a position-dependent derivative of the second order partial differential equation. Therefore, the following equation can be given,

$$\int_C \left[T_Q \cdot \frac{\partial}{\partial n_Q}\left(\ln\frac{1}{r_{PQ}}\right) \quad \ln\frac{1}{r_{PQ}} \cdot \frac{\partial T_Q}{\partial n_Q}\right] ds = -a\pi T_p \qquad \cdots\cdots(5\text{-}9)$$

a = 1, if point P is on the boundary,

a = 2, when point P is in the boundary.

where subscripts P and Q mean a point in an arbitrary region, a point on an arbitrary boundary, and $r_{PQ} = |\overline{PQ}|$, respectively.

To divide Eq. (5-9) to boundary elements, boundary C is separated to n-elements which has Q with a subscript of j, (j = 1, 2, 3, ·····, n) and P with a

subscript of i, (i =1, 2, ·····, N). Subsequently, the following equation can be given,

$$\sum_{j=1}^{n} W_{ij} \cdot T_{Qj} - \sum_{j=1}^{n} V_{ij} \cdot \frac{\partial T_{Qj}}{\partial n_{Qj}} = -\pi T_{Pi} \quad (P \in C) \ (i=1, 2, \cdots, n) \qquad \cdots\cdots(5\text{-}10)$$

$$\sum_{j=1}^{n} W_{ij} \cdot T_{Qj} - \sum_{j=1}^{n} V_{ij} \cdot \frac{\partial T_{Qj}}{\partial n_{Qj}} = -2\pi T_{Pi} \quad (P \in D) \ (i=1, 2, \cdots, N) \qquad \cdots\cdots(5\text{-}11)$$

where,

$$W_{ij} = \int_j \frac{\partial}{\partial n_Q}\left(\ln \frac{1}{r_{PiQ}}\right) ds,$$

$$V_{ij} = \int_j \ln \frac{1}{r_{PiQ}} ds$$

5.2.2 Process of the analysis

To determine the inside temperature and heat flux, 2-dimensional analysis code has been developed. This code based on the inverse analysis of heat conduction problems consists of two parts as follows,

Part 1: as seen in Fig. 5-8 (1), all boundaries are given, e. g., heat fluxes on the outside of the test sample (C1) and on both edge regions due to symmetrical structure, temperature on inside region where corresponds to the thermocouple position along the circumference (C2) by interpolating the experimental data. Therefore, normal heat conduction problem can be applied to calculate temperatures in the test sample which is closed with above boundaries. In the heat conduction analysis, the following equation is given by arranging known terms in left side and unknown terms in right side,

$$\sum_{j=1}^{n1} W_{ij} \cdot T_{Qj} - \sum_{j=n1+1}^{n1+n2} V_{ij} \cdot q_{Qj} + \pi T_{Pi} = \sum_{j=1}^{n1} V_{ij} \cdot q_{Qj} - \sum_{j=n1+1}^{n1+n2} W_{ij} \cdot T_{Qj}$$

$$(P \in C1) \ (\ i = 1,2,\cdots,n1\ ) \qquad \cdots\cdots(5\text{-}12)$$

$$\sum_{j=1}^{n1} W_{ij} \cdot T_{Qj} - \sum_{j=n1+1}^{n1+n2} V_{ij} \cdot q_{Qj} = \sum_{j=1}^{n1} V_{ij} \cdot q_{Qj} - \sum_{j=n1+1}^{n1+n2} W_{ij} \cdot T_{Qj} - \pi T_{Pi}$$

$$(P \in C2) \ (\quad i = n1+1, n1+2, \cdots, n) \qquad \cdots\cdots(5\text{-}13)$$

Therefore, these simultaneous equations can be solved applying Gauss formula, and have solutions which correspond to temperatures Tpi in the boundary as follows,

$$T_{Pi} = -\frac{1}{2\pi}\left\{ \sum_{j=1}^{n1}{}_1 \; W_{ij}\cdot T_{Qj} - \sum_{j=1}^{n1}{}_1 \; V_{ij}\cdot q_{Qj} + \sum_{j=n1+1}^{n1+n2}{}_2 \; W_{ij}\cdot T_{Qj} - \sum_{j=n1+1}^{n1+n2}{}_2 \; V_{ij}\cdot q_{Qj} \right\}$$

$$(P \in D) \quad (\, i = 1,2,\cdots; N\,) \qquad \cdots\cdots(5\text{-}14)$$

Part 2: using the calculation results obtained in Eq. (5-14), inverse analysis of heat conduction problems is performed to predict temperatures and heat fluxes on a new boundary where is defined at inside of the previous boundary C2 with an infinitely small distance, DR, as shown in Fig. 5-8 (2). However new boundary is not defined in this process, it can be given by the following equations,

$$\sum_{j=n1+1}^{n1+n2}{}_2 \; W_{ij}\cdot T_{Qj} - \sum_{j=n1+1}^{n1+n2}{}_2 \; V_{ij}\cdot q_{Qj} = -\sum_{j=1}^{n1}{}_1 \; W_{ij}\cdot T_{Qj} + \sum_{j=1}^{n1}{}_1 \; V_{ij}\cdot q_{Qj} - \pi T_{Pi}\,,$$

$$(P \in C1) \quad (\, i = 1,2,\cdots; n2\,) \qquad \cdots\cdots(5\text{-}15)$$

$$\sum_{j=n1+1}^{n1+n2}{}_2 \; W_{ij}\cdot T_{Qj} - \sum_{j=n1+1}^{n1+n2}{}_2 \; V_{ij}\cdot q_{Qj} - \pi T_{Pi} = -\sum_{j=1}^{n1}{}_1 \; W_{ij}\cdot T_{Qj} + \sum_{j=1}^{n1}{}_1 \; V_{ij}\cdot q_{Qj}\,,$$

$$(P \in C2) \quad (\, i = 1,2,\cdots; n1) \qquad \cdots\cdots(5\text{-}16)$$

$$\sum_{j=n1+1}^{n1+n2}{}_2 \; W_{ij}\cdot T_{Qj} - \sum_{j=n1+1}^{n1+n2}{}_2 \; V_{ij}\cdot q_{Qj} = -\sum_{j=1}^{n1}{}_1 \; W_{ij}\cdot T_{Qj} + \sum_{j=1}^{n1}{}_1 \; V_{ij}\cdot q_{Qj} - 2\pi T_{pi}\,.$$

$$(P \in D) \quad (\, i = 1,2,\cdots; N\,) \qquad \cdots\cdots(5\text{-}17)$$

From Eqs. (5-15), (5-16), and (5-17), (n + N) numbers of simultaneous equations for the boundary with n-unknown values, $AX = y$, are obtained. Since these simultaneous equations have many solutions, therefore a solution on X which corresponds to the boundary condition is determined by a least squares method. In the preliminary investigation, it was confirmed that a number of simultaneous equations is required to be at least twice of a number of unknown values to obtain reasonable solution. By iterating these processes which the boundary condition obtained by part 2) is used as an input condition, the boundary condition can consequently be converged and determined. These

processes are iterated till the inside wall of the test sample. Subsequently, the inside temperature and the heat flux can finally be determined.

Although an infinitely small distance, DR, as shown in Fig. 5-8 (2) can arbitrarily be defined, it should be optimized to obtain accurate solution. With decreasing distance DR, accurate solution by the inverse analysis of heat conduction problems in part 2) would be obtained, however, a number of the iteration process also increases, resulting increase of sum of errors induced by processes of inverse analyses of heat conduction problems. On the other hand, with increasing a number of fine boundaries, accurate solution by normal heat conduction analysis would also be obtained, while a number of unknown values also increases. Subsequently, sum of errors induced by processes of inverse analyses of heat conduction problems should increase. After optimizing, in the analyses a distance DR and a number of fine boundaries were selected to be 0.1 mm, 64 for boundary along the circumference, and 16 in radial, respectively.

6. CONCLUSIONS

1) Heat transfer experiments for the smooth tube and the swirl tube have been performed under conditions that the flow rate, the local pressure, and the subcooling ranged from 4 to 16 m/s, 0.3 to 1.4 MPa, and 80 to 170 K, respectively, at the surface heat fluxes from 2 MW/m^2 to burnout.

2) The inverse analysis code of heat conduction problems was developed to determine heat transfer coefficient under one sided heating conditions.

3) In the simple comparisons between the experimental data and the existing correlations for heat transfer in non-boiling region under one-sided heating conditions, the existing heat transfer correlations proposed by Dittus-Boelter and Gambill applying a friction factor can be applied for both tube configurations.

4) In the subcooled partial nucleate boiling region, existing heat transfer correlations proposed by Thom, Shah, and Jens-Lottes were roughly applicable for the heat transfer prediction under one sided heating conditions with an accuracy of ± 30 %, although a small discrepancy between the experiments and the analyses was found.

processes are iterated till the inside wall of the test sample. Subsequently, the inside temperature and the heat flux can finally be determined.

Although an infinitely small distance, DR, as shown in Fig. 5-8 (2) can arbitrarily be defined, it should be optimized to obtain accurate solution. With decreasing distance DR, accurate solution by the inverse analysis of heat conduction problems in part 2) would be obtained, however, a number of the iteration process also increases, resulting increase of sum of errors induced by processes of inverse analyses of heat conduction problems. On the other hand, with increasing a number of fine boundaries, accurate solution by normal heat conduction analysis would also be obtained, while a number of unknown values also increases. Subsequently, sum of errors induced by processes of inverse analyses of heat conduction problems should increase. After optimizing, in the analyses a distance DR and a number of fine boundaries were selected to be 0.1 mm, 64 for boundary along the circumference, and 16 in radial, respectively.

6. CONCLUSIONS

1) Heat transfer experiments for the smooth tube and the swirl tube have been performed under conditions that the flow rate, the local pressure, and the subcooling ranged from 4 to 16 m/s, 0.3 to 1.4 MPa, and 80 to 170 K, respectively, at the surface heat fluxes from 2 MW/m^2 to burnout.

2) The inverse analysis code of heat conduction problems was developed to determine heat transfer coefficient under one sided heating conditions.

3) In the simple comparisons between the experimental data and the existing correlations for heat transfer in non-boiling region under one-sided heating conditions, the existing heat transfer correlations proposed by Dittus-Boelter and Gambill applying a friction factor can be applied for both tube configurations.

4) In the subcooled partial nucleate boiling region, existing heat transfer correlations proposed by Thom, Shah, and Jens-Lottes were roughly applicable for the heat transfer prediction under one sided heating conditions with an accuracy of ± 30 %, although a small discrepancy between the experiments and the analyses was found.

5) To determine the heat transfer coefficients under one sided heating conditions, we will develop a new heat transfer correlation which can cover from non-boiling to the subcooled partial nucleate boiling regions.

Acknowledgment

The authors would like to thank Dr. Y. Ohara and the other NBI heating laboratory for their valuable discussions and comments. The authors wish to thank Mr. W. Hashimoto of Nikon Systems co. Ltd. for his assistance on the calculations. The authors would deeply like to thank Drs. S. Shimamoto, M. Ohta and Dr. Y. Tanaka for their support and encouragement.

5) To determine the heat transfer coefficients under one sided heating conditions, we will develop a new heat transfer correlation which can cover from non-boiling to the subcooled partial nucleate boiling regions.

Acknowledgment

The authors would like to thank Dr. Y. Ohara and the other NBI heating laboratory for their valuable discussions and comments. The authors wish to thank Mr. W. Hashimoto of Nikon Systems co. Ltd. for his assistance on the calculations. The authors would deeply like to thank Drs. S. Shimamoto, M. Ohta and Dr. Y. Tanaka for their support and encouragement.

References

[1] T. Kuroda, et al., ITER Documentation Series, No. 30, IAEA (1991).

[2] M. Araki, et al., Fusion Engineering and Design, 22, (1993) 217.

[3] T. Hino and T. Yamashina, in Proc. of 10th Plasma Surface Interactions, (1992).

[4] G. Janeschitz, et al., in Proc. of 15th Int. Conf. on Plasma Physics and Controlled Nuclear Fusion Research, Seville, Spain (1994).

[5] F.W. Dittus and L. M. K. Boelter,Univ.Calif.Publs Engnrs, Vol.2, (1930) 443.

[6] W. H. Jens and P. A. Lottes, A.N.L.Report 4627, (May, 1951).

[7] W. R. Gambill, R. D. Bundy, and R. W. Wansbrough, ORNL-2911, Oakridge National Laboratory, (1960).

[8] A. E. Berges and W. M. Rohsenow, Journal Heat Transfer, (August, 1964) 365.

[9] J. R. S. Thom, W. M. Walker, T. A. Fallon, and G. F. S. Reising, in Proc. Inst. Mech. Engrs., Vol.180, Prat 3C (1966) 266.

[10] M. M. Shah, Heat Transfer Engineering, 4 (1983) 24.

[11] J. Schlosser and J. Boscary, in Proc. of NURETH6, Grenoble, (Oct. 1993) 815.

[12] M. Araki, et al., Fusion Engineering and Design, Vol. 9, (1988) 131.

[13] M. Matsuoka, et al., JAERI-M 84-112, Japan Atomic Energy Research Institute, (1984).

[14] S. Ikeda, et al., JAERI-M 893-070, Japan Atomic Energy Research Institute, (1993) and also see M. Araki, M. Akiba R. D. Watson, C. B. Baxi and D. L. Youchison, to be published for Atomic and Plasma-Material Interaction Processes in Controlled Thermonuclear Fusion, Vol. 5 (1994).

[15] C. A. Brebbia, The Boundary Element Method for Engineers, Pentech Press Limited., London, (1978) .

Table2-1 Fundamental Specifications of PBEF Power Supply System.

	Voltage	Current	Duration	Duty
Accel P.S.				
plasma grid	20-100 kV	80 A	10 s	1/30
gradient grid	20-90 kV	-2 - +2 A	10 s	1/30
Suppressor Grid P.S.	-(.5-3) kV	22 A	10 s	1/30
Arc P.S.	120 V	2000 A × 2	10.5 s	-
	or 180 V	1000 A × 2		
Filament P.S.	12 V	400 A × 8 × 2	14 s	-

Table2-2 Specifications of the Gate Turn Off Thyristors.

	Accel P.S.
Type	SG600EX21 (Toshiba)
Voltage Range (V)	2500
I_T(RMS) (A)	420
I_{TGQ}^{*} (A)	600
I_{TSM}^{**} (A)	6000
t_{gq}^{***} (μs)	20

* turn off current

** surge on current

*** turn off time

Table3-1 Thermal and Mechanical Properties of OFHC – Cu.

Density at RT, kg/m^3	: 8.9 x10^3
Elastic Modulus, GPa	
at 20°C	82.4
at 100°C	78.5
at 200°C	73.5
at 500°C	65.7
at 800°C	58.8
Yield Strength, MPa	
at 20°C	44.1, 0.2%
	103.0, 4.0%
at 400°C	34.3, 0.2%
	66.7, 4.0%
Ultimate Strength, MPa	
at RT	245.0
Poisson Ratio	0.33
Thermal Conductivity, W/m•K	
at 27°C	398.0
at 400°C	383.0
at 527°C	371.0
at 727°C	357.0
at 927°C	342.0
Thermal Expansion Coefficients, x10^{-6}/K	
at 27°C	15.0
at 300°C	16.6
at 400°C	18.3
at 500°C	19.1
at 600°C	20.0
at 800°C	21.6

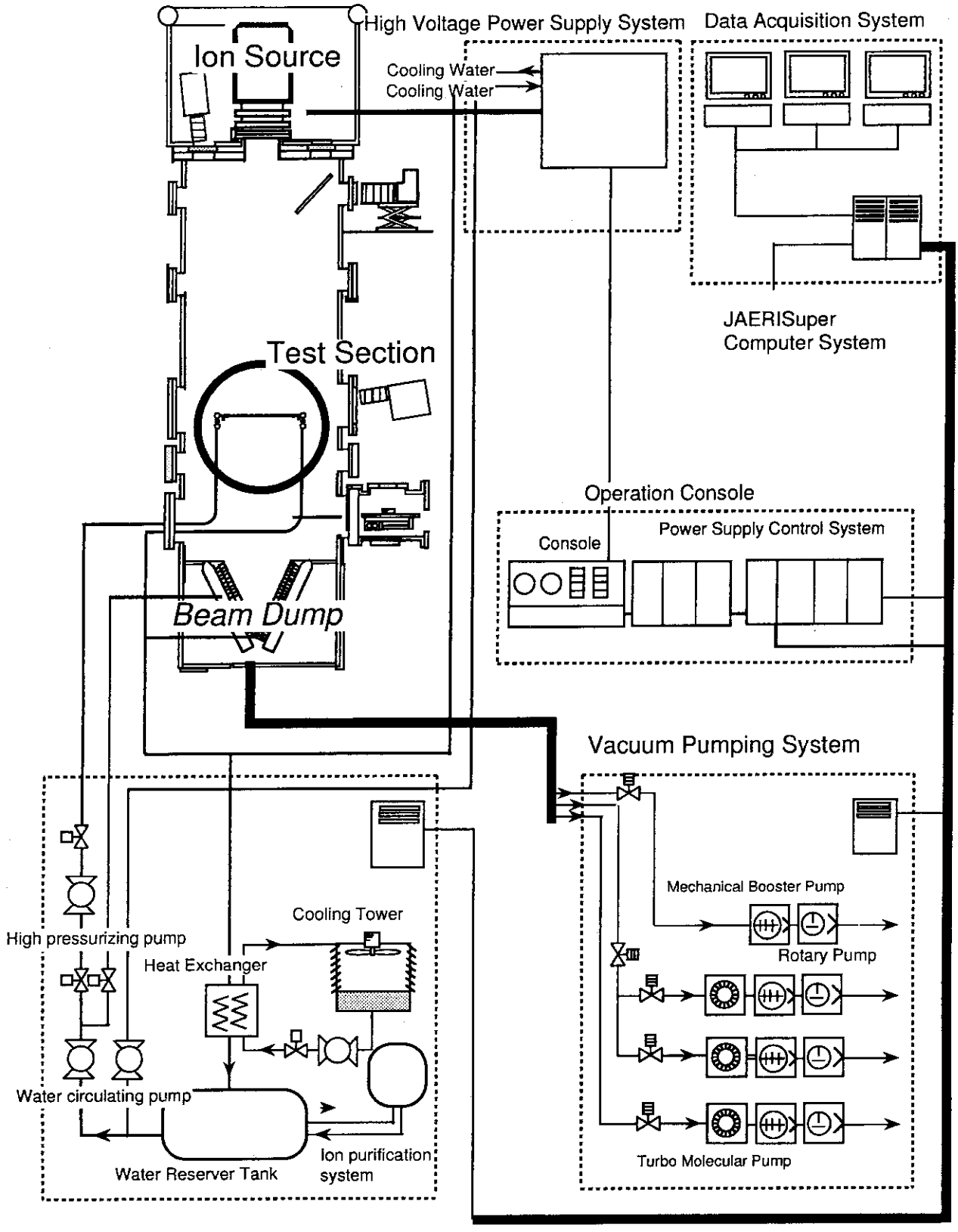

Figure2-1 System Diagram of JAERI PBEF.

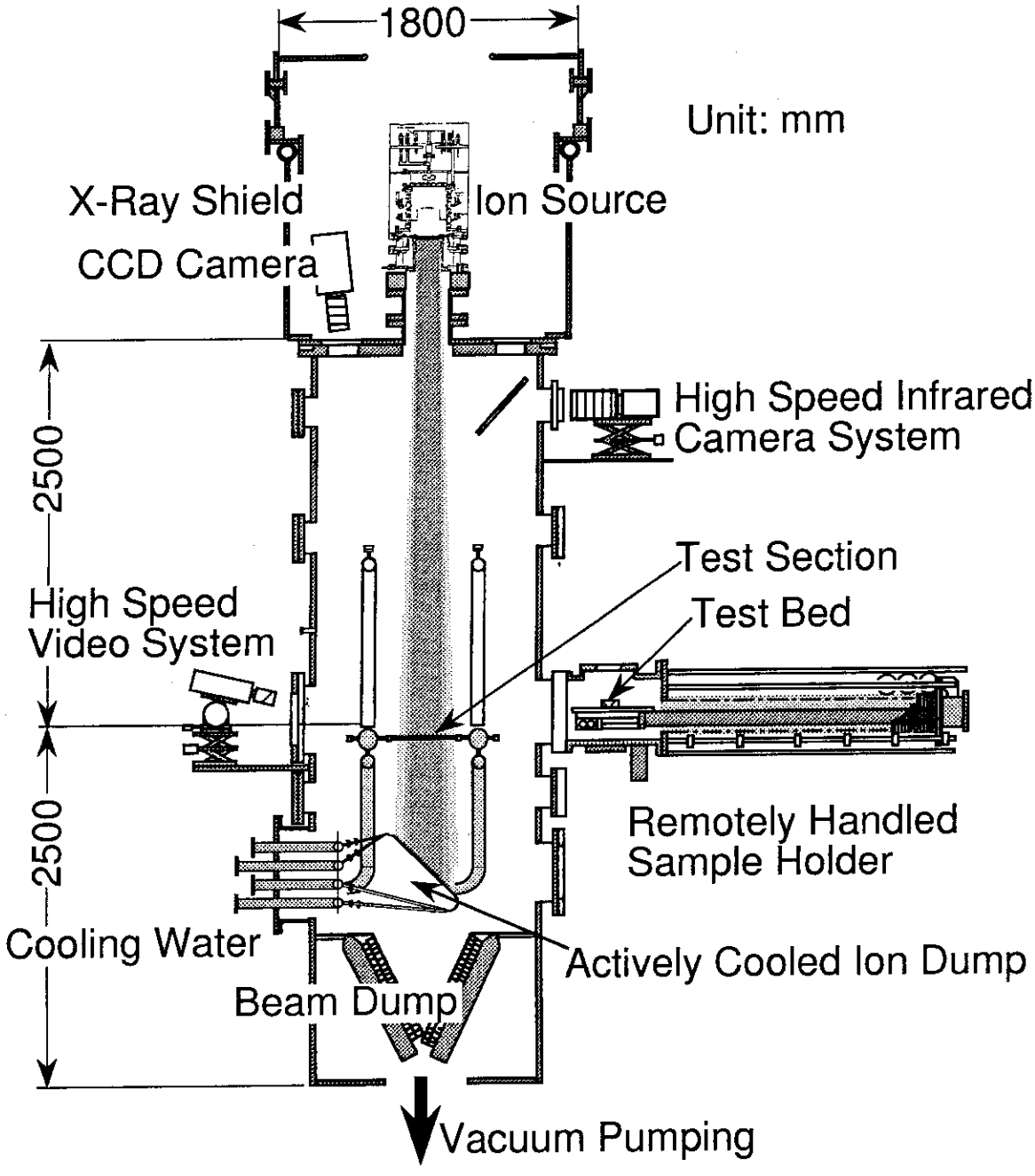

Figure2-2 Schematic of JAERI Particle Beam Engineering Facility.

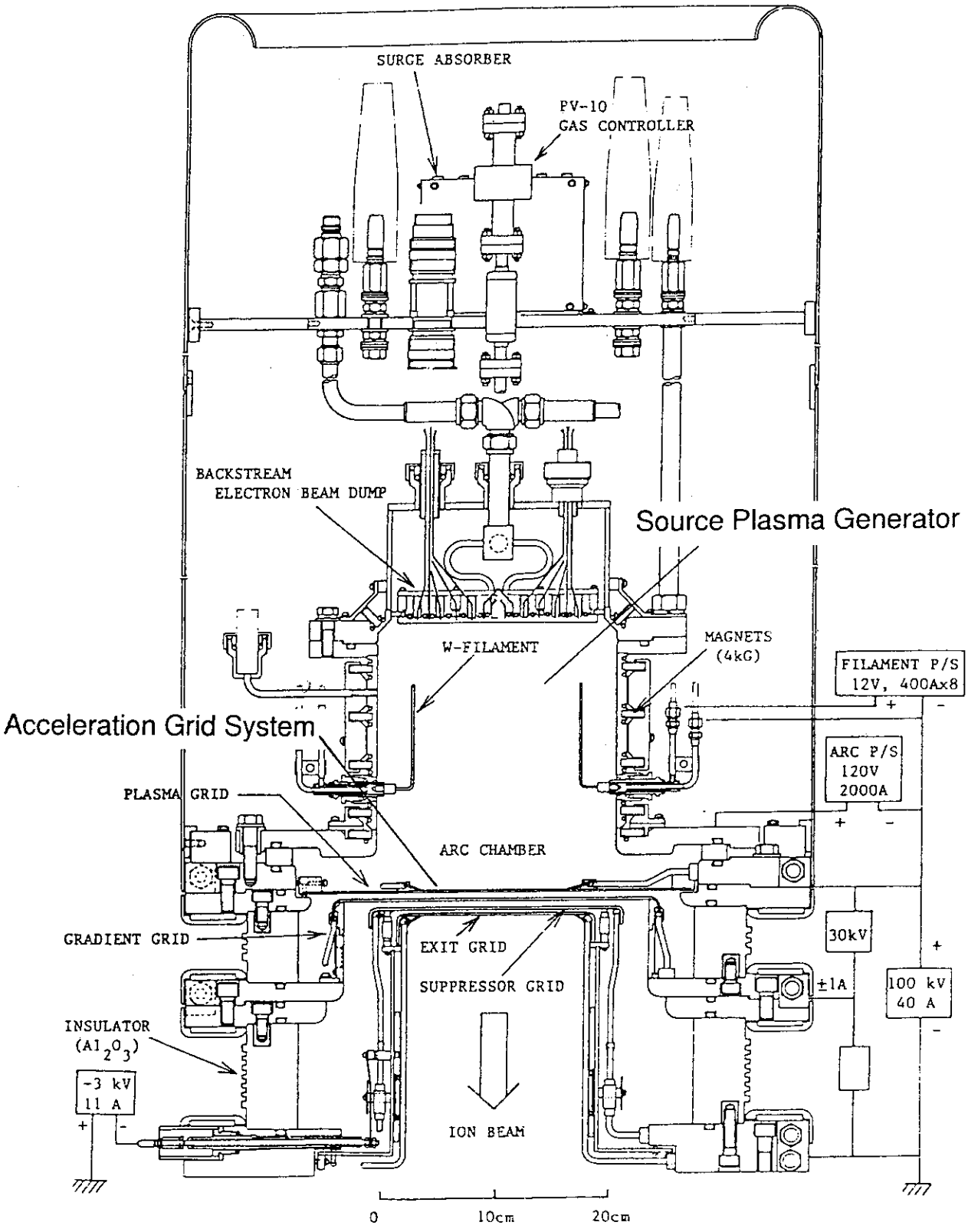

Figure2-3 Schematic of PBEF Ion Source.

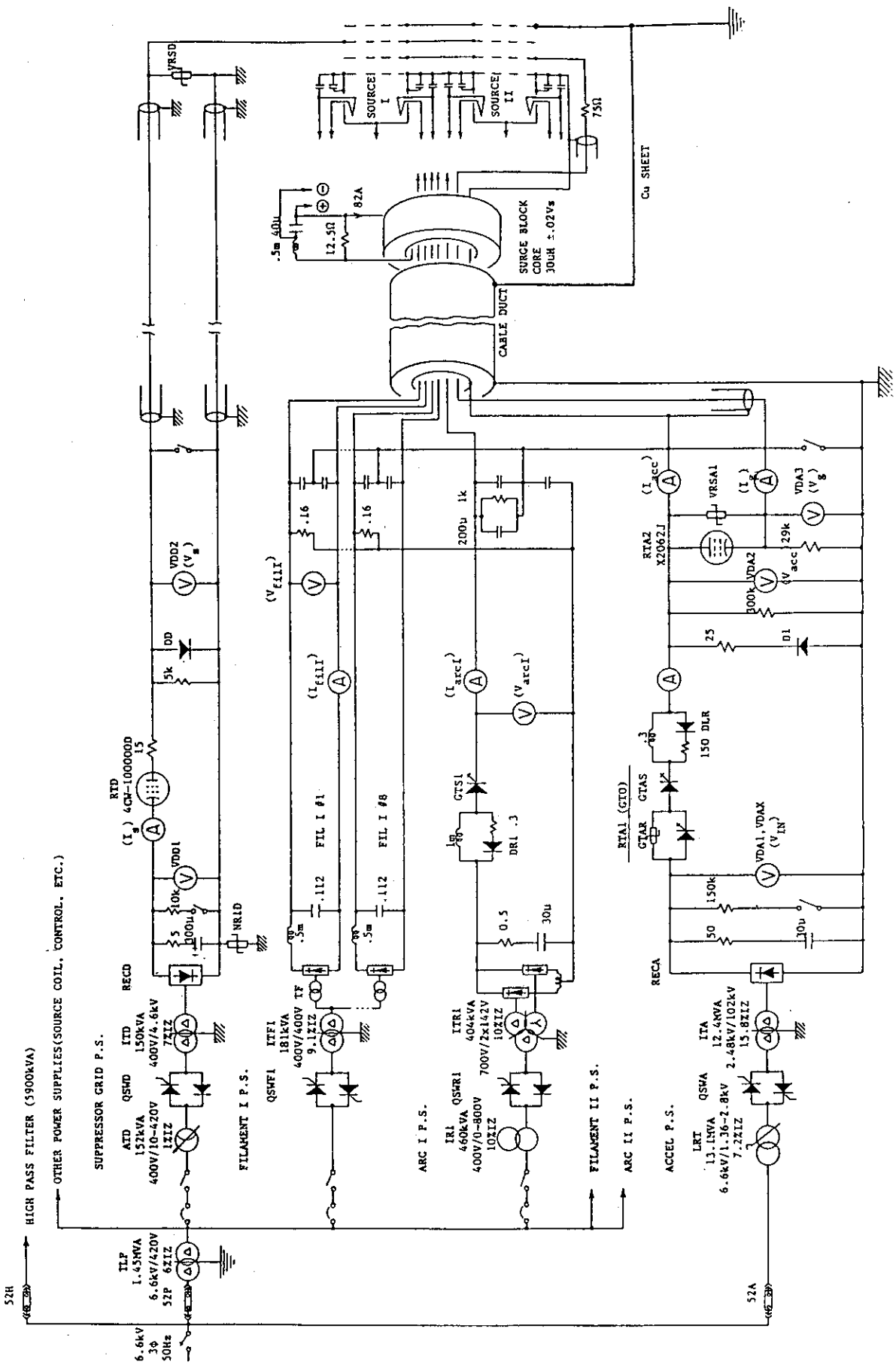

Figure2-4 A Schematic Diagram of PBEF Power Supply System.

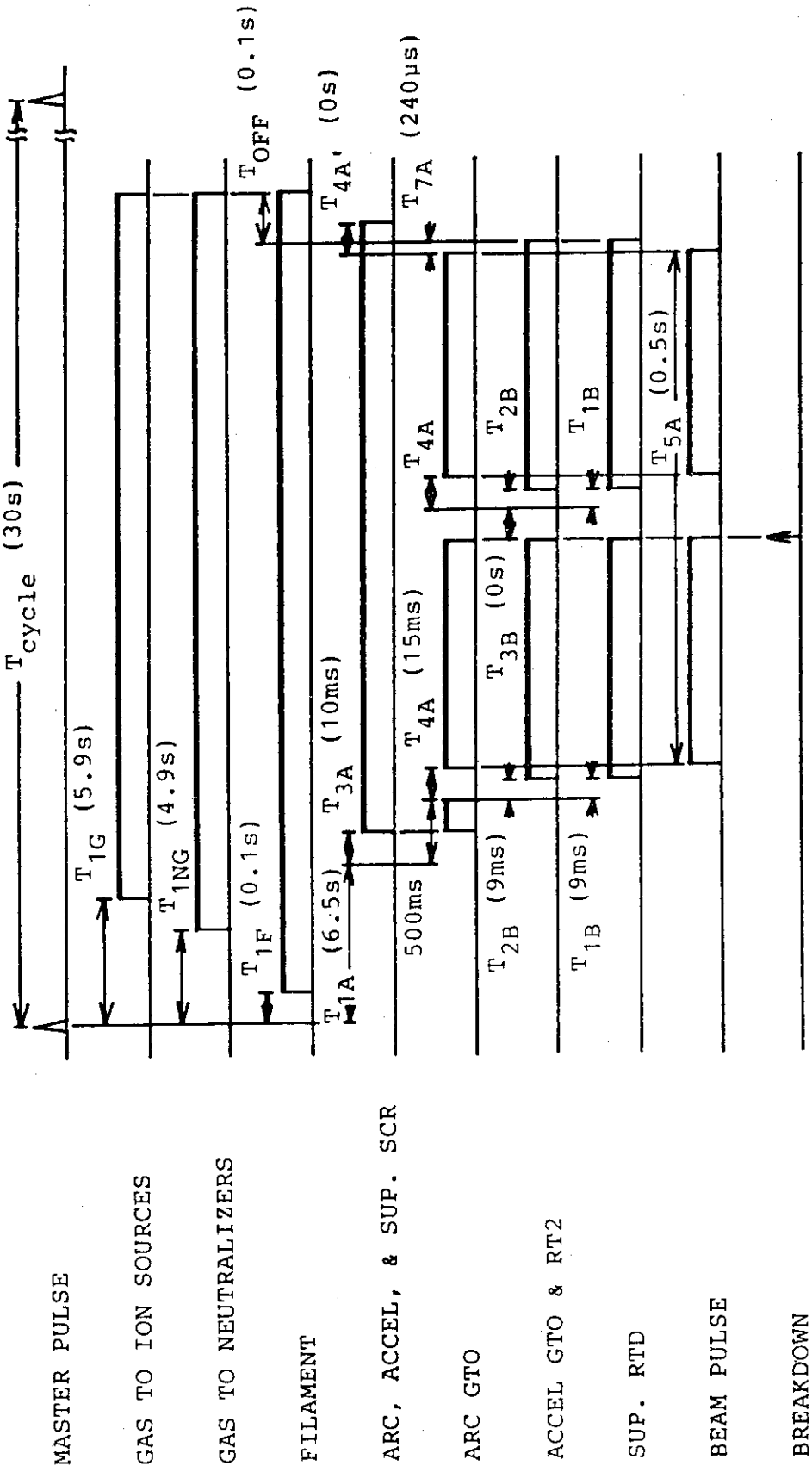

Figure2-5 A Typical Timing Chart.

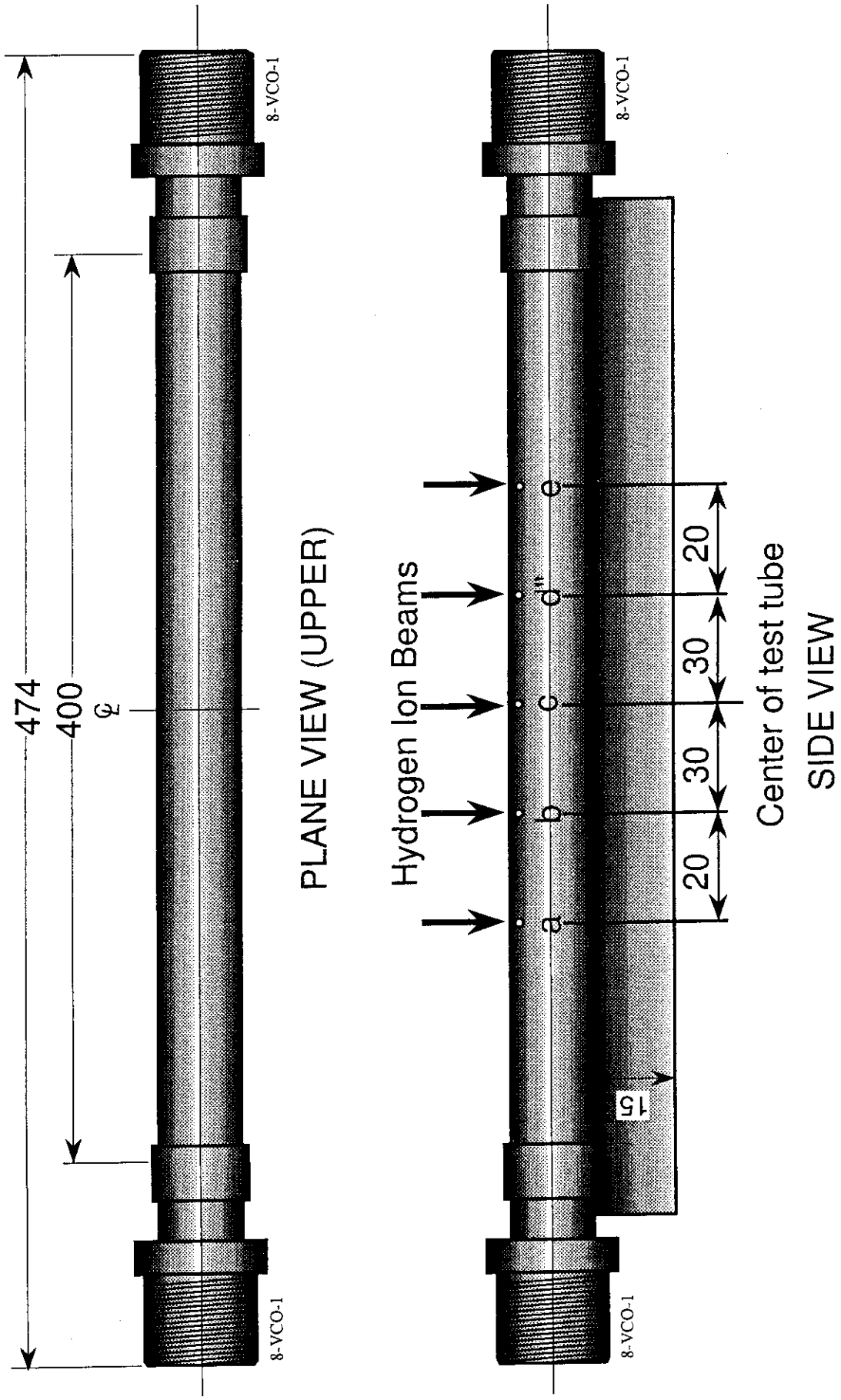

Figure3-1 Schematic of test sample for heat transter experiment.

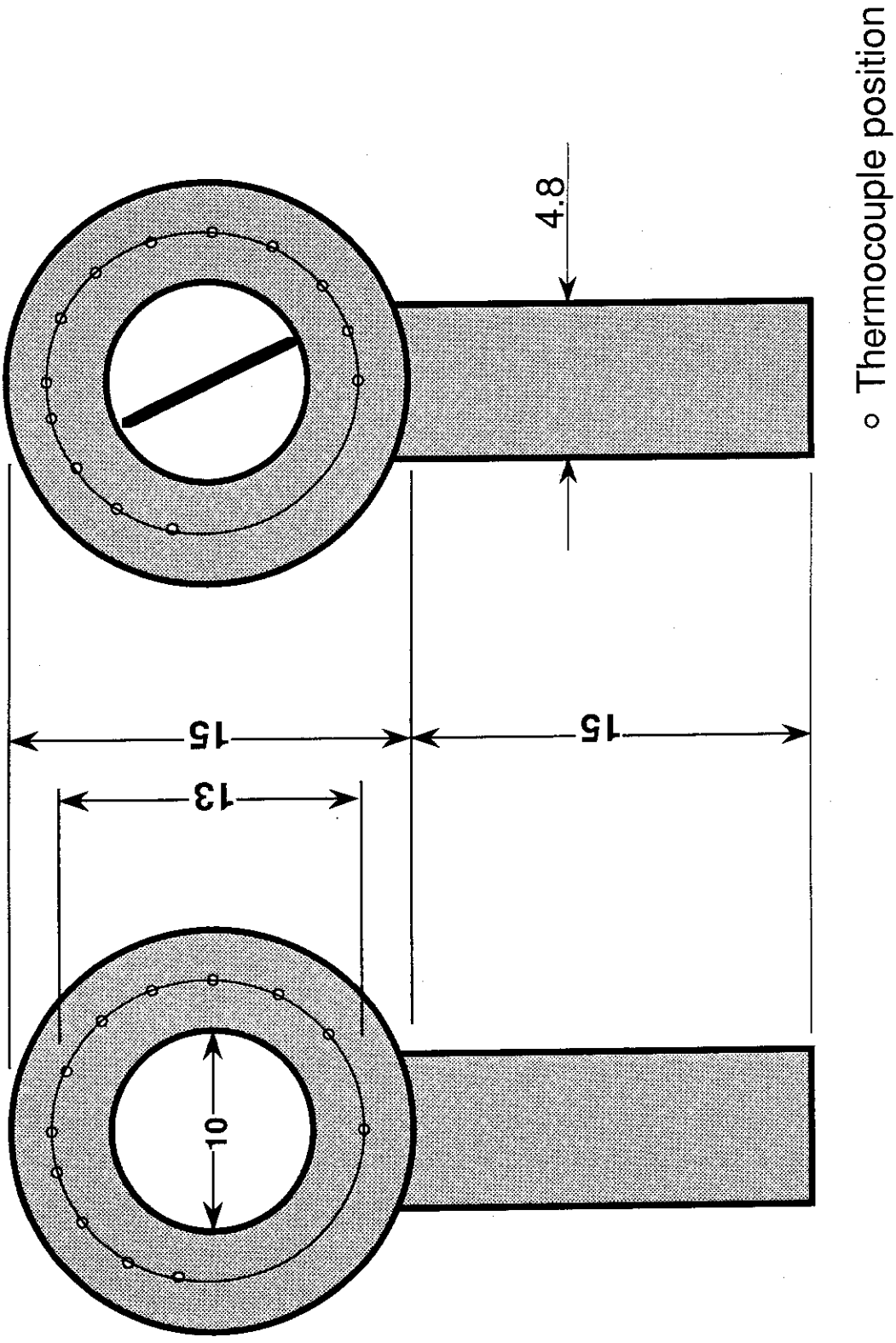

Figure3-2 Detailed crossectional view at "d" point.

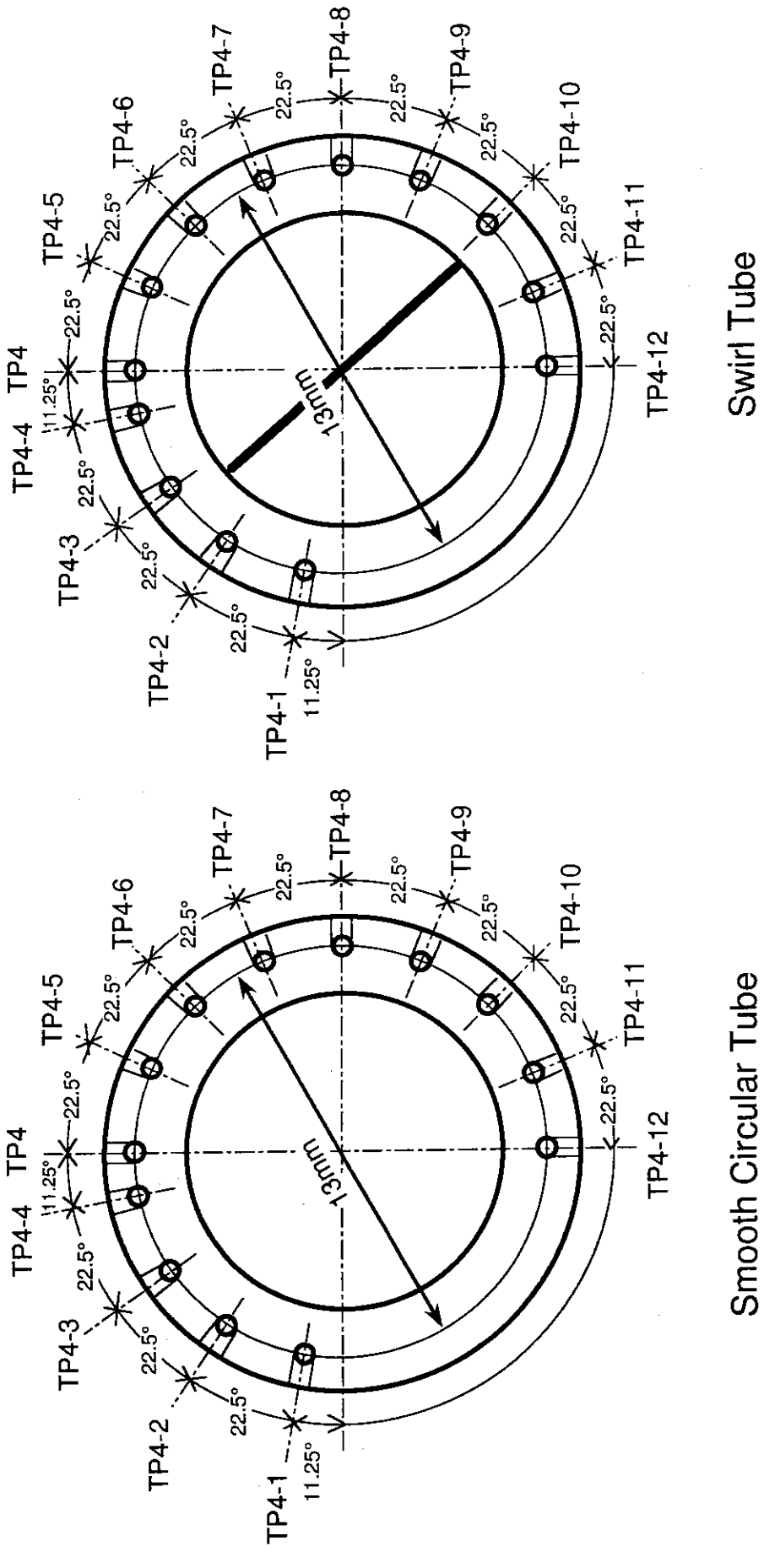

Figure3-3 Thermocouple Position along the Circumfential Direction of the Test Sample.

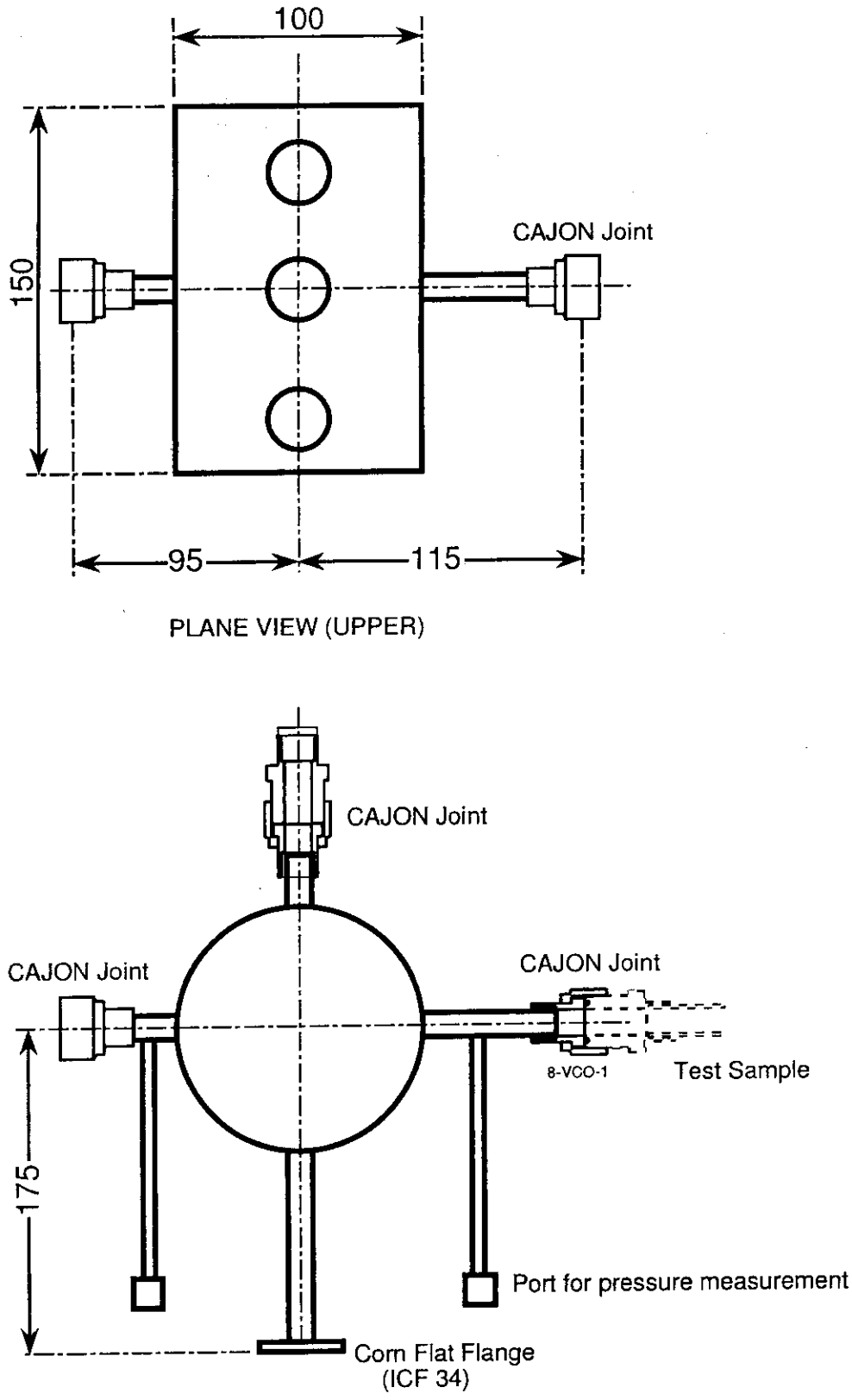

Figure3-4 Test sample manifold.

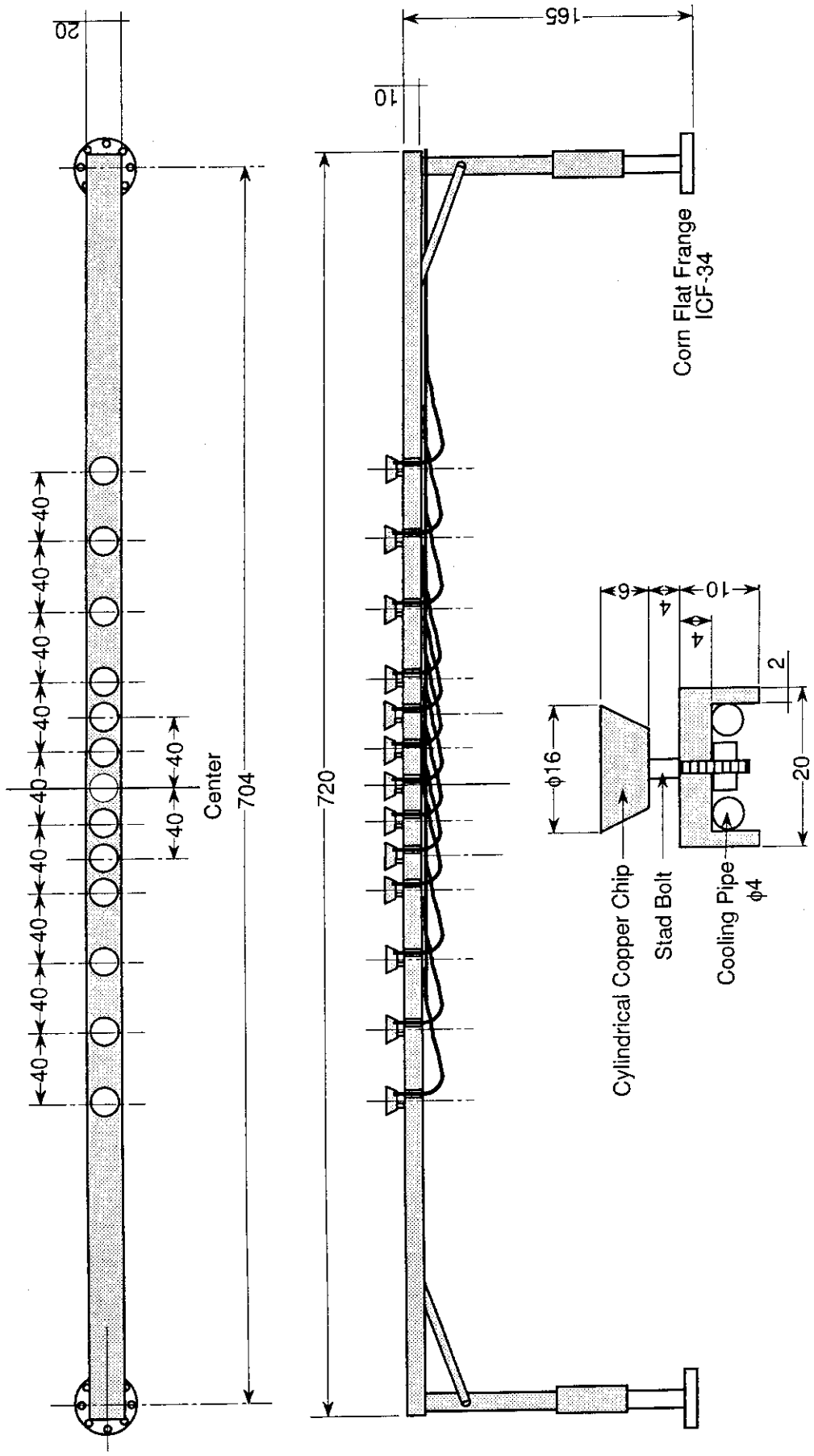

Figure3-5 Schematic of a Multi-Channel Calorimeter.

Major dimensions of each cylindrical copper chip are 2.0 cm^2 of surface area and 1.0 cm^3 of volume.

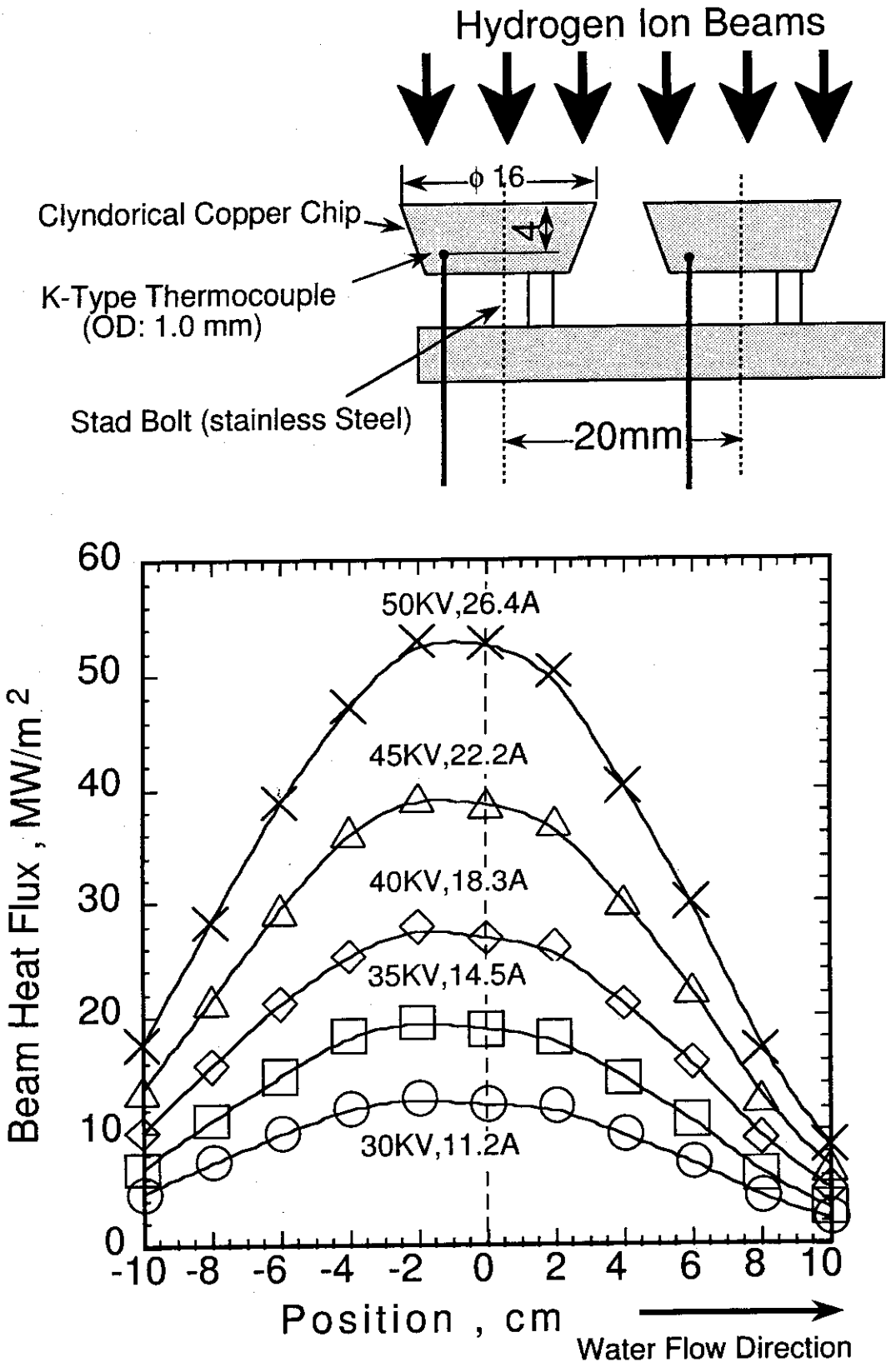

Figure3-6 Surface Heat Flux Distributions at the Test Sample Position.

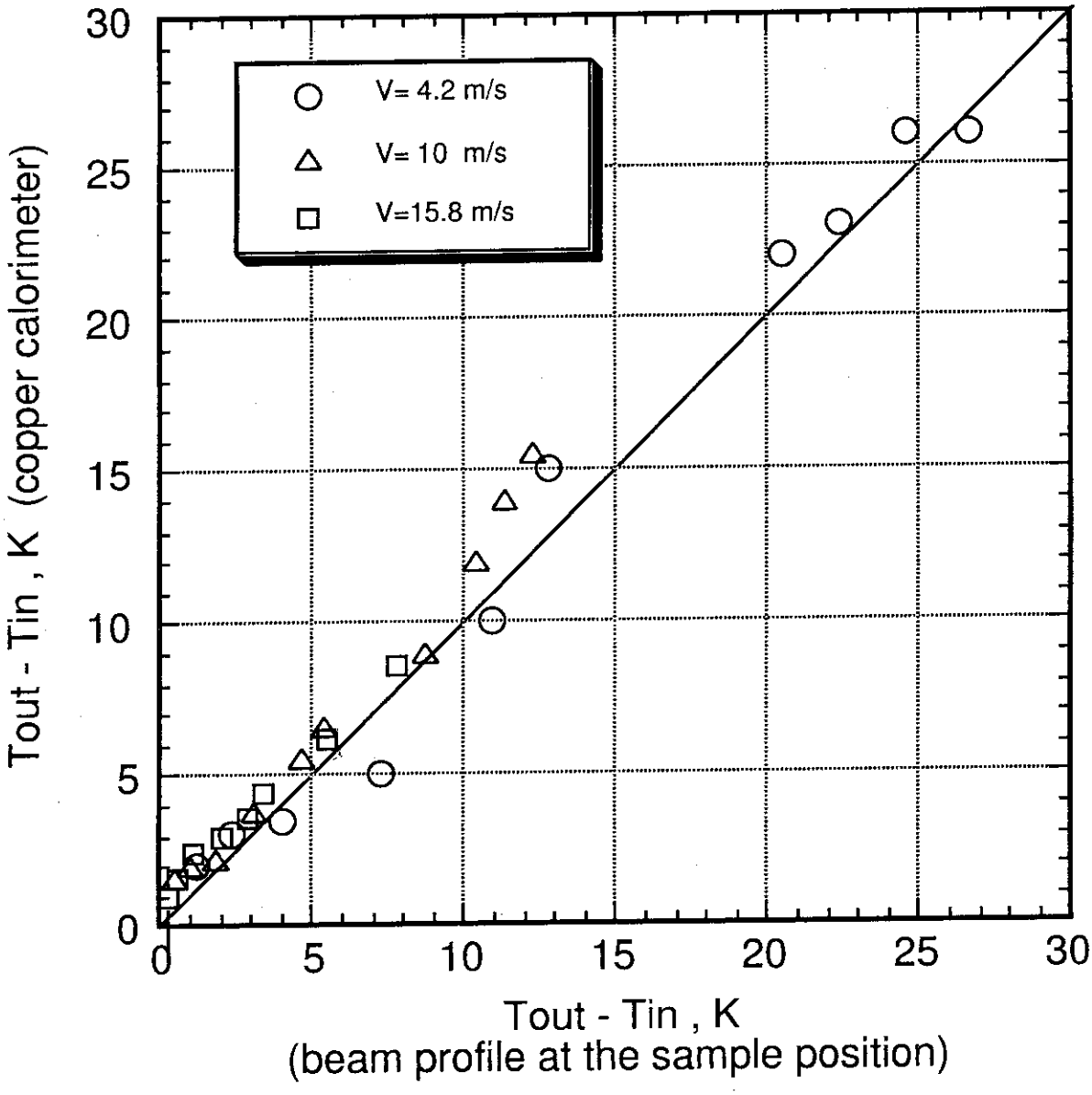

Figure3-7 Comparison of deposited power with different measurement method.

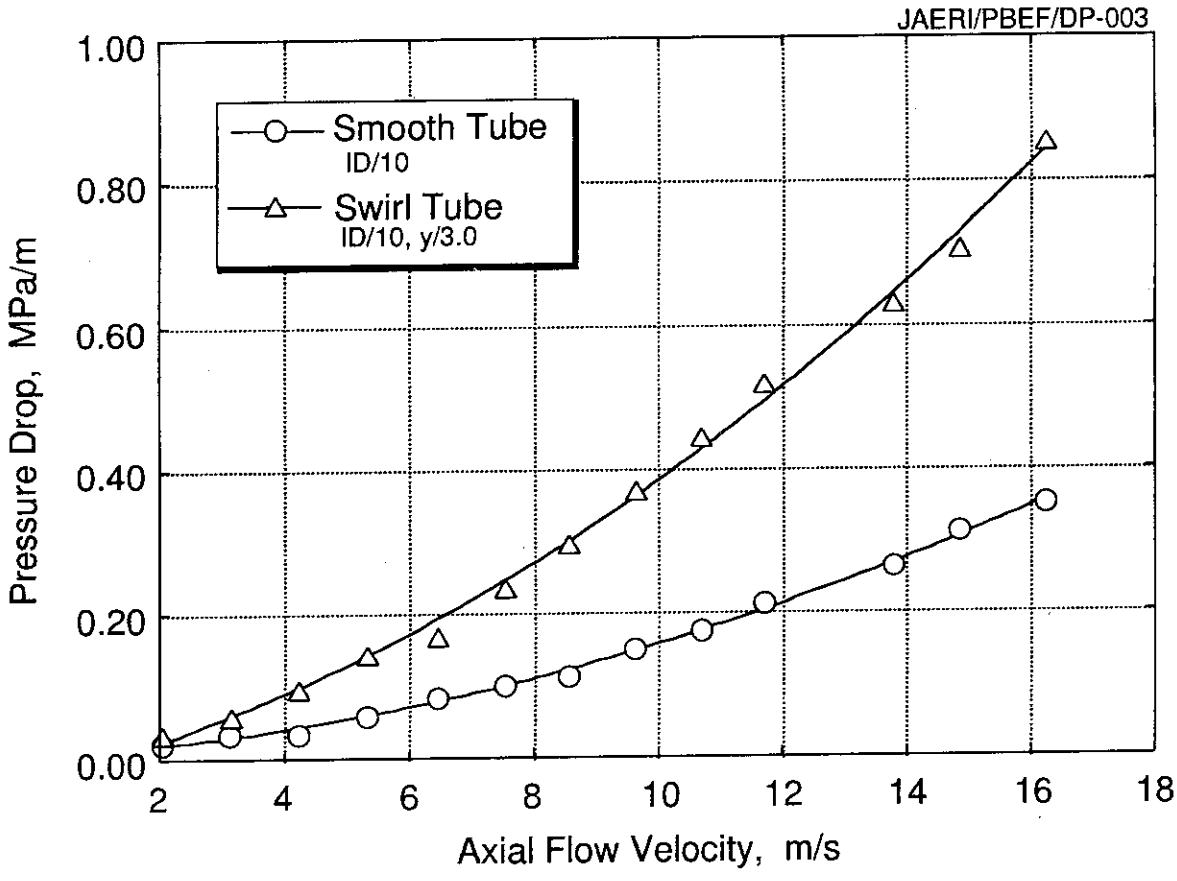

Figure4-1 Pressure Drops of Smooth and Swirl tubes.

All data were measured at temperature around 20 °C.

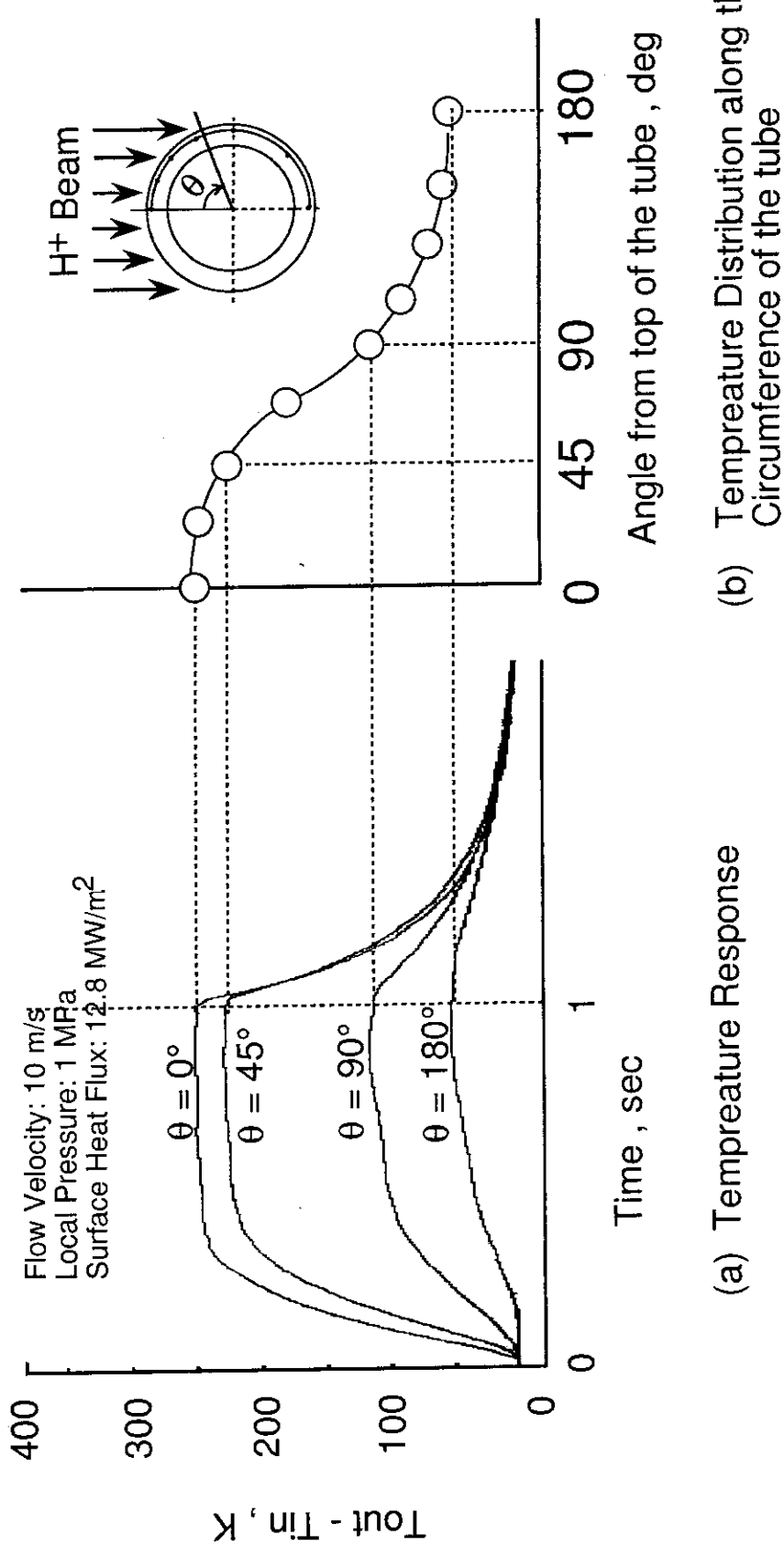

Figure4-2 Typical Temperature Responses of Thermocouples Bonded in the Test Sample.

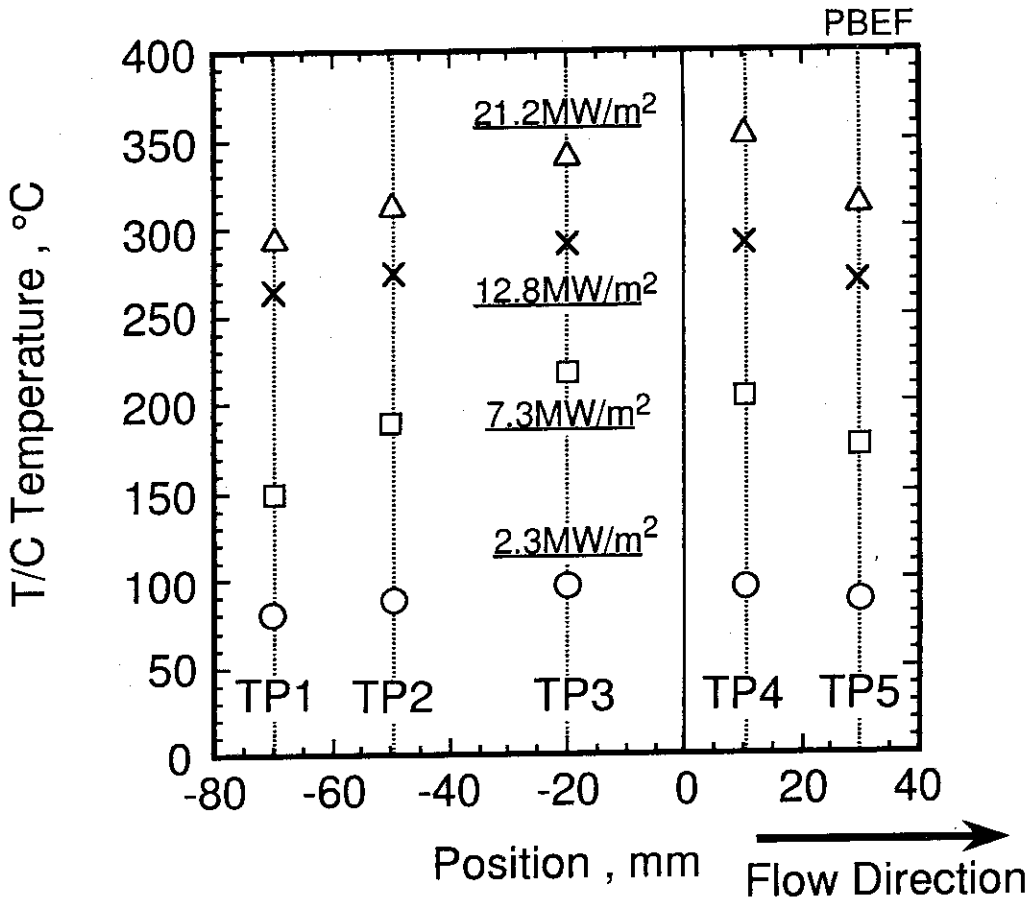

Figure4-3 Temperature Distribution in the Flow Direction.

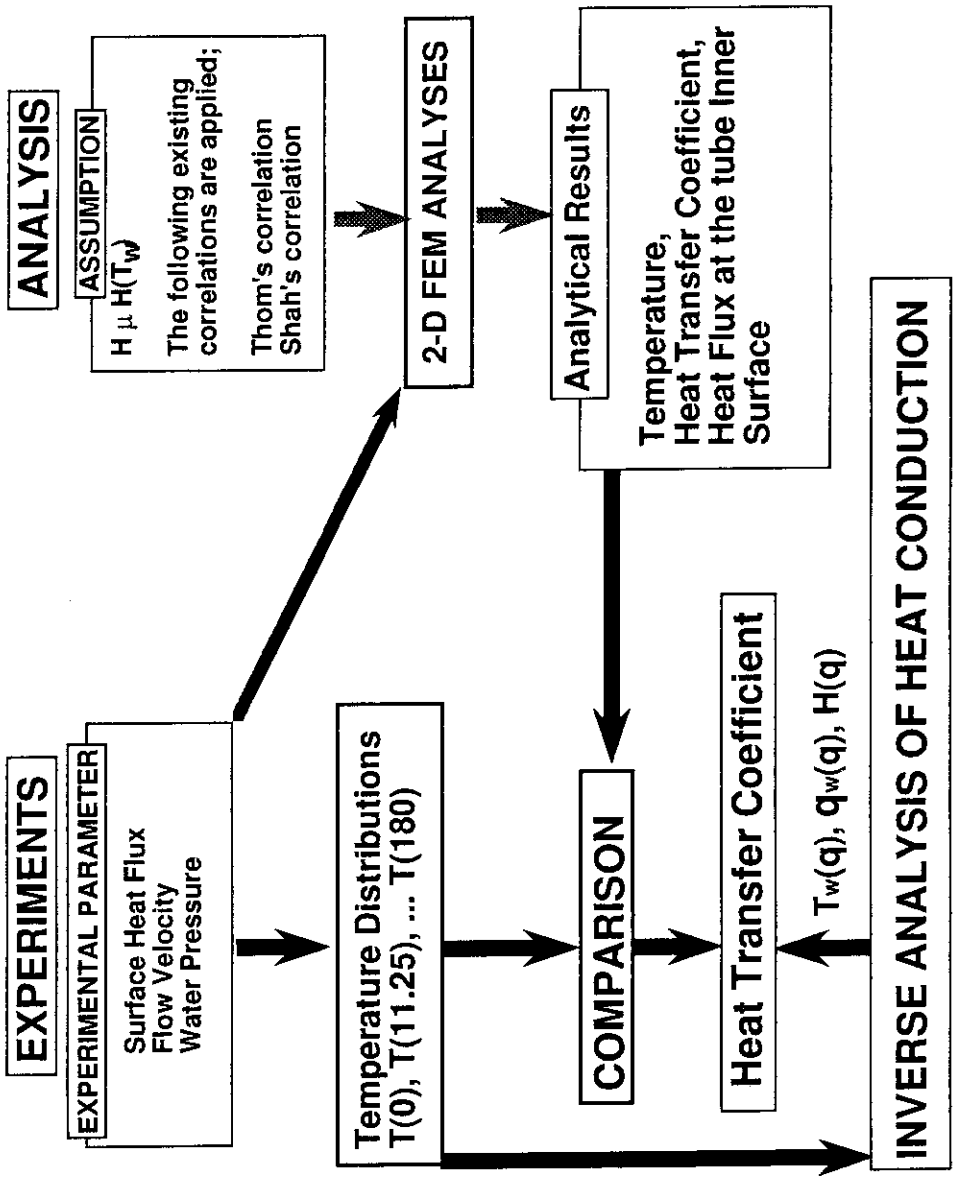

Figure5-1 Evaluation Procedure for the Prediction of Heat Transfer Coefficients.

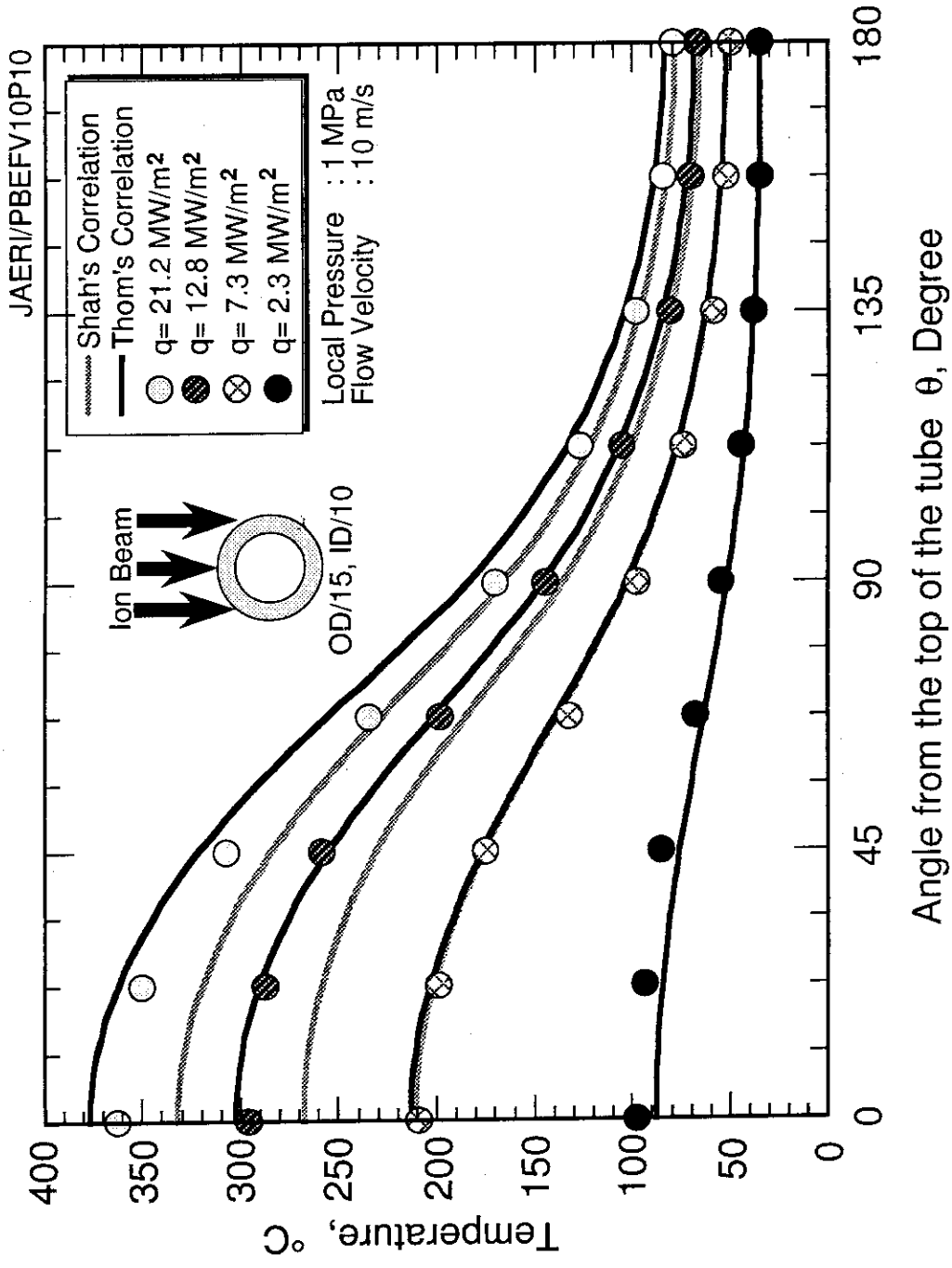

Figure5-2 Typical Temperature Distributions from Thermocouples.

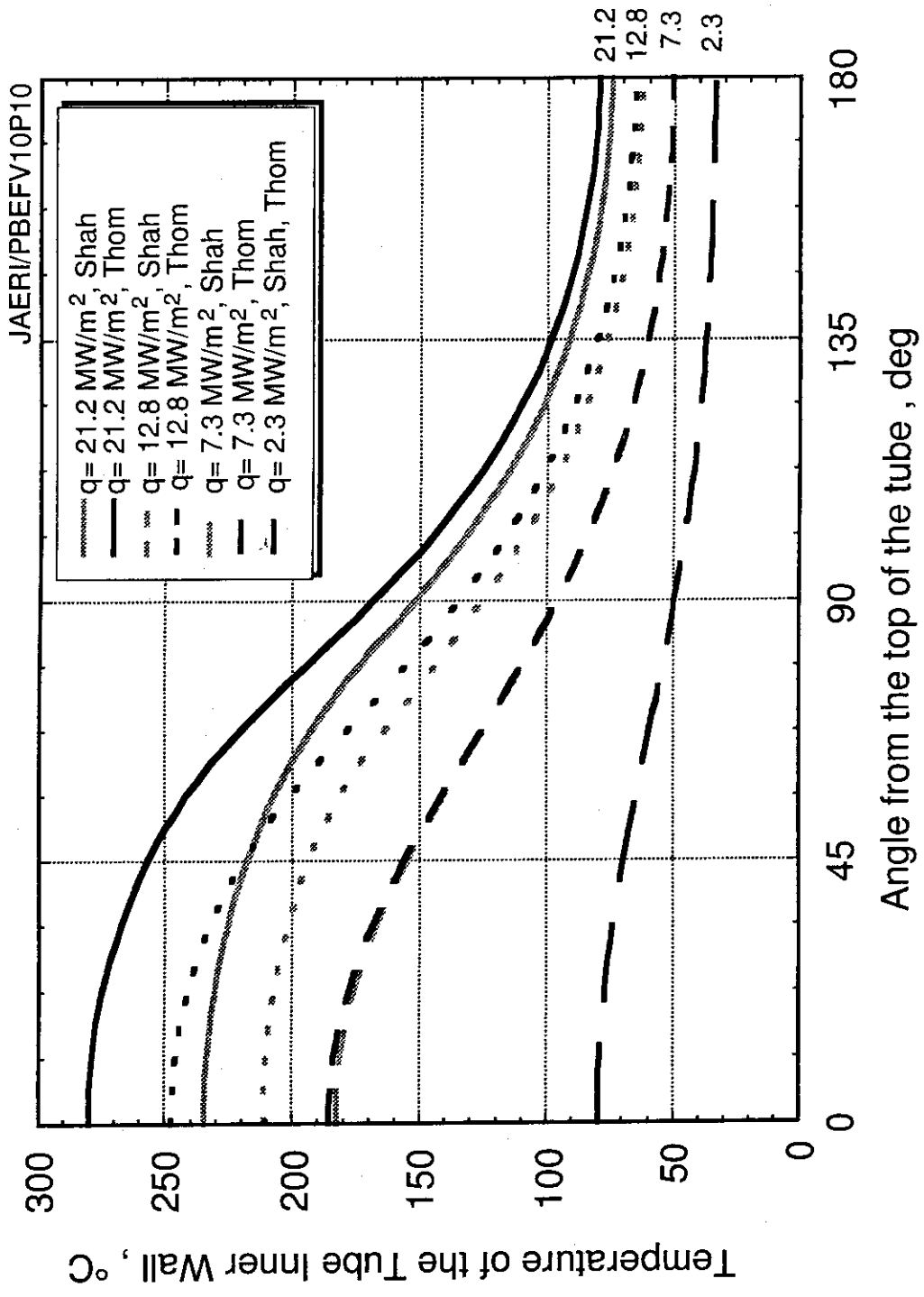

Figure5-3 Temperature Distributions of the Tube Inner Wall.

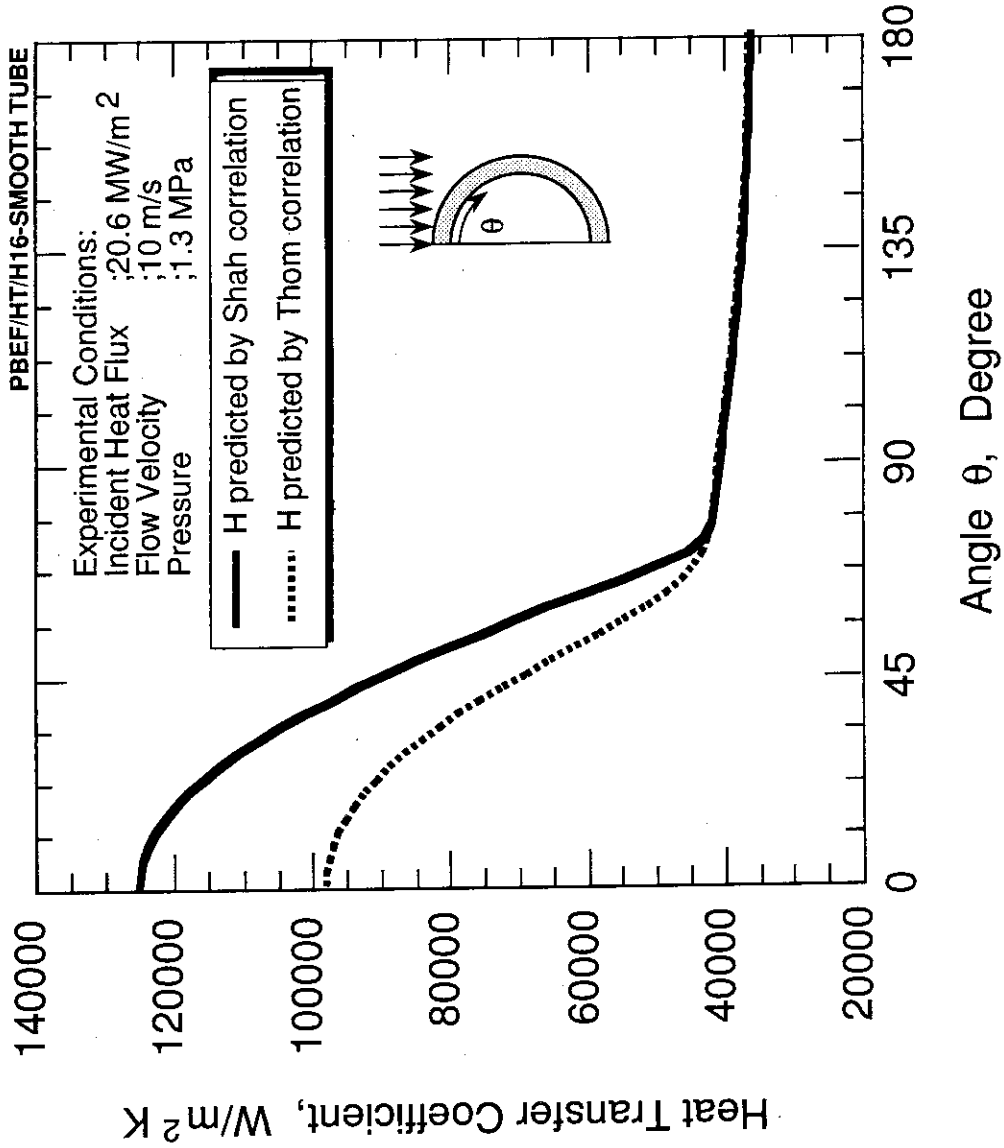

Figure5-4 Predicted Heat Transfer Coefficient Distributions at the Tube Inner Wall.

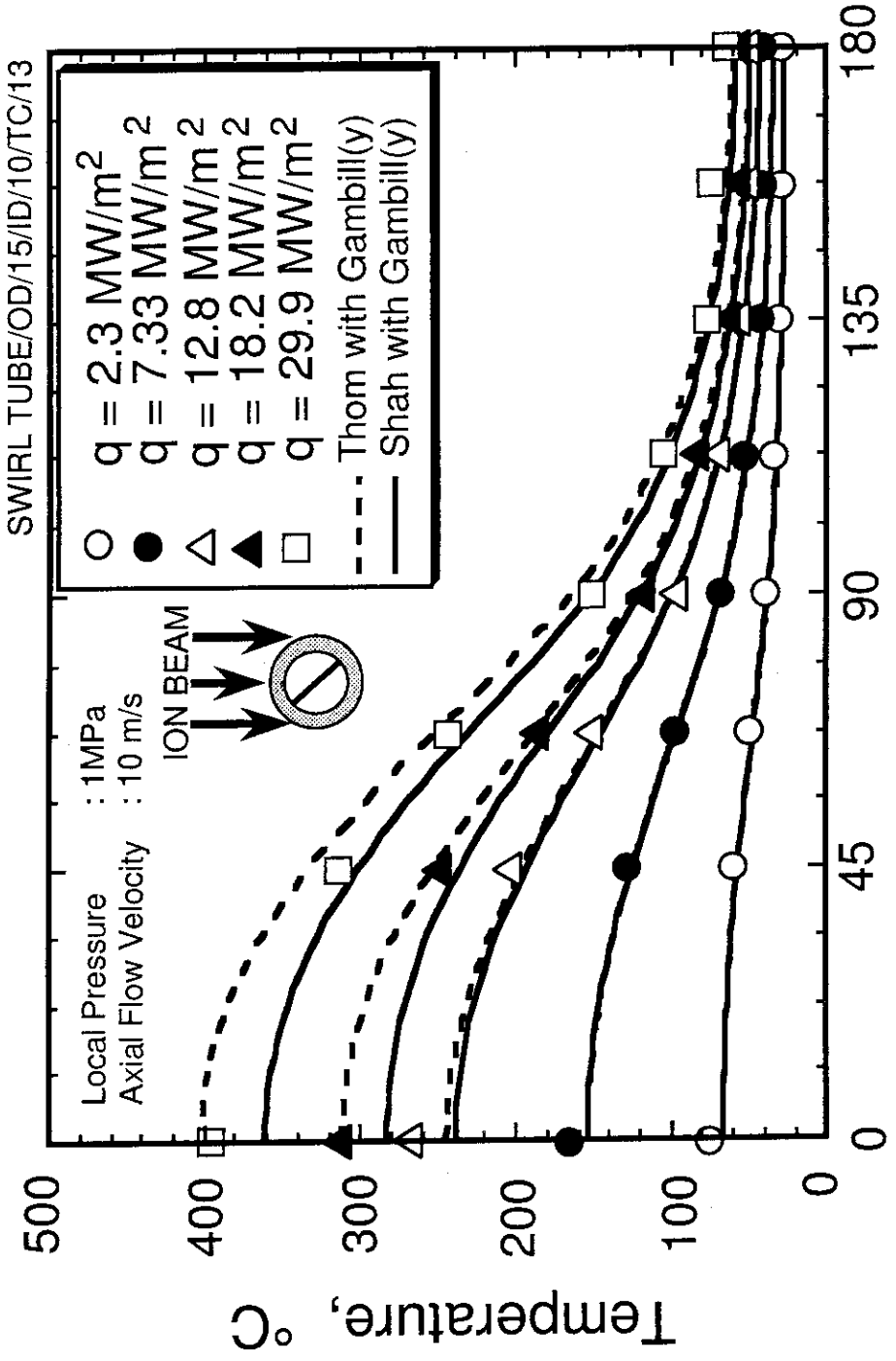

Figure5-5 Temperature Distributions of the Swirl Tube at the Thermocouple Positions.

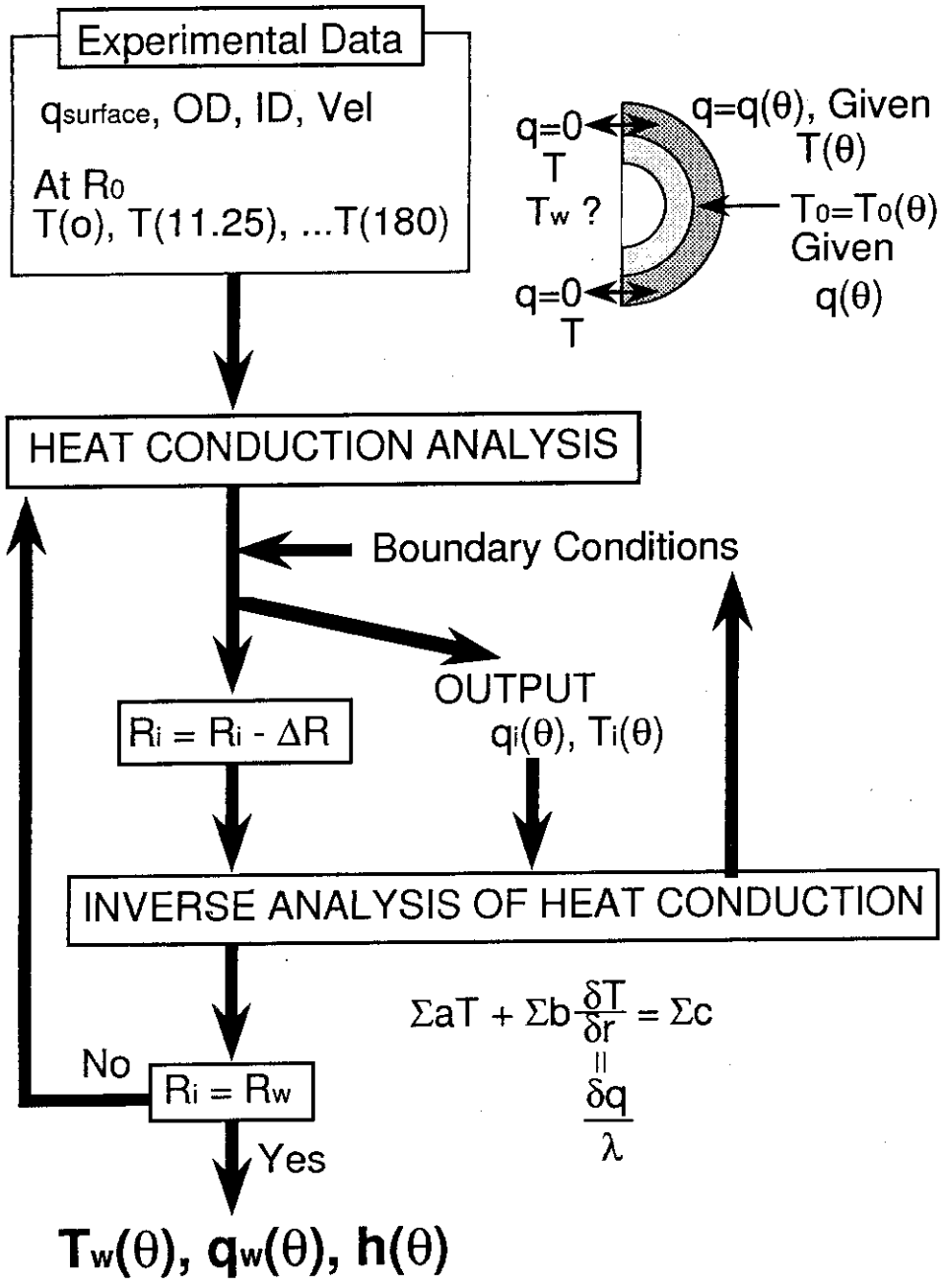

Figure5-6 Conceptual Diagram of Inverse Analysis of Heat Conduction Problems.

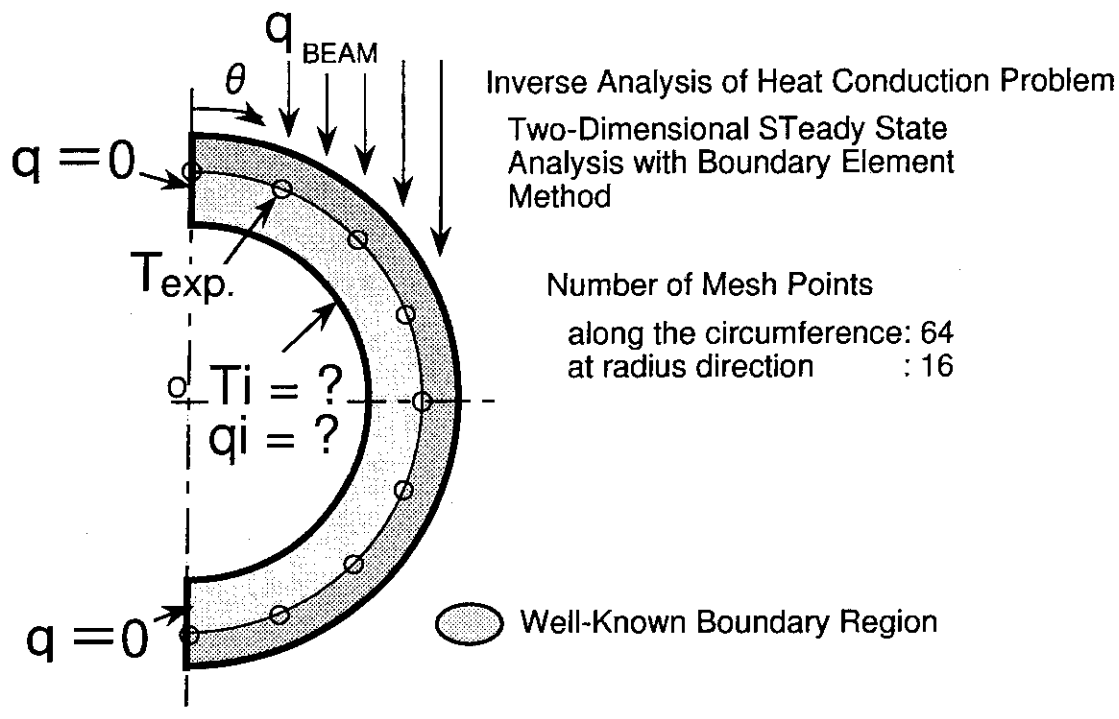

Figure5-7 Analytical Model.

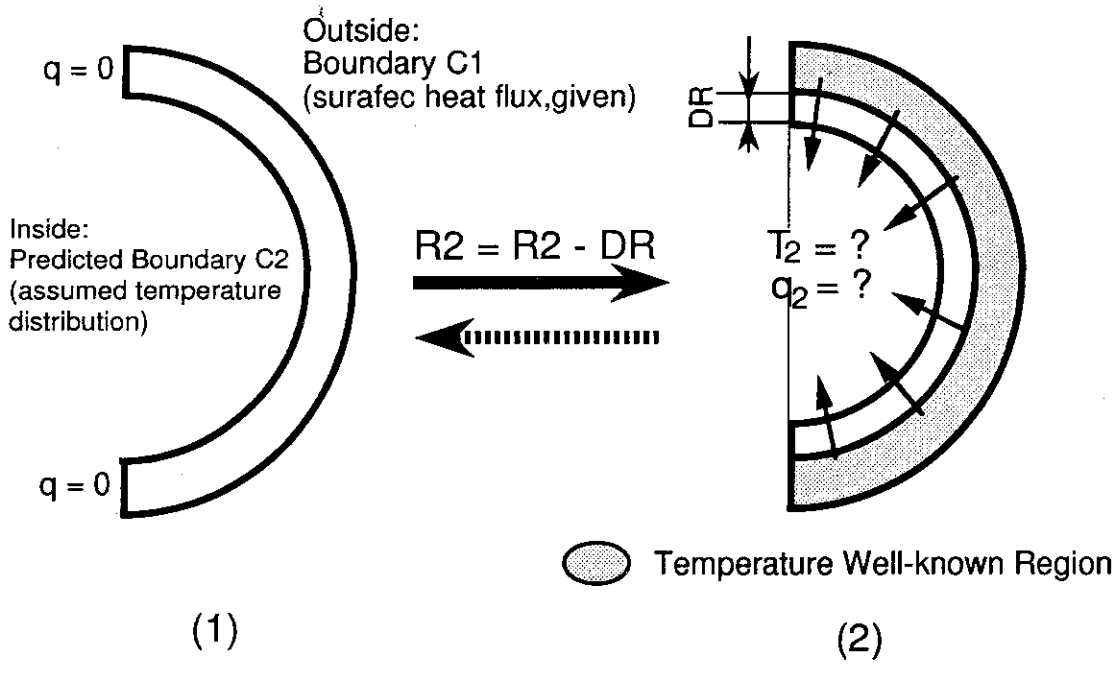

Figure5-8 Conceptual Diagram of Inverse Analysis of Heat Conduction Problems.

APPENDIX: Experimental Data

Table 4-1. Temperature data for smooth tube test sample.

Notation:

Q; flow rate, l/min
V; flow velocity, m/s
P; local pressure, MPa
Vacc; acceleration voltage, kV
Iacc; acceleration current, A
q; peak surface heat flux on the test sample, MW/m^2
T0; inlet water temperature, °C
Tbulk; local water temperature, °C
Tsat; saturation temperature at the local pressure, °C

In the table, only thermocouple channel numbers and temperatures indicate. Each channel corresponds to the position described in **Fig. 3-3**.

ITER TASK/JB-DPI-3/JAPAN

Continue (Table 4-1.)

920625

92062501	Q=65.0	V=13.8	P=1.03	Tsat=181.17			
	NO.	Vacc(kv)	Iacc(A)	q(MW/m2)	T0(°C)	Tbulk(°C)	t(sec)
1	H45	30.0	3.0	0.77	21.5	22.5	1.0
2	H46		4.8	2.04	21.5	23.5	1.0
3	H47		6.9	6.96	21.5	25.5	1.0
4	H48		11.5	12.80	20.5	26.5	1.0
5	H49	34.0	13.9	18.20	21.5	30.5	1.0
6	H50	36.0	15.3	21.20	21.0	31.0	1.0
7	H51	38.0	17.0	24.50	21.0	33.0	1.0
8	H52	39.0	17.5	26.20	22.0	36.0	0.5
92062502	Q=60.63	V=12.9	P=1.05	Tsat=182.01			
	NO.	Vacc(kv)	Iacc(A)	q(MW/m2)	T0(°C)	Tbulk(°C)	t(sec)
1	H53	30.0	3.0	0.77	22.0	23.0	1.0
2	H54		5.0	2.35	21.0	23.0	1.0
3	H55		6.0	4.40	21.0	24.0	1.0
4	H56		7.0	7.29	21.0	26.0	1.0
5	H57		11.3	12.80	22.0	30.0	1.0
6	H58	32.0	12.5	15.40	21.0	31.0	1.0
7	H59	34.0	14.4	18.20	21.0	33.0	1.0
8	H60	36.0	15.3	21.20	21.0	35.0	1.0
9	H61	37.0	16.3	22.90	22.0	38.0	1.0
10	H62	38.0	16.6	24.50	22.0	39.0	0.5
92062503	Q=55.63	V=11.81	P=1.08	Tsat=183.25			
	NO.	Vacc(kv)	Iacc(A)	q(MW/m2)	T0(°C)	Tbulk(°C)	t(sec)
1	H63	30.0	3.0	0.77	22.0	23.0	1.0
2	H64		4.8	2.04	22.0	24.0	1.0
3	H65		6.0	4.40	22.0	25.0	1.0
4	H66		7.0	7.29	22.0	27.0	1.0
5	H67		11.0	12.80	22.0	29.0	1.0
6	H68	32.0	12.5	15.40	22.0	31.0	1.0
7	H69	34.0	14.3	18.20	21.0	32.0	1.0
8	H70	36.0	15.3	21.20	20.0	33.0	1.0
9	H71	37.0	16.3	22.90	22.0	36.0	1.0
92062504	Q=47.0	V=9.97	P=1.16	Tsat=186.43			
	NO.	Vacc(kv)	Iacc(A)	q(MW/m2)	T0(°C)	Tbulk(°C)	t(sec)
1	H72	30.0	2.8	0.77	21.5	22.5	1.0
2	H73		6.0	4.40	22.0	26.0	1.0
3	H74		6.8	6.65	21.5	26.5	1.0
4	H75		11.0	12.80	22.0	31.0	1.0
5	H76		5.0	2.35	20.5	22.5	1.0
6	H77		8.9	11.00	20.5	27.5	1.0
7	H78	32.0	12.6	15.40	21.5	32.5	1.0
8	H79	34.0	14.3	18.2	20.5	32.5	1.0
9	H80	36.0	15.6	21.2	20.0	34.0	1.0
10	H81	37.0	16.2	22.9	20.0	35.0	0.5

Continue (Table 4-1.)

92062601	Q=40.6	V=8.62	P=1.14	Tsat=185.5			
	NO.	Vacc(kv)	Iacc(A)	q(MW/m2)	T0(°C)	Tbulk(°C)	t(sec)
1	H82	30.0	3.0	0.77	23.5	24.5	1.0
2	H83		5.0	2.35	22.0	24.0	1.0
3	H84		6.2	4.91	22.5	25.5	1.0
4	H85		7.0	7.29	23.5	28.5	1.0
5	H86		8.0	9.50	23.0	31.0	1.0
6	H87		11.3	12.80	23.5	32.5	1.0
7	H88	32.0	12.6	15.40	23.5	34.5	1.0
8	H89	34.0	14.3	18.20	24.0	37.0	1.0
9	H90	36.0	14.8	21.20	24.0	39.0	0.7
92062602	Q=31.0	V=6.58	P=1.18	Tsat=187.2			
	NO.	Vacc(kv)	Iacc(A)	q(MW/m2)	T0(°C)	Tbulk(°C)	t(sec)
1	H91	30.0	3.2	0.78	23.0	24.0	1.0
2	H92		5.0	2.35	23.5	25.5	1.0
3	H93		6.0	4.40	24.0	27.0	1.0
4	H94		7.0	7.29	23.5	28.5	1.0
5	H95		8.2	9.87	22.0	29.0	1.0
6	H96		11.3	12.80	22.0	31.0	1.0
7	H97	32.0	12.5	15.40	22.0	33.0	1.0
8	H98	34.0	14.0	18.20	24.0	37.0	1.0
9	H99	35.0	15.0	19.70	23.5	37.5	0.5
92062603	Q=20.25	V=4.3	P=1.19	Tsat=187.58			
	NO.	Vacc(kv)	Iacc(A)	q(MW/m2)	T0(°C)	Tbulk(°C)	t(sec)
1	I00	30.0	3.1	0.77	22.0	23.0	1.0
2	I01		5.3	2.87	22.0	24.0	1.0
3	I02		6.0	4.40	23.5	26.5	1.0
4	I03		7.0	7.29	23.5	28.5	1.0
5	I04		11.0	12.75	22.0	29.0	1.0
6	I05	32.0	12.6	15.40	22.5	31.5	1.0
7	I06	33.0	13.0	16.70	23.5	33.5	0.8
92062604	Q=55.38	V=11.76	P=0.8	Tsat=170.41			
	NO.	Vacc(kv)	Iacc(A)	q(MW/m2)	T0(°C)	Tbulk(°C)	t(sec)
1	I07	30.0	3.0	0.77	22.5	23.5	1.0
2	I08		5.0	2.35	22.5	24.5	1.0
3	I09		7.0	7.29	22.5	25.5	1.0
4	I10		6.2	4.91	22.5	27.5	1.0
5	I11		7.9	9.31	22.5	29.5	1.0
6	I12		9.2	11.40	22.5	31.5	1.0
7	I13		11.2	12.80	21.5	32.5	1.0
8	I14	32.0	12.6	15.4	21.0	33.0	1.0
9	I15	34.0	13.7	18.2	21.5	34.5	1.0
10	I16	36.0	15.3	21.2	22.0	36.0	1.0
11	I17	37.0	16.1	22.9	20.5	35.5	0.98(1.0)
92062605	Q=47.5	V=10.08	P1=11.25	P2=5.8	P=8.525	Tsat=172.25	
	NO.	Vacc(kv)	Iacc(A)	q(MW/m2)	T0(°C)	Tbulk(°C)	t(sec)
1	I18	30.0	3.0	0.78	22.0	23.0	1.0
2	I19		5.0	2.35	21.5	23.5	1.0
3	I20		6.0	4.40	22.0	24.0	1.0
4	I21		7.1	7.29	20.5	25.5	1.0
5	I22		9.2	11.40	21.0	28.0	1.0
6	I23		11.0	12.80	22.0	31.0	1.0
7	I24	32.0	12.5	15.40	21.5	32.5	1.0
8	I25	34.0	13.8	18.20	22.0	35.0	1.0
9	I26	35.0	14.6	19.70	22.0	36.0	1.0
10	I27	36.0	15.0	21.2	21.5	36.5	0.5

ITER TASK/JB-DPI-3/JAPAN

Continue (Table 4-1.)

92062901	Q=41.25	V=8.75	P=0.851	Tsat=172.94			
	NO.	Vacc(kv)	Iacc(A)	q(MW/m2)	T0(°C)	Tbulk(°C)	t(sec)
1	I28	30.0	3.0	0.77	25.0	26.0	1.0
2	H01		5.0	2.35	25.0	27.0	1.0
3	H02		7.0	7.29	24.5	30.5	1.0
4	H03		6.0	4.40	24.0	28.0	1.0
5	H04		8.0	9.50	24.0	32.0	1.0
6	H05		11.3	12.80	24.0	34.0	1.0
7	H06	32.0	12.8	15.40	24.0	36.5	1.0
8	H07	34.0	14.2	16.70	24.5	36.7	1.0
9	H08	35.0	14.7	19.70	24.7	39.0	1.0
10	H09	36.0	14.8	21.20	26.0	37.7	0.62(1.0)
92062902	Q=32.13	V=6.82	P=0.898	Tsat=175.21			
	NO.	Vacc(kv)	Iacc(A)	q(MW/m2)	T0(°C)	Tbulk(°C)	t(sec)
1	H10	30.0	2.9	0.77	25.2	26.2	1.0
2	H11		5.0	2.35	25.0	27.0	1.0
3	H12		6.0	4.40	25.0	28.0	1.0
4	H13		7.0	7.29	25.5	30.5	1.0
5	H14		10.9	12.72	26.0	33.0	1.0
6	H15	32.0	12.2	15.40	26.0	35.0	1.0
7	H16	33.0	13.2	16.70	26.0	37.0	1.0
8	H17	34.0	13.8	18.20	25.0	38.0	1.0
92062903	Q=20.38	V=4.32	P=0.912	Tsat=175.92			
	NO.	Vacc(kv)	Iacc(A)	q(MW/m2)	T0(°C)	Tbulk(°C)	t(sec)
1	H18	30.0	3.0	0.77	26.0	27.0	1.0
2	H19		5.2	2.69	25.5	29.5	1.0
3	H20		4.0	1.14	25.5	27.5	1.0
4	H21		6.0	4.40	25.5	31.5	1.0
5	H22		7.0	7.29	25.0	33.0	1.0
6	H23		11.3	12.80	25.5	35.5	1.0
7	H24	32.0	12.3	15.40	26.0	38.0	1.0
8	H25	33.0	13.3	16.70	25.5	39.5	0.8

920630

92063001	Q=41.6	V=8.83	P=0.345	Tsat=138.37			
	NO.	Vacc(kv)	Iacc(A)	q(MW/m2)	T0(°C)	Tbulk(°C)	t(sec)
1	H26	30.0	11.4	12.80	22.5	30.5	1.0
2	H27		3.0	0.77	24.0	25.0	1.0
3	H28		5.0	2.35	22.5	24.5	1.0
4	H29		6.0	4.40	22.5	26.5	1.0
5	H30		7.0	7.29	24.0	30.0	1.0
6	H31	32.0	12.4	15.40	23.0	33.0	1.0
7	H32	34.0	13.7	18.20	24.0	36.0	1.0
8	H33	36.0	15.5	21.20	22.0	36.0	0.8
9	H34	36.0	14.8	21.20	23.0	37.0	1.0
92063004	Q=19.5	V=4.14	P=0.192	Tsat=190.28			
	NO.	Vacc(kv)	Iacc(A)	q(MW/m2)	T0(°C)	Tbulk(°C)	t(sec)
1	H48	30.0	3.0	0.77	22.0	23.0	1.0
2	H49		5.1	2.51	21.0	23.0	1.0
3	H50		6.1	4.65	22.0	26.0	1.0
4	H51		7.0	7.29	22.0	28.0	1.0
5	H52		11.4	12.80	22.0	30.0	1.0
6	H53	31.0	11.8	14.00	22.0	31.0	1.0
7	H54	32.0	12.6	15.40	21.0	31.0	1.0
8	H55	33.0	13.4	16.70	22.0	33.0	1.0

ITER TASK/JB-DPI-3/JAPAN

Continue (Table 4-1.)

920702

92070201	Q=30.34	V=6.44	P=1.386	Tsat=194.57			
	NO.	Vacc(kv)	Iacc(A)	q(MW/m2)	T0(°C)	Tbulk(°C)	t(sec)
1	H01	30.0	3.0	0.77	23.5	24.0	1.0
2	H02		5.2	2.69	23.2	25.2	1.0
3	H03		4.0	1.14	24.3	25.3	1.0
4	H04		6.1	4.65	23.5	26.5	1.0
5	H05		6.8	6.65	23.5	27.0	1.0
6	H06		11.0	12.75	23.0	29.0	1.0
7	H07	32.0	12.6	15.40	23.0	31.0	1.0
8	H08	33.0	13.5	16.70	23.9	33.9	1.0
9	H09	34.0	14.2	18.20	24.0	35.0	0.80
92070202	Q=19.5	V=4.14	P=1.41	Tsat=195.37			
	NO.	Vacc(kv)	Iacc(A)	q(MW/m2)	T0(°C)	Tbulk(°C)	t(sec)
1	H10	30.0	3.0	0.77	23.5	24.0	1.0
2	H11		4.5	1.64	23.5	24.5	1.0
3	H12		5.0	2.35	25.0	27.0	1.0
4	H13		6.3	5.18	23.5	26.5	1.0
5	H14		7.1	7.55	24.0	29.0	1.0
6	H15		11.0	12.75	23.3	31.3	1.0
7	H16		9.3	11.53	24.2	32.2	1.0
8	H17	31.0	12.0	14.00	25.0	33.0	1.0
9	H18	32.0	12.3	15.40	25.0	35.0	0.98(1.0)
92070203	Q=60.36	V=12.82	P1=1.263	Tsat=190.28			
	NO.	Vacc(kv)	Iacc(A)	q(MW/m2)	T0(°C)	Tbulk(°C)	t(sec)
1	H19	30.0	3.0	0.77	23.5	24.0	1.0
2	H20		5.0	2.35	24.0	25.0	1.0
3	H21		7.1	7.55	23.5	27.5	1.0
4	H22		6.2	4.91	23.5	25.5	1.0
5	H23		11.5	12.80	23.5	26.5	1.0
6	H24	31.0	12.0	14.00	24.0	30.0	1.0
7	H25	32.0	12.3	15.40	24.0	32.0	1.0
8	H26	34.0	13.5	18.20	23.5	33.5	1.0
9	H27	36.0	15.0	21.20	24.3	36.3	1.0
10	H28	38.0	16.5	24.50	23.5	37.5	0.6(0.8)
11	H29	37.0	16.5	22.90	25.0	38.0	0.8

ITER TASK/JB-DPI-3/JAPAN

Continue (Table 4-1.)

920703

92070301	Q=59.88	V=12.71	P=0.75	Tsat=167.92			
	NO.	Vacc(kv)	Iacc(A)	q(MW/m2)	T0(°C)	Tbulk(°C)	t(sec)
1	H30	30.0	3.0	0.77	24.0	25.0	1.0
2	H31		5.0	2.33	24.0	26.0	1.0
3	H32		7.0	7.29	24.2	28.2	1.0
4	H33		5.8	3.92	25.5	28.5	1.0
5	H34		10.8	12.69	25.6	31.6	1.0
6	H35	32.0	12.3	15.40	25.9	32.9	1.0
7	H36	34.0	14.1	18.20	24.2	32.2	1.0
8	H37	36.0	15.0	21.20	25.3	35.5	1.0
9	H38	37.0	15.6	22.90	25.0	37.0	0.75(1.0)
92070304	Q=30.5	V=6.48	P=0.381	Tsat=141.88			
	NO.	Vacc(kv)	Iacc(A)	q(MW/m2)	T0(°C)	Tbulk(°C)	t(sec)
1	H48	30.0	3.0	0.77	24.5	25.5	1.0
2	H49		5.0	2.33	25.3	27.3	1.0
3	H50		6.0	4.40	26.2	29.2	1.0
4	H51		7.1	7.63	25.0	29.0	1.0
5	H52		9.0	11.14	25.8	31.8	1.0
6	H53		11.0	12.75	25.2	33.2	1.0
7	H54	32.0	12.3	15.40	25.2	35.2	1.0
8	H55	34.0	13.8	18.20	26.2	37.2	1.0
9	H56	33.0	12.9	16.70	26.2	38.2	1.0
92070305	Q=19.75	V=4.19	P=0.4	Tsat=144.78			
	NO.	Vacc(kv)	Iacc(A)	q(MW/m2)	T0(°C)	Tbulk(°C)	t(sec)
1	H57	30.0	3.0	0.77	24.3	25.3	1.0
2	H58		5.0	2.33	25.0	27.0	1.0
3	H59		7.0	7.29	25.2	28.2	1.0
4	H60		6.1	4.65	24.3	29.3	1.0
5	H61		9.2	11.40	25.0	32.5	1.0
6	H62		11.3	12.80	24.2	34.2	1.0
92070306	Q=30.13	V=6.4	P=0.581	Tsat=157.58			
	NO.	Vacc(kv)	Iacc(A)	q(MW/m2)	T0(°C)	Tbulk(°C)	t(sec)
	H63	30.0	3.0	0.77	24.0	24.5	1.0
	H01		5.0	2.30	25.0	26.0	1.0
	H02		6.1	4.40	24.0	26.0	1.0
	H03		7.0	7.29	25.0	29.0	1.0
	H04		9.2	11.20	25.0	32.0	1.0
	H05		11.3	12.80	25.0	33.0	1.0
	H06	32.0	12.5	15.40	25.0	34.0	1.0
	H07	34.0	14.1	18.20	24.0	34.0	0.5
	H08		14.2	18.20	24.0	34.0	0.8

ITER TASK/JB-DPI-3/JAPAN

Continue (Table 4-1.)

920930

92093001	Q=20	V=4.24	P=0.98	Tsat=179.05			
	NO.	Vacc(kv)	Iacc(A)	q(MW/m2)	T0(°C)	Tbulk(°C)	t(sec)
1	H11	30.0	3.0	0.77	28.0	29.0	1.0
2	H12		4.0	1.14	27.6	29.1	1.0
3	H13		5.0	2.35	27.8	29.5	1.0
4	H14		6.1	4.62	27.0	29.5	1.0
5	H15		7.1	7.55	28.2	33.2	1.0
6	H16		8.0	9.50	27.8	35.3	1.0
7	H17		11.0	12.75	27.8	38.3	1.0
8	H18		11.5	12.80	27.0	38.0	1.0
9	H19	31.0	12.0	14.00	27.0	38.5	1.0
10	H20	32.0	12.5	15.40	22.5	35.5	1.0
11	H21	33.0	13.0	16.7	24.7	37.7	1.0
12	H22	34.0	14.0	18.2	24.2		1.0

921001

92100102	Q=47	V=9.99	P=0.977	Tsat=178.85			
	NO.	Vacc(kv)	Iacc(A)	q(MW/m2)	T0(°C)	Tbulk(°C)	t(sec)
1	H23	30.0	2.9	0.77	22.4	23.2	1.0
2	H24		4.0	1.14	24.0	25.0	1.0
3	H25		5.1	2.51	24.0	25.1	1.0
4	H26		6.0	4.40	24.0	25.9	1.0
5	H27		7.0	7.29	23.0	25.8	1.0
6	H28		8.1	9.69	23.8	27.1	1.0
7	H29		11.2	12.80	23.5	28.0	1.0
8	H30	32.0	12.5	15.40	23.5	29.5	1.0
9	H31	33.0	13.0	16.70	24.0	31.0	1.0
10	H32	34.0	13.8	18.20	23.8	31.6	1.0
11	H33	36.0	15.2	21.2	23.0	31.3	1.0
12	H34	37.0	16.3	22.9	23.0	31.8	0.51(1.0)
13	H35	38.0	16.2				
92100103	Q=47	V=9.99	P=1.275	Tsat=190.72			
	NO.	Vacc(kv)	Iacc(A)	q(MW/m2)	T0(°C)	Tbulk(°C)	t(sec)
1	H36	30.0	3.0	0.77	23.8	24.6	1.0
2	H37		5.0	2.4	23.2	24.4	1.0
3	H38		6.0	4.4	22.5	24.3	1.0
4	H39		7.0	7.3	22.8	25.6	1.0
5	H40		8.0	9.5	23.0	26.3	1.0
6	H41		11.2	12.8	24.5	29.5	1.0
7	H42	34.0	13.9	18.2	24.0	30.0	1.0
8	H43	37.0	15.9	22.9	23.0	31.5	1.0
9	H44	38.0	16.6		24.2		0.6

ITER TASK/JB-DPI-3/JAPAN

Continue (Table 4-1.)

921002

92100201	Q=74.5	V=15.81	P=0.98	Tsat=179.05			
	NO.	Vacc(kv)	Iacc(A)	q(MW/m2)	T0(°C)	Tbulk(°C)	t(sec)
1	H01	30.0	3.0	0.77	23.0	23.5	1.0
2	H02		4.2	1.31	24.5	25.3	1.0
3	H03		5.0	2.35	23.0	24.2	1.0
4	H04		6.1	4.65	24.5	26.0	1.0
5	H05		7.1	7.55	24.5	26.3	1.0
6	H06		8.2	9.87	23.5	25.7	1.0
7	H07		11.1	12.80	23.0	26.1	1.0
8	H08	34.0	14.0	18.20	23.2	27.5	1.0
9	H09	37.0	15.8	22.90	23.2	28.7	1.0
10	H10	39.0	17.5	26.20	24.5	31.5	1.0
11	H11	40.0	18.0	28.1	23.2		0.72(1.0)
92100202	Q=47.5	V=10.08	P=0.493	Tsat=151.31			
	NO.	Vacc(kv)	Iacc(A)	q(MW/m2)	T0(°C)	Tbulk(°C)	t(sec)
1	H12	30.0	3.0	0.77	23.5	24.0	1.0
2	H13		5.0	2.4	22.5	23.5	1.0
3	H14		6.0	4.4	24.0	25.5	1.0
4	H15		7.0	7.3	23.0	25.5	1.0
5	H16		7.9	9.3	23.5	27.0	1.0
6	H17		11.2	12.8	22.5	27.0	1.0
7	H18	34.0	14.0	18.2	22.5	29.5	1.0
8	H19	36.0	15.0	21.2	23.2	31.7	1.0
9	H20	37.0	15.9	22.9	24.0	34.5	1.0
10	H21	38.0	16.0	24.5	23.5		0.52(1.0)

ITER TASK/JB-DPI-3/JAPAN

Continue (Table 4-1.)

062501

ch	H45	H46	H47	H48	H49	H50	H51	H52
TP1	35.5	61.6	126.9	248.3	292.7	307.6	315.9	319.8
TP2	35.5	65.8	157.2	281	315.8	332.5	351.3	356.4
TP3	36.7	71.8	186.6	295.9	331.2	352	382.3	425.2
TP4-1	28.2	40.9	83.1	132.5	155.4	164.7	169.5	171.7
TP4-2	32.4	54.9	125.2	213.5	250.5	266.5	278	303.9
TP4-3	35.5	65.8	160.2	275.1	314	332.5	357.8	425.2
TP4-4	37.3	71.1	175.5	295.9	333.6	355.5	393.3	469.4
TP4	36.8	70.5	176.2	293.7	327.6	351.6	404	452.9
TP4-5	36.1	68.8	169.4	284.6	320.5	345.5	410.8	399.4
TP4-6	33.6	62.9	147.7	250.1	287.9	305.4	355	325.2
TP4-7	30	50.1	110.3	183.7	214.5	229.3	245.2	236.4
TP4-8	28.2	40.9	78.2	127	145.8	156.6	162.3	155.2
TP4-9	26.3	34.3	57.9	88.6	100.8	108	111.6	99.6
TP4-10	25.2	30.7	46.5	65	76	79.1	82.6	74.2
TP4-11	24.5	28.2	40.9	55.7	63.4	66.5	68.3	62.1
TP4-12	24	28.2	39.1	51.4	59.1	61.7	62.9	58.5
TP5	36.2	67.1	150.2	269.6	304	322.4	350.3	388.9

062502

ch	H53	H54	H55	H56	H57	H58	H59	H60	H61	H62
TP1	34.7	69.5	100	130	256	278.1	293.6	307.2	309.9	309.3
TP2	37.2	77.2	119.4	161	282.6	298.2	314.2	330.8	338.9	344.2
TP3	37.3	83.3	134.9	190.3	296.9	313.1	328.5	53.9	366.6	407.8
TP4-1	28.1	46.5	64.8	57.9	138.2	148.5	158	165.4	171.3	170
TP4-2	32.3	62.3	94.5	127	218.2	236.7	249.5	267.2	273.1	299.2
TP4-3	35.3	76	118.8	162.8	278.4	296.5	311.3	333.8	346.1	415.4
TP4-4	36.6	83.1	130.7	178.6	298.6	314.8	330.8	360.8	372.3	467.2
TP4	36.6	84.3	131	179.2	295	310.9	327.6	353.7	368.2	449.9
TP4-5	35.4	80.1	127.1	173.2	287.4	302.4	318.9	343.3	356	389.2
TP4-6	35.4	71.9	111.2	150.2	254.9	270.9	288.1	303	314.7	310.5
TP4-7	30.5	56.2	83.8	112.8	189.5	202	217.2	228.2	236	222.4
TP4-8	28.7	44.7	63.1	81.4	144	138.3	150.8	156.8	162.7	147
TP4-9	26.8	36.2	47.2	59.9	94.3	95.7	104.5	109.3	112.7	96.7
TP4-10	25.7	32.6	39.4	47.8	70.1	70.3	75.7	79.2	84.9	71.9
TP4-11	25.6	29.5	35.7	41.7	58.5	60.6	64.3	66	70	60.3
TP4-12	24.5	28.3	33.8	38.6	55.5	57	60.6	63	64.7	56.8
TP5	36	76.6	114.1	152.1	273.1	289.3	304.2	322.5	331.2	378.7

ITER TASK/JB-DPI-3/JAPAN

Continue (Table 4-1.)

062601.

ch	H82	H83	H84	H85	H86	H87	H88	H89	H90
TP1	38.1	78.8	126.2	162.2	205	270.2	287	297.5	297.5
TP2	15.7	63.9	128.6	180.2	240	265.8	280.6	296.7	304.3
TP3	17.6	72.8	151.6	216.3	248.5	277.7	292.5	332.8	373.5
TP4-1	8.5	31.6	62.7	88.8	109	135.7	146.1	152.8	155.2
TP4-2	12.7	49.1	99.5	140	173.5	213.2	229	237.5	272.9
TP4-3	15.8	63.9	129.8	182.7	224.2	264.1	280.6	302	403.6
TP4-4	17.6	71	143.7	201.6	243.7	279.5	295.5	333.8	490.4
TP4	17.1	72.3	145.5	199.8	241.9	275.8	291.3	329.6	489.8
TP4-5	17	69.8	140	193.7	234.6	269.4	285.4	313.2	432.8
TP4-6	15.2	60.4	120.9	166.2	205.3	244.3	259.3	273.6	318.6
TP4-7	9.6	43.1	88.8	120.3	151	183.9	197.4	207.1	214.4
TP4-8	7.9	29	62	82.7	105.4	127.9	134.5	143.7	141.3
TP4-9	4.9	19.4	42.4	56.1	71	86.3	91.1	98.8	95.3
TP4-10	4.2	15.8	30.4	40.1	50.3	61.6	66.3	69.3	69.3
TP4-11	3	12.8	24.3	32.8	41.3	51.4	55.6	58	56.2
TP4-12	3.6	11.5	21.9	30.3	37.6	47.3	52	55	50.2
TP5	16.4	64.5	122.1	166.8	213.2	256.8	272.9	290	352.4

062602.

ch	H91	H92	H93	H94	H95	H96	H97	H98	H99
TP1	43.1	85	125.9	178.1	231.5	275.4	286.6	293.9	300.5
TP2	44.2	94.4	150.2	228.1	265.1	291.3	312.2	324.8	330.7
TP3	46.1	104	172.5	253.1	278.4	302.1	337.1	365.5	387
TP4-1	33.3	61.1	91.5	127.8	150	170.5	176	184.8	167.1
TP4-2	41.2	80.3	125.3	184.3	216.3	245	259.6	276.8	263.5
TP4-3	44.9	96.3	153.2	229.4	260.7	292	319.1	356.2	349.7
TP4-4	47.3	104	166.5	246.5	276	304.3	345.8	378.2	403.3
TP4	46.1	105.9	166.5	247.7	273	302.1	342.4	377	417.8
TP4-5	46.7	99.8	162.8	239.2	268.1	295.5	328.1	365.4	410.3
TP4-6	43.1	90.4	143.7	211.7	242.5	273	289.1	321.3	337.8
TP4-7	37.6	73.2	112.8	163.5	190.1	216.9	226.7	239	239.6
TP4-8	33.8	58.1	86.6	123.6	139.9	161.9	169.4	175	167.1
TP4-9	30.2	47.7	67	92.7	106	120.8	126.8	131.1	120.5
TP4-10	29.7	42.3	56.8	76.7	85.9	95.4	97.8	102.1	91.4
TP4-11	27.8	39.9	52	66.6	75.8	85.3	87.1	90.9	78.4
TP4-12	27.8	38.7	50.7	64.2	71.7	81.8	83.5	86.7	74.2
TP5	45.5	96.3	146.1	214.7	254.7	284.3	307.3	329.5	350.9

ITER TASK/JB-DPI-3/JAPAN

Continue (Table 4-1.)

062503.

ch	H63	H64	H65	H66	H67	H68	H69	H70	H71
TP1	36.2	66.5	105.1	143.1	263.4	282.7	296.6	304.9	307.4
TP2	37.3	72.4	126.4	181	286.8	302.7	315.4	332.1	339.4
TP3	38.6	77.8	144.3	212.8	299.3	316	329.2	354.7	393.3
TP4-1	28.2	45.3	68.8	95.6	144.3	154.3	160.5	169.2	171.2
TP4-2	33.1	59.1	100.3	142.4	224.4	242	253.2	266.7	288.4
TP4-3	37.4	71.8	125.8	181	282.6	299.8	313	336.3	389.7
TP4-4	39.2	77.7	137	198.8	301	318.2	331.4	360.9	426.9
TP4	37.9	77.6	136.3	198.1	297.3	313.3	326.9	354.4	426.8
TP4-5	37.9	75.9	134.1	191.5	290.5	306.4	319.5	345.2	422.8
TP4-6	35.5	68.9	118.1	167.7	259.1	276.8	290	288.7	356.1
TP4-7	31.8	54.9	90.9	125.3	194.5	210.4	221	232.6	244.4
TP4-8	30.1	44	67	89.6	136.8	146	153.8	162.4	162.7
TP4-9	26.9	36.7	51.3	65.8	97.9	103.2	107	115.4	114.4
TP4-10	25.8	32.5	43.4	52	73.7	78.5	79.8	82.9	85.4
TP4-11	25.1	30.6	38.5	45.8	62.2	66.5	68.5	70.3	73.6
TP4-12	24	29.5	36.1	44.1	58.7	71.6	63	65.5	68.1
TP5	37.4	72.5	120.5	167.1	276.8	292.8	304.7	319.7	366.4

062504.

ch	H72	H73	H74	H75	H76	H77	H78	H79	H80	H81
TP1	35.5	109.2	141.9	266.9	73.8	231.3	285	296.4	307.2	308.4
TP2	36.8	132.2	176.1	288.4	82.8	273.3	303.4	315.4	330.9	337.4
TP3	37.4	149.5	208.5	300.4	88.7	285.9	315.4	329.2	359.3	404.7
TP4-1	28.9	75.3	96.8	150.1	49.7	137.3	160.9	167.9	175.3	159.4
TP4-2	33.1	106.8	143.1	230.3	67.3	211.8	246.3	258	268.5	264.3
TP4-3	36.2	132.9	180.5	284.9	81.5	266.1	301	313.7	337.5	352.8
TP4-4	38	143.6	196.9	301.5	88.1	284	318.2	332	364.4	428.4
TP4	37.4	143.5	196.8	299.8	88.1	282.2	314	327.1	360.8	453.2
TP4-5	37.4	138.8	190.2	292	86.3	276.4	308.2	320.1	351.6	453.5
TP4-6	34.9	122.8	165.2	264.5	76.8	245.3	281	293	310.3	367.5
TP4-7	31.3	93.7	124.7	203	61.9	186.2	216.4	228.3	235.1	245.5
TP4-8	28.2	70.5	90.1	145.2	47.8	133	156	163	166	161.2
TP4-9	26.3	54.8	67	107.2	39.3	96.3	113.9	117.1	118.9	112.4
TP4-10	25.8	45.8	54.3	80.7	34.5	73.8	86.8	86.9	87.6	83.6
TP4-11	24.5	40.8	48.9	70	32.1	63.7	74.8	75	75.1	68
TP4-12	25.3	39.7	45.9	65.2	30.9	60	68.9	70.8	72.2	61.3
TP5	36.1	125.8	166.5	280.3	81.5	259.3	294.6	306.5	326.1	372

ITER TASK/JB-DPI-3/JAPAN

Continue (Table 4-1.)

062603.

ch	HI00	HI01	HI02	HI03	HI04	HI05	HI06
TP1	43.3	111.4	139.6	207.4	275.4	279.5	282.2
TP2	45.7	131	170.2	247.6	299.1	312.5	319.5
TP3	47.5	145.8	198.2	262.9	330.5	357.6	411.6
TP4-1	34.8	82.4	106.4	149.1	180.9	179.5	201.3
TP4-2	41.4	110.3	145	205.5	344.3	272.3	321.9
TP4-3	45.7	132.8	176.9	245.8	315.7	345.8	438.8
TP4-4	47.5	143.5	191	259.2	346.5	367.5	484.6
TP4	47.7	144.2	194.1	258.1	344.3	360.1	464.9
TP4-5	46.9	139.2	187.3	253.2	331	355.1	388.2
TP4-6	43.9	125.7	166	231.8	288.4	323.3	326.1
TP4-7	38.4	100.2	131.9	186.1	224.2	246.7	239.2
TP4-8	34.1	78.7	102.1	143.1	171.7	188.1	174.4
TP4-9	31.7	62.7	81.3	112.2	135.2	145	135.5
TP4-10	29.9	54.8	69.6	93.3	110.8	118.4	111.3
TP4-11	28	50.6	63.6	84.4	98.9	104.8	101.1
TP4-12	28.1	49.4	61.1	81.5	95.4	99.4	98.7
TP5	46.3	128.7	166	237.9	301.5	316.2	338.4

062604.

ch	HI07	HI08	HI09	HI10	HI11	HI12	HI13	HI14
TP1	37.1	84.6	162.5	123.2	188.1	236.9	264	274.4
TP2	37.7	98.3	214.9	156.4	251.5	274.7	278.5	291.6
TP3	38.9	110.7	247.9	184.5	266.2	286	290.3	303.5
TP4-1	29.2	57.1	110.1	84.1	123.8	138.6	141.2	149
TP4-2	33.4	80.5	168	126.2	191.8	214.9	220.7	234.8
TP4-3	37.7	98.3	216.1	159.4	242.4	269.8	275.5	290.4
TP4-4	39.5	108.4	236.3	175.3	261.9	287.7	292.7	307.6
TP4	40.2	107.7	235.7	175.3	259	284.8	289.8	305
TP4-5	38.3	105.4	228.4	169.8	252.1	277.1	283.2	296.3
TP4-6	37.1	93.5	198.5	148.2	220.4	247.9	254.2	268.9
TP4-7	32.2	72.2	147.6	112.5	162.5	186.9	192	205.5
TP4-8	29.8	56.5	107.1	81.6	114.8	131.4	137	145.3
TP4-9	27.3	45	78.1	62	82.3	94.7	96.1	103.3
TP4-10	26.1	38.4	60.9	49.9	64.5	71.1	71.8	78.5
TP4-11	25.5	34.6	52.3	44.4	55.9	61.4	61	65.3
TP4-12	24.9	34	49.2	41.3	52.3	57.8	58	61.1
TP5	38.9	95.3	197.9	147.6	228.4	261.3	270	283.9

ITER TASK/JB-DPI-3/JAPAN

Continue (Table 4-1.)

062605.

ch	HI18	HI19	HI20	HI21	HI22	HI23	HI24	HI25	HI26	HI27
TP1	41.5	82.5	122.2	167.3	247.1	267.5	277.3	288.4	290.8	289.2
TP2	42.7	95.5	152.3	222.1	276.7	283.1	296.3	309.8	315.1	322.2
TP3	44.6	106.9	179.7	248.9	288.1	293.9	308.2	327.6	341.8	395.2
TP4-1	32.3	57.4	85.9	113.5	145	149.5	157.8	164.4	166.9	156.1
TP4-2	38.5	78.3	125.1	172.7	221.9	228.5	241.4	252.2	256.6	260.3
TP4-3	42.6	96.1	155.9	220.3	273.8	280.7	295	313.3	323.4	369.4
TP4-4	45.1	105	169.9	240.4	290.4	296.8	311.7	335.9	348.3	448.5
TP4	44.5	106.3	170.6	241.7	287.7	293.8	308.2	332.9	345.3	466.5
TP4-5	42.7	102.6	164.4	232.4	280.5	287.3	301	325.2	334.1	443.9
TP4-6	40.9	91.5	144.1	203.2	251.3	260.2	273.7	287.3	294.4	342
TP4-7	35.3	71.8	109.8	152.7	191	200.4	211.5	219.4	224.2	226.7
TP4-8	31.7	57.4	80.5	110.5	136.5	144.1	152.4	157.6	160.7	151.8
TP4-9	28.1	44.6	60.3	79.6	97.9	103.7	110.3	113.2	115.6	103.2
TP4-10	27.5	38.6	50	62.5	77.3	78.9	83.8	88.4	87.2	76
TP4-11	26.2	34.8	44.5	53.9	65.9	67.5	71.2	74.6	74	64
TP4-12	25.6	33	42.6	50.3	61.1	63.9	67	69.9	70.5	60.4
TP5	43.3	94.9	145.3	204.4	265.9	274.2	286.8	301.5	311	356

062901.

ch	I28	H01	H02	H03	H04	H05	H06	H07	H08	H09
TP1	42.6	86.4	165.7	123.5	217.6	263.2	279.1	286.4	290.6	295.3
TP2	43.9	96	210.3	147.8	255.6	279.7	295.7	308.9	322	337.9
TP3	45.6	106.7	244.4	170.7	269.5	289.1	312.3	330.3	351	458.1
TP4-1	33.5	60.2	113.9	84.3	134.8	153.2	161.5	167.8	172.6	170.8
TP4-2	39	80.6	167	122.3	201.9	228.7	243.8	253.8	263.6	288.7
TP4-3	43.8	96.6	211.4	150.8	250	277.3	298.6	316	336.9	444.7
TP4-4	45.7	104.3	229.2	164.1	267.1	292.2	324.1	337.9	366.8	560.1
TP4	46.2	105.5	232.2	164	266.5	290	327.7	336.8	365.5	584
TP4-5	45.1	100.8	223.7	160.2	259	283.3	315.8	327.9	366.8	547.9
TP4-6	42.5	90.7	197.3	140.2	231.1	259.6	278.4	292.8	316.7	382.5
TP4-7	37.8	71	148.8	109.7	178.5	201.3	218.1	224.5	234.3	251.3
TP4-8	33.5	57.9	109.7	82.5	130.6	147.2	160.9	166	172.8	172.7
TP4-9	31.1	46.9	82.5	63.6	96.2	108	118.6	121.8	127.3	121.8
TP4-10	29.8	42	66.5	53.8	76	83.1	93.1	93.9	96.9	90.9
TP4-11	28.1	37.8	57.4	47.1	65.3	72.4	78.3	80.8	82.7	76.1
TP4-12	28.7	37.7	55.5	45.8	62.3	70.6	73.5	76.1	78	71.4
TP5	44.5	96	196.2	143.1	243.2	271.4	[illegible]	304.7	[illegible]	[illegible]

ITER TASK/JB-DPI-3/JAPAN

Continue (Table 4-1.)

062902.

ch	H10	H11	H12	H13	H14	H15	H16	H17
TP1	44	98.9	144	193.5	269.7	273.4	282.9	281.9
TP2	45.9	115	181.5	250.9	287.1	303.1	308.4	315.7
TP3	48.9	130.4	216.8	257.6	312.6	323.8	333.3	360.8
TP4-1	35.5	72.3	106	134.4	168.5	173.8	177.6	174.7
TP4-2	40.9	97.8	150.6	193	245.9	252.6	255.1	266.3
TP4-3	45.3	118.4	188.2	238	303.1	313.8	315.6	351.3
TP4-4	47.7	127.5	205.2	254	326.8	333.9	341	383.3
TP4	47.1	128.6	206.5	253.4	326.7	329.7	337.9	376.8
TP4-5	47.7	123.9	199.2	246.7	307.2	322	329.1	369.9
TP4-6	44.6	110.1	175.4	222.2	272	284.7	290.6	331.1
TP4-7	38.6	85.9	136.4	174	214.2	219.1	223.3	240.1
TP4-8	35.6	68.1	103.7	130.9	160.5	163.6	165.5	174.2
TP4-9	32.5	54.8	79.4	100.7	120.1	124.9	124.3	131
TP4-10	31.9	48.7	65.7	81.1	96.5	101.2	99.4	103.1
TP4-11	30.1	43.9	57.9	70.4	84.6	88.1	89.3	89.4
TP4-12	29.5	42.6	56	67.4	79.8	82.7	86.3	84.1
TP5	46.4	114.4	174.2	226.5	284.1	300.1	307.8	325.8

062903.

ch	H18	H19	H20	H21	H22	H23	H24	H25
TP1	51.6	119.6	75.6	165.4	226.6	269.2	269.7	274.7
TP2	53.9	140.4	82.2	210.7	245.6	292.5	304.3	319.2
TP3	57	159.4	88.2	232	260.8	323.3	347	368.7
TP4-1	40.6	89.9	56.5	128	151.2	174.7	173.3	170.9
TP4-2	48.5	120.2	70.4	175.3	208.3	254	258.1	268.5
TP4-3	53.9	144	82.8	210.7	246.8	315.1	335.1	344.1
TP4-4	56.4	156.4	87.6	226.5	259.5	331	366.3	400.1
TP4	57.5	156.9	88.8	227.2	258.4	328.6	364.4	446
TP4-5	55.8	153.4	86.4	221.1	253.5	322.8	354.6	474.4
TP4-6	52.7	136.7	78.6	197.7	232.7	293	322.6	400.6
TP4-7	45.5	109	65.7	155.8	190	2045.6	242.1	274.7
TP4-8	40.6	87	54.7	121.4	148.2	177.1	183.8	192.4
TP4-9	37	69.2	46.2	95.3	117.3	139.2	143.3	145.7
TP4-10	34.4	59.5	41.8	81.7	97.2	116.1	118.4	117.9
TP4-11	33.9	55.3	40.1	73.4	86.5	101.8	103.5	103.6
TP4-12	33.3	54.5	38.9	71.5	83	97.1	100	96.5
TP5	54.5	139.8	82.8	197.8	238.9	290.7	319.7	235.1

ITER TASK/JB-DPI-3/JAPAN

Continue (Table 4-1.)

063001.

ch	H26	H27	H28	H29	H30	H31	H32	H33	H34
TP1	237.5	38.6	79.9	111.3	157.9	248.4	263.4	280.1	282.3
TP2	252.8	41	88.7	132.7	199.3	273.4	294.6	312.7	319.6
TP3	266.2	41.6	97.1	151.1	217	289.4	320.7	351.9	362.2
TP4-1	141	31.9	54.7	75.7	108	148.6	154.9	168.1	175.2
TP4-2	209.5	36.7	73.3	108.4	156.7	221.6	236	271.8	297.8
TP4-3	256.5	39.8	89.3	133.9	194.5	273.4	303.5	367	443.1
TP4-4	275.9	41.6	95.9	145.7	211	296.5	331.4	392.6	527.4
TP4	272.4	42.3	95.9	146.6	210.4	296.1	329.5	375.7	530.8
TP4-5	261.3	41	93	141.6	204.9	285.9	317.1	353.6	474.9
TP4-6	235.7	39.2	83.5	125	181.7	251.4	276.8	301.5	371.5
TP4-7	184.5	34.9	66.2	95.9	139.6	194.7	207.3	215	245.3
TP4-8	135	31.9	52.9	72	102.6	144.9	151.9	151.8	169.7
TP4-9	99.5	29.5	41.37	55.9	77.1	108.3	115.2	109.6	123.1
TP4-10	76.9	28.8	38.3	48	62.2	83.3	89.8	84.3	94.1
TP4-11	67.4	27.6	35.3	43.2	56.2	71.4	77.2	75.2	79.8
TP4-12	64.4	27	33.4	40.7	53.2	67.3	73	71.7	76.8
TP5	257.2	41	88.2	128	181.6	270.4	301.3	326.4	350.5

063004.

ch	H48	H49	H50	H51	H52	H53	H54	H55
TP1	43.9	105.1	159	189.8	230.3	237.1	247.2	259.6
TP2	45.1	122.9	182.9	201.5	258.9	270.7	281.7	296.1
TP3	47.6	134.7	184.7	211.8	284.9	304	324.4	382.7
TP4	47	133.6	184.1	210	310.3	320.8	339.9	425.6
TP4-1	35.4	78.4	109.1	129.1	152.4	157.8	163.6	167.5
TP4-2	40.8	103.9	147.7	172.2	216.3	229.2	247.8	265.1
TP4-3	45.7	124.1	175.5	202.1	278.3	296.9	318.5	346.6
TP4-4	47.5	133	185.3	212.4	306.2	325.9	345.2	392.6
TP4	47	133.6	184.1	210	310.3	320.8	339.9	425.6
TP4-5	46.9	130	181	207.5	299.7	299.8	326.2	433.9
TP4-6	43.9	115.8	165.8	192.3	252.2	254.8	266.7	361.3
TP4-7	39	92.6	135.2	158.1	192.5	190.8	197.8	238.3
TP4-8	34.7	73.7	107.4	124.9	149.4	148.8	150.2	171.1
TP4-9	31.1	59.3	84.8	98.7	118	117.5	120.1	133.4
TP4-10	31.2	52.1	72.4	82.8	99.7	99.2	103.6	111.5
TP4-11	29.3	50.3	64.7	76.2	90.1	90.8	94	99.5
TP4-12	28.7	47.1	63.4	73.2	85.9	87.8	89.9	94.2
TP5	46.4	121.2	171.3	195.4	277.3	287.3	290	306.2

ITER TASK/JB-DPI-3/JAPAN

Continue (Table 4-1.)

070201.

ch	H01	H02	H03	H04	H05	H06	H07	H08	H09
TP1	42.9	64.5	100.6	143.8	161.6	281	294.2	296.3	299.8
TP2	43.6	68	113.7	176.2	200.8	296.5	318.4	319.9	336.1
TP3	45.4	72.3	125.6	205	237.3	307.8	363.3	363.6	423.1
TP4	45.3	73.1	123.8	196.5	226.3	307.7	354.5	365.5	514.4
TP4-1	33.8	45.6	70.3	102.7	115.9	170.8	178.1	176.6	185.3
TP4-2	40.5	57.9	95.3	144.8	163.4	248.9	261.7	269.3	301
TP4-3	44.1	67.4	115.5	179.3	203.7	296	336.8	344.8	425.9
TP4-4	46.6	71.6	123.7	193.9	223.2	310.2	363.2	370.5	506.4
TP4	45.3	73.1	123.8	196.5	226.3	307.7	354.5	365.5	514.4
TP4-5	45.3	71	120.1	188.4	217.7	301.2	350.4	362.3	470.1
TP4-6	42.9	65.8	108.3	167.2	192.8	278.1	307.1	321.2	355.6
TP4-7	37.5	53.5	85.8	129.6	147.8	224	238.1	241.3	252.3
TP4-8	33.7	46.2	67.4	98	112.3	167.9	176.4	182.3	181.8
TP4-9	30.2	38.9	54.9	75.5	84.4	127.3	132	137.5	133.6
TP4-10	29.6	35.3	47.4	63.6	69.6	100.5	105.9	108.5	103.9
TP4-11	27.8	32.3	43.7	55.7	61.2	87.9	91.5	93.1	91.5
TP4-12	27.7	32.2	42.4	55	59.2	83.3	86.2	86.5	86.6
TP5	44.7	69.3	113	167.8	192.2	287	316	323	364.2

070202.

CH	H10	H11	H12	H13	H14	H15	H16	H17	H18
TP1	47.8	92.1	100.6	173.2	228.7	283.8	274.6	290.8	290.2
TP2	49.7	102.7	114.4	215.4	254.9	307.5	293	316.3	332.3
TP3	52.1	111.1	125.1	250.1	270.1	353.1	370.9	385.1	585.2
TP4	52.8	111.3	123.7	236.7	266.5	352.1	350	380.7	557.8
TP4-1	37.5	64.8	71.6	127	156	189.6	187.3	185.7	186.9
TP4-2	45.4	86.2	96	176.2	213.4	268.2	261.7	274.7	288.9
TP4-3	49.6	101.5	113.7	217.1	254.2	336.6	324.4	345.9	434.4
TP4-4	52	109.8	122.6	236	268.8	359.5	354	374	539.7
TP4	52.8	111.3	123.7	236.7	266.5	352.1	350	380.7	557.8
TP4-5	51.4	108.1	121.4	230.5	260.9	339.5	324.3	369.3	519
TP4-6	48.4	97.5	110.9	205.6	238.4	290.2	283.4	319.8	410.1
TP4-7	41.6	80.9	89.9	162.2	192	229.1	230.1	244.2	275.4
TP4-8	36.8	66	74	125.9	149	176.1	178.3	187	196.1
TP4-9	33.1	53.3	60.2	98.7	115.2	137.7	139.1	144.7	149.4
TP4-10	32.6	47.8	53.6	82.6	96.2	114.5	116.6	117.4	122.7
TP4-11	31.3	44.2	48.7	74.4	87.2	104.3	104.1	106	108.4
TP4-12	30.7	43.5	46.9	71.9	83.7	100.8	100	102.5	103.7
TP5	50.2	102.8	113.6	202.7	247.5	324.4	294.7	325.2	352.4

Continue (Table 4-1.)

070203.

	A	B	C	D	E	F	G	H	I	J	K	L
1	ch	H19	H20	H21	H22	H23	H24	H25	H26	H27	H28	H29
2	TP1	38.1	73.1	146	109.9	262.9	273.1	287.4	301.7	318	324.2	321
3	TP2	39.3	81.8	186.1	134.3	288.7	298.1	307	324.3	342.6	360.8	348.3
4	TP3	41.1	87.9	217.8	153.8	304.8	315.4	324.8	342.7	362.9	515.8	396
5	TP4	41.2	87.9	203.2	146.8	304.2	314.8	321.8	339.2	358.5	600	429.6
6	TP4-1	30.2	48.9	95.1	72	138.5	146	151.9	162.2	171	175.1	168.6
7	TP4-2	36.3	65.9	147.2	106.4	223.2	234.2	243.2	259.9	276.5	333.2	276
8	TP4-3	39.2	80.7	186.7	133.1	284.6	295.1	305.2	321.9	342.3	496.7	362.3
9	TP4-4	41	86.1	203.7	146.2	305.9	315.9	325.4	343.8	363.4	588.3	415.9
10	TP4	41.2	87.9	203.2	146.8	304.2	314.8	321.8	339.2	358.5	600	429.6
11	TP4-5	39.9	84.3	197.1	142	295.1	304.1	313.4	329.6	348.8	557.7	422.8
12	TP4-6	37.4	75.4	170.7	124.1	261	271.2	280.3	297	315	410.8	359.9
13	TP4-7	32.6	58.6	125.9	93.8	192.7	201.1	210.3	225	239.9	257.3	358.9
14	TP4-8	30.2	47.7	89.7	68.9	135.4	140.7	148.4	156.2	167.4	167.8	165.7
15	TP4-9	27.8	38.6	65.4	52.7	94.5	98.5	105.1	108.1	116.1	111.1	115
16	TP4-10	28.3	34.9	52.1	44.2	72.6	74.8	79.6	79.1	85.2	79.7	86.5
17	TP4-11	26.5	31.9	46	39.3	60.6	62.9	65.9	66	71.6	65.9	71.6
18	TP4-12	25.9	30.7	44.2	37.5	57	58.6	61.1	62.4	67.4	61.8	66.3
19	TP5	40.5	80.8	173.2	127.8	279.2	288.6	296.4	312.4	329.2	423.2	360

070301.

ch	H30	H31	H32	H33	H34	H35	H36	H37	H38
TP1	40.4	71.1	134.3	92.8	228.6	273.3	283.4	291.7	291.4
TP2	41	79	167.9	107.2	250.6	289.9	304.2	320.1	327.6
TP3	42.1	86.6	197.1	120.7	264.3	303.6	317.9	352.1	394.9
TP4-1	31.3	48.9	87.5	62	114.6	145	154.5	159.8	174.2
TP4-2	37.3	65.3	132.6	88.1	193.2	231.2	244.8	256.9	323.4
TP4-3	40.4	80.2	167.9	107.8	247.5	287.6	301.8	327.9	482.6
TP4-4	41.7	85.5	185	117.3	266.6	306.5	321.5	358.5	573
TP4	43.4	86.1	187.4	118.5	263.5	302.8	318.1	361.3	574.1
TP4-5	41.7	83.7	179.5	114.3	255.9	294.7	308.4	354.5	516.6
TP4-6	39.7	75.9	158	100	226.2	266.6	279.4	299.4	382.7
TP4-7	35	59.2	117.1	76.9	162.8	201.9	212.4	221.5	245.6
TP4-8	31.3	47.1	85.7	59.5	107.4	142.6	149.8	154.4	161.4
TP4-9	28.9	38.6	64.4	46.8	71.2	101.6	104.1	108.7	109
TP4-10	27.5	34.8	51	42.5	47.4	76.7	77.3	80.3	80
TP4-11	26.5	31.9	44.9	37.7	37.2	64.2	65.5	67.8	67.5
TP4-12	26.4	31.3	42.5	35.8	34.2	59.9	61.9	64.2	64.6
TP5	41.6	80.1	158.1	105.3	240.8	279.3	292.9	314.3	374

ITER TASK/JB-DPI-3/JAPAN

Continue (Table 4-1.)

070304.

ch	H48	H49	H50	H51	H52	H53	H54	H55	H56
TP1	42.6	85.6	129.9	183.4	223.1	235.4	245.2	267.5	257.2
TP2	44	96.9	156.5	209.6	244.5	257.3	279.1	305	291.4
TP3	45.2	105.2	179.6	222.9	264.7	279.8	308.2	356.6	330
TP4-1	34.3	59.9	93.6	120.9	143.7	148.4	154.4	172.3	165.6
TP4-2	39.7	79.1	130.5	171.7	205.5	213.4	227.5	281.3	252.2
TP4-3	43.4	95.1	158.9	207.7	251.2	264.7	292.2	386.8	333
TP4-4	46.4	104	172.3	221.2	271.3	289.8	319.5	482.6	363.5
TP4	47.1	105.1	173.5	221.2	266.4	288	325.3	512.5	356.3
TP4-5	44.6	102.8	167.5	215.6	253.7	278.5	315.9	494.8	334.7
TP4-6	42.2	92.7	148.8	195.5	227.4	243.3	267.7	376.4	287.9
TP4-7	37.9	75	116.8	153.5	182.3	189	200.6	241.8	209.5
TP4-8	34.3	61.2	90.1	117.9	138.9	143.1	149.6	171.2	154.7
TP4-9	31.2	50.3	69.9	90.6	106.3	109.8	115.8	127.5	119.1
TP4-10	30	44.2	59.1	75.1	84.4	86.1	93.7	100.7	97.1
TP4-11	28.8	40.5	54.1	66.3	76.6	77.8	83.2	88.9	86.5
TP4-12	28.8	39.3	88.4	63.3	73.7	74.8	78.4	84.2	81.8
TP5	45.1	95.7	150	201	237.8	259.1	288	343	304.5

070306.

ch	H63	H01	H02	H03	H04	H05	H06	H07	H08
TP1	41.2	84.4	133.3	177.1	240.4	255	260.3	266.4	272.8
TP2	42	93.9	162	215	261.8	270.9	291.7	298.1	308.5
TP3	44.4	101.6	188.2	230.9	273.4	310.7	325.5	349.7	362.3
TP4-1	32.8	59.3	96.6	121.5	154.6	162.3	158	162.8	164.3
TP4-2	38.8	78.4	135.1	172.3	219.1	232.9	235.4	271.2	263.8
TP4-3	41.3	93.3	165.1	210.8	261.2	285.2	300	370.1	382.5
TP4-4	44.4	100.4	178.4	226.6	274.6	314.2	340.3	400.3	484.2
TP4	43.2	103.4	179.1	226.6	272.2	313.5	340.9	391.7	514.3
TP4-5	43.2	98.6	172.9	220.6	264.9	300.6	326.7	359	501.5
TP4-6	41.2	89.1	152.4	197.9	241	262.8	283.9	285.6	395.9
TP4-7	37.6	72.4	118	155.3	192.8	205	212.8	204.2	259.3
TP4-8	32.8	59.3	90.6	119.1	145	153.9	159.9	144.3	177.1
TP4-9	30.4	48.4	69.3	91.2	108.8	116.5	121.8	106.3	130.9
TP4-10	29.1	43.5	59.7	74.1	86.7	92.8	96.9	84.4	101.2
TP4-11	29.2	39.9	53.6	66.3	78.6	83.1	84.4	73	88.1
TP4-12	28.5	39.8	52.3	63.2	76.7	79.7	80.2	69.5	82.1
TP5	42.6	93.8	154.8	202.3	249	281	302.4	304.1	332.1

ITER TASK/JB-DPI-3/JAPAN

Continue (Table 4-1.)

093001.

ch	H11	H12	H13	H14	H15	H16	H17	H18	H19	H20	H21	H22
TP1	47.5	68.9	97	161.6	203	244	264.8	266.4	267	270.5	278.6	278.8
TP2	49.2	73.5	108.7	200.6	236.5	260.5	281	281.4	282.5	288.3	298.8	322
TP3	49.9	76.6	118.3	226.2	250.6	273.4	320.9	327.8	331.2	331	354.8	424.8
TP4-1	40.2	53.1	73.8	125.3	146	165.4	172.1	186.6	176.2	177.7	176.9	214.2
TP4-2	44.4	64.7	95.2	170	198.7	225.1	242.2	264.4	249.3	262.3	265.4	355.1
TP4-3	48	72.9	110.6	203.6	235.9	261.1	301.7	331.2	313.4	337.5	349.2	484.7
TP4-4	51.1	78.4	117.7	218.9	247.5	270.9	332	349.6	339.5	358.7	394.1	529.6
TP4	49.8	78.4	120.1	221.9	247.5	269.7	337.5	339.1	337.7	358.9	395.6	507.7
TP4-5	51.1	76.7	116	215.2	241.4	263.6	333.9	335.5	330.1	344.7	355.4	406.9
TP4-6	47.4	71.2	104	193.3	221.3	244	292.9	295	292.1	297.8	316	329.7
TP4-7	43.2	61.1	86.9	154.9	180.4	200.1	224.5	226.8	223.1	219.2	234.2	244.9
TP4-8	40.2	52	70.3	121.1	141.9	153.9	172.1	175.5	170	165.6	171.4	176.3
TP4-9	37.1	45.8	60	96.1	113.3	123	136.1	141.8	135.8	132.6	132.4	134.9
TP4-10	35.3	41.5	52.6	80.7	93.9	102.3	111.8	119.9	113.4	110.2	108.7	112.9
TP4-11	34	39.7	49.7	72.9	84.8	92.1	99.2	107.4	101.4	97.5	98.6	103.5
TP4-12	32.8	38.5	47.9	71.7	81.9	89.7	95.7	102.6	96.6	94.1	95.1	102.3
TP5	49.3	74.1	109.9	193.3	229.8	253.8	297	299.2	301	315	339.1	348.7

100102.

ch	H23	H24	H25	H26	H27	H28	H29	H30	H31	H32	H33	H34	H35
TP1	36.4	5.5	80.2	115.8	150.4	187	263.5	272	281	285.5	296	298.3	302.9
TP2	36.9	58	88.9	138.2	189.3	238.2	274.5	289.9	296.9	302.1	314.9	321.4	332.5
TP3	38.3	58.6	96.8	155.4	218.6	257.8	290.6	304.2	312.3	316.3	342.8	353.3	394.3
TP4-1	30.3	40.4	55	78.4	101.2	122.1	146.1	155.7	162.8	163.8	167.9	167.3	164
TP4-2	33.9	49.5	73.5	112.8	149.7	184.6	220.2	237.9	246.4	250.4	258.9	283.4	282.6
TP4-3	37	57.4	88.4	138.9	189.2	231.5	273.8	290.4	299.8	303.9	325	381.3	409.7
TP4-4	38.2	61	95.6	149.6	205	250.4	290.5	307.1	315.2	322.2	357.4	433.1	507.5
TP4	38.3	60.5	96.2	150.1	206.3	251.7	291.1	305.5	312.3	318	354.2	451.1	529.4
TP4-5	38.3	58.7	92.6	144.1	196.6	241.3	282.8	296.5	303.3	309.2	341.2	434.2	484.4
TP4-6	35.8	55	84.4	127.1	172.1	212.6	253.8	270.8	277.4	284.9	298.8	362.7	361.3
TP4-7	32.1	46.5	67.1	97.4	129.5	158.3	193.4	209.9	214.5	223	226.4	246.6	239
TP4-8	29.7	39.2	53.8	72.4	94.6	113.8	140.2	149.7	153.2	160.1	161.8	167.9	162.8
TP4-9	27.9	34.9	43.5	58	71.4	83.8	101.1	109.4	109.3	116.8	119	119.4	112.2
TP4-10	26.6	31.3	37.4	47.7	56.4	65.1	76.7	82.6	82.8	88.9	90.5	90.5	80.8
TP4-11	25.4	30.7	33.7	42.8	49.1	57.8	65.5	70.8	71.3	74.6	76.2	74.9	67.6
TP4-12	23.6	28.9	33.7	39.8	47.3	54.2	62.4	65.4	67.7	69.8	71.4	69.7	64.7
TP5	37.6	59.3	88.9	132.4	176.4	220.6	269	284	292.8	298.5	316.1	365	416.6

ITER TASK/JB-DPI-3/JAPAN

Continue (Table 4-1.)

100201.

ch	H01	H02	H03	H04	H05	H06	H07	H08	H09	H10	H11
TP1	35.2	52.5	69.1	96.7	127.6	156.8	214.9	274.2	302.7	309.3	324
TP2	35.2	54.8	75	113.3	156	198.3	257.6	299	328.1	343	350.5
TP3	36.3	57.3	81.6	127.4	176.8	222.1	277.6	315.7	346	392.5	420
TP4-1	28.4	36.6	45.4	62.7	79.5	95.6	122.5	142.2	158.3	166.9	169.2
TP4-2	32	46.3	61.8	91.3	122.8	152.5	197.2	234.6	262.1	296.9	303.8
TP4-3	35.1	53.5	75.5	113.3	154.8	194	255.2	299.7	331.1	412.5	430.9
TP4-4	36.3	57.2	80.8	123.3	167.6	212.3	277.6	321	353	468.3	521.7
TP4	37	57.9	82.9	124	168.8	214.2	279.5	321.8	349.7	484.3	531.2
TP4-5	36.4	56.1	79.3	118.5	160.9	205.1	267.9	309.8	339	457.6	482.9
TP4-6	34.5	51.9	70.1	106.2	141.8	176.9	232.4	275.4	303.3	367.6	379.7
TP4-7	32.1	42.6	55.7	80	104.4	127.8	167.8	201.7	224.1	243.2	246.1
TP4-8	28.5	36	44.9	59.8	75.2	89.7	115.3	135.7	150.5	159	155.8
TP4-9	26.5	32.4	36.3	46.3	57.2	64.8	79.2	91.8	101.9	108.5	105.9
TP4-10	24.7	29.3	31.4	38.4	43.9	48.9	58.7	66.8	73.4	77	75.1
TP4-11	24.7	28.2	29.6	34.8	39.7	41.8	50.3	55.9	60.3	63.4	61.4
TP4-12	24.8	27.6	28.5	33	37.3	40	46.8	53	56.6	59.1	57.2
TP5	35.8	56	76.2	109.1	145.9	184.9	253.9	296.1	323.4	383.3	411.7

100103.

ch	H36	H37	H38	H39	H40	H41	H42	H43	H44
TP1	39	75.9	107.2	154.4	188	267.6	295.1	309.6	310.2
TP2	39	82.8	127.9	195	238.6	284.4	313.5	332.1	338.6
TP3	42	90.2	144.2	222.7	265.5	298.5	327.8	369.8	391.6
TP4-1	32.3	51.8	71.6	101.5	122.5	149	167.1	173.4	181.9
TP4-2	35.3	68.6	101.7	150.7	184.9	227.9	257.8	284.6	316
TP4-3	40.8	83	127.3	191.5	234.4	282.6	313.6	377.8	447.7
TP4-4	42	89.4	138	209.2	255.1	301.6	332.5	415.7	515.3
TP4	42.1	89.6	140.1	210.4	256.4	301	330.7	417.6	508.8
TP4-5	41.4	87.2	135.3	201.3	245.4	291.4	321.3	404.8	444.5
TP4-6	38.4	77.6	118.5	176.2	213.6	260.8	293.4	347	347.5
TP4-7	34.7	62.7	90.4	132.9	158.7	198.6	227.4	240.5	236.1
TP4-8	31.1	49.9	68.6	98	116	141.8	162.8	167.3	161.1
TP4-9	30.5	42.6	53.5	74.8	85.1	105	118.1	120.1	113.6
TP4-10	28	36.6	44.4	57.5	65	80.1	89.7	90.5	85.1
TP4-11	27.4	32.9	40.1	49.5	55.7	67.5	75.4	76.8	72.7
TP4-12	26.2	31.7	38.3	47.8	54	64.1	71.3	72	69.7
TP5	40.8	33.6	123.2	179.2	220.4	279.1	308.2	357.4	385.9

ITER TASK/JB-DPI-3/JAPAN

Continue (Table 4-1.)

100202.

ch	H12	H13	H14	H15	H16	H17	H18	H19	H20	H21
TP1	39.3	76.9	109.9	147.5	184.3	239.9	262.6	275.1	282.7	281.6
TP2	40.4	85.1	131.1	184.4	233.7	253.5	278.2	304.7	314.1	314.8
TP3	41.8	92.5	148.4	212.5	239.1	263.8	298.5	337.4	344.8	376.5
TP4-1	32	52.8	74.8	98.2	118.9	137.4	151.7	161.6	165.2	167.2
TP4-2	36.3	71	107.4	146.9	175.6	208.8	230.8	250.7	258.5	295.9
TP4-3	40.5	86.4	133	185	218.3	253.4	290.1	320.2	336.1	428.9
TP4-4	42.3	92.3	143.7	200.8	234.2	267.3	314.4	359.6	377	523.7
TP4	42.4	93.2	144.3	202.1	234.8	266.9	310.5	264	376.4	528.9
TP4-5	41.8	90.2	138.9	194.2	226.2	258.3	299.2	338.7	364.1	477.6
TP4-6	39.3	81.1	123.5	169.7	202.6	235.7	264.3	286.3	312.3	371.3
TP4-7	35	63.8	95.6	128.4	151.4	180.7	202.2	213.5	227.4	237.9
TP4-8	32	51.1	71.3	95.2	110.5	131.5	144.6	151.5	160.2	154.9
TP4-9	30.2	42.6	56.8	72.1	82	97.1	104.1	109.2	116.9	109.2
TP4-10	27.7	36.5	45.9	57	63.6	74.5	78.7	83.9	89.7	82
TP4-11	27.1	33.4	40.9	49.7	55	63.8	68	70.6	74.2	67.1
TP4-12	25.9	31.6	39.2	46.7	52.1	59	63.8	67.2	70	62.5
TP5	41.7	85.8	127.5	173.4	211	249.1	283.6	324.9	333.1	390.5

ITER TASK/JB-DPI-3/JAPAN

Table 4-2. Temperature data for swirl tube test sample.

Notation:

Q; flow rate, l/min
V; axial flow velocity, m/s
P; local pressure, MPa
Vacc; acceleration voltage, kV
Iacc; acceleration current, A
q; peak surface heat flux on the test sample, MW/m^2
T0; inlet water temperature, °C
Tbulk; local water temperature, °C
Tsat; saturation temperature at the local pressure, °C

In the table, only thermocouple channel numbers and temperatures indicate. Each channel corresponds to the position described in **Fig. 3-3**.

ITER TASK/JB-DPI-3/JAPAN

Table 4-2. Temperature data for swirl tube test sample.

Notation:

Q; flow rate, l/min
V; axial flow velocity, m/s
P; local pressure, MPa
Vacc; acceleration voltage, kV
Iacc; acceleration current, A
q; peak surface heat flux on the test sample, MW/m^2
T0; inlet water temperature, °C
Tbulk; local water temperature, °C
Tsat; saturation temperature at the local pressure, °C

In the table, only thermocouple channel numbers and temperatures indicate. Each channel corresponds to the position described in **Fig. 3-3**.

ITER TASK/JB-DPI-3/JAPAN

Continue (Table 4-2.)

920709

92070901	Q=47.0	V=9.97	P=0.461	Tsat=148.81			
	NO.	Vacc(kv)	Iacc(A)	q(MW/m2)	T0(°C)	Tbulk(°C)	t(sec)
1	H20	30.0	3.1	0.77	26.0	27.0	1.0
2	H21		5.2	2.69	24.7	26.7	1.0
3	H22		7.0	7.30	25.0	28.5	1.0
4	H23		11.4	12.80	26.0	33.0	1.0
5	H24	32.0	12.5	15.40	25.0	33.5	1.0
6	H25	34.0	14.2	18.20	24.4	34.4	1.0
7	H26	36.0	15.5	21.20	24.4	36.4	1.0
8	H27	38.0	16.6	24.50	26.0	39.0	1.0
9	H28	39.0	17.6	26.20	26.0	40.0	1.0
10	H29	40.0	18.5	28.10	25.8	40.8	1.0
11	H30	41.0	19.0	30.00	24.3	42.3	1.0
12	H31	42.0	19.8	32.10			0.78(1.0)
92070902	Q=40.38	V=8.57	P=0.512	Tsat=152.74			
	NO.	Vacc(kv)	Iacc(A)	q(MW/m2)	T0(°C)	Tbulk(°C)	t(sec)
1	H32	30.0	3.1	0.77	25.8	26.8	1.0
2	H33		5.2	2.69	25.5	27.5	1.0
3	H34		7.0	7.29	25.8	30.3	1.0
4	H35		6.0	4.40	25.8	28.8	1.0
5	H36		11.5	12.80	25.0	33.0	1.0
6	H37		9.0	11.14	25.8	32.8	1.0
7	H38	32.0	12.7	15.40	25.5	35.0	1.0
8	H39	34.0	14.0	18.20	24.3	35.3	1.0
9	H40	36.0	15.4	21.20	26.0	39.0	1.0
10	H41	38.0	16.5	24.50	26.0	41.0	1.0
11	H42	39.0	17.5	26.20	25.8	41.8	1.0
12	H43	40.0	18.2	28.10	25.0	42.0	0.8(1.0)
92070903	Q=30.63	V=6.5	P=0.56	Tsat=156.16			
	NO.	Vacc(kv)	Iacc(A)	q(MW/m2)	T0(°C)	Tbulk(°C)	t(sec)
1	H44	30.0	3.1	0.77	25.8	26.8	1.0
2	H45		5.1	2.51	24.5	26.5	1.0
3	H46		6.2	4.91	25.5	28.5	1.0
4	H47		7.0	7.30	25.3	29.5	1.0
5	H48		8.2	9.87	24.0	30.0	1.0
6	H49		11.0	12.80	24.5	32.5	1.0
7	H50	32.0	12.7	15.40	24.8	34.3	1.0
8	H51	34.0	13.9	18.20	25.0	36.0	1.0
9	H52	36.0	15.4	21.20	24.2	37.2	1.0
10	H53	38.0	17.0	24.50	25.5	40.5	1.0
11	H54	39.0	17.0	26.20	25.0	41.0	0.64(1.0)

ITER TASK/JB-DPI-3/JAPAN

Continue (Table 4-2.)

920710

92071001	Q=20.0	V=4.25	P=0.582	Tsat=157.65			
	NO.	Vacc(kv)	Iacc(A)	q(MW/m2)	T0(°C)	Tbulk(°C)	t(sec)
1	H55	30.0	3.2	0.77	23.0	24.0	1.0
2	H56		5.0	2.35	22.5	24.5	1.0
3	H57		7.0	7.30	23.0	27.5	1.0
4	H58		5.8	3.92	24.2	27.2	1.0
5	H59		11.2	12.80	23.5	31.5	1.0
6	H60	32.0	12.4	15.40	23.2	32.7	1.0
7	H61	34.0	13.7	18.20	24.0	35.0	1.0
8	H62	36.0	15.1	21.20	24.0	37.0	1.0
9	H63	37.0	15.9	22.80	23.9	37.9	1.0
10	H64	38.0	16.4	24.50	24.0	39.0	1.0
92071002	Q=36.88	V=7.83	P=0.321	Tsat=135.86			
	NO.	Vacc(kv)	Iacc(A)	q(MW/m2)	T0(°C)	Tbulk(°C)	t(sec)
1	H65	30.0	2.9	0.77	24.4	25.4	1.0
2	H66		5.0	2.35	23.8	25.8	1.0
3	H67		7.1	7.55	23.5	28.0	1.0
4	H68		6.4	5.45	24.5	27.5	1.0
5	H69		11.0	12.80	24.2	32.2	1.0
6	H70		7.9	9.31	23.0	29.0	1.0
7	H71	32.0	12.6	15.40	23.3	32.8	1.0
8	H72	34.0	14.0	18.20	24.5	35.5	1.0
9	H73	36.0	15.6	21.20	24.5	37.5	1.0
10	H74	38.0	16.7	24.50	23.5	38.5	1.0
11	H75	39.0	17.6	26.20	23.0	39.0	1.0
12	H76	40.0	18.4	28.10	24.5	41.5	1.0
13	H77	41.0	18.5	30.00	23.0	41.0	0.6(1.0)
92071003	Q=30.3	V=6.42	P=0.362	Tsat=140.06			
	NO.	Vacc(kv)	Iacc(A)	q(MW/m2)	T0(°C)	Tbulk(°C)	t(sec)
1	H78	30.0	3.4	0.82	24.0	25.0	1.0
2	H79		4.8	2.04	23.0	25.0	1.0
3	H80		6.0	4.40	24.0	27.0	1.0
4	H81		7.1	7.55	23.6	28.1	1.0
5	H82		11.3	12.80	24.6	32.6	1.0
6	H83	32.0	12.6	15.40	23.5	33.0	1.0
7	H84	34.0	14.1	18.20	23.9	34.9	1.0
8	H85	36.0	15.1	21.20	25.0	38.0	1.0
9	H86	38.0	16.6	24.50	23.8	38.8	1.0
10	H87	39.0	17.2	26.20	23.5	39.5	1.0

ITER TASK/JB-DPI-3/JAPAN

Continue (Table 4-2.)

920713

92071301	Q=20.38	V=4.33	P=0.382	Tsat=141.97			
	NO.	Vacc(kv)	Iacc(A)	q(MW/m2)	T0(°C)	Tbulk(°C)	t(sec)
	H88	30.0	3.2	0.77	23.0	24.0	1.0
	H89		5.3	2.87	23.0	25.0	1.0
	H90		7.0	7.30	22.8	27.3	1.0
	H91		6.0	4.40	22.0	25.0	1.0
	H92		11.0	12.80	22.5	30.5	1.0
	H93	32.0	12.5	15.40	23.2	32.7	1.0
	H94	34.0	14.2	18.20	21.5	32.5	1.0
	H95	36.0	15.2	21.20	22.0	35.0	1.0
	H96	38.0	16.0	24.50	23.2	38.2	0.93(1.0)
	H97	37.0	15.8	22.80	22.5	36.5	1.0
92071302	Q=70.0	V=14.86	P=0.978	Tsat=178.92			
	NO.	Vacc(kv)	Iacc(A)	q(MW/m2)	T0(°C)	Tbulk(°C)	t(sec)
	H98	30.0	3.0	0.77	23.0	23.4	1.0
	H99		5.1	2.51	23.8	24.5	1.0
	I01		5.9	4.15	23.2	24.4	1.0
	I02		7.0	7.30	22.2	23.7	1.0
	I03		11.5	12.80	23.8	26.8	1.0
	I04	34.0	13.9	15.40	23.5	28.0	1.0
	I05	36.0	15.4	18.20	23.5	29.0	1.0
	I06	38.0	16.8	24.50	22.2	28.2	1.0
	I07	40.0	18.0	28.10	23.0	31.0	1.0
	I08	41.0	19.0	30.00	22.2	30.7	1.0
	I09	42.0	19.2	32.10	23.8	32.8	1.0
	I10	43.0	20.6	34.30	23.8	33.8	1.0
	I11	44.0	21.5	36.60	23.0	33.5	1.0
	I12	45.0	21.9	39.10	23.0	34.8	1.0
	I13	46.0	22.0		22.2	34.0	0.44(1.0)

ITER TASK/JB-DPI-3/JAPAN

Continue (Table 4-2.)

920714

92071401	Q=60.5	V=12.85	P=0.98	Tsat=179.01			
	NO.	Vacc(kv)	Iacc(A)	q(MW/m2)	T0(°C)	Tbulk(°C)	t(sec)
1	I14	30.0	3.1	0.77	24.5	24.9	1.0
2	I15		5.3	2.87	23.0	23.7	1.0
3	I16		6.2	4.91	23.0	24.3	1.0
4	I17		7.1	7.55	23.9	25.4	1.0
5	I18		11.3	12.80	23.8	27.3	1.0
6	I19		7.9	9.31	23.0	25.0	1.0
7	I20	34.0	14.0	18.20	24.0	29.0	1.0
8	I21	36.0	15.5	21.20	24.2	30.2	1.0
9	I22	38.0	17.0	24.50	23.5	31.0	1.0
10	I23	40.0	18.2	28.10	24.2	32.7	1.0
11	I24	42.0	20.3	32.10	24.5	34.5	1.0
12	I25	43.0	20.4	34.30	24.8	35.8	1.0
13	I26	44.0	21.4	36.60	24.2	36.2	1.0
14	H01	45.0	21.4	39.10	25.0	37.8	0.44(1.0)
92071402	Q=47.88	V=10.17	P=0.974	Tsat=178.74			
	NO.	Vacc(kv)	Iacc(A)	q(MW/m2)	T0(°C)	Tbulk(°C)	t(sec)
1	H02	30.0	3.2	0.77	25.0	25.4	1.0
2	H03		5.0	2.35	23.5	24.2	1.0
3	H04		7.1	7.55	24.2	25.9	1.0
4	H05		6.0	4.40	23.5	24.8	1.0
5	H06		11.0	12.80	25.0	28.5	1.0
6	H07		8.2	9.87	24.8	27.8	1.0
7	H08	34.0	14.2	18.20	25.0	30.4	1.0
8	H09	38.0	16.6	24.50	24.5	32.5	1.0
9	H10	41.0	19.2	30.00	23.2	31.2	1.0
10	H11	42.0	19.9	32.10	23.2	34.2	0.84(1.0)
92071403	Q=40.63	V=8.63	P=0.98	Tsat=179.05			
	NO.	Vacc(kv)	Iacc(A)	q(MW/m2)	T0(°C)	Tbulk(°C)	t(sec)
1	H12	30.0	3.2	0.77	24.5	24.9	1.0
2	H13		5.0	2.35	24.5	25.2	1.0
3	H14		6.2	4.91	23.5	24.8	1.0
4	H15		7.0	7.30	23.0	24.7	1.0
5	H16		8.0	9.50	23.5	25.6	1.0
6	H17		11.2	12.80	23.5	27.0	1.0
7	H18	34.0	14.0	18.20	24.8	32.8	1.0
8	H19	38.0	16.7	24.50	24.5	36.0	1.0
9	H20	40.0	18.0	28.10	23.5	35.5	1.0
10	H21	41.0	18.6	30.00	23.0	35.2	0.49(0.5)
11	H22	39.0	17.5	26.20	24.8	36.6	1.0

ITER TASK/JB-DPI-3/JAPAN

Continue (Table 4-2.)

920715

92071501	Q=30.0	V=6.37	P=0.989	Tsat=179.4			
	NO.	Vacc(kv)	Iacc(A)	q(MW/m2)	T0(°C)	Tbulk(°C)	t(sec)
1	H23	30.0	3.0	0.77	23.6	24.0	1.0
2	H24		5.1	2.51	23.0	23.7	1.0
3	H25		5.9	4.15	25.0	26.7	1.0
4	H26		7.1	7.55	23.5	27.0	1.0
5	H27		8.0	9.50	25.2	29.0	1.0
6	H28		11.3	12.80	25.4	32.4	1.0
7	H29	34.0	13.8	18.20	24.3	34.8	1.0
8	H30	36.0	15.0	21.20	24.3	36.3	1.0
9	H31	38.0	16.8	24.50	25.0	36.5	1.0
10	H32	39.0	17.3	26.20	25.0	38.0	0.96(1.0)
92071502	Q=20.1	V=4.27	P=0.984	Tsat=179.18			
	NO.	Vacc(kv)	Iacc(A)	q(MW/m2)	T0(°C)	Tbulk(°C)	t(sec)
1	H33	30.0	3.0	0.77	25.3	26.3	1.0
2	H34		5.0	2.35	25.0	27.0	1.0
3	H35		6.2	4.91	24.2	27.2	1.0
4	H36		6.9	6.96	24.2	28.7	1.0
5	H37		8.1	9.69	25.3	31.3	1.0
6	H38		11.2	12.80	2.8	33.8	1.0
7	H39	34.0	13.9	18.20	25.3	36.3	1.0
8	H40	36.0	15.2	21.20	25.0	38.0	1.0
9	H41	37.0	16.0	22.80	24.0	38.0	1.0
10	H42	38.0	16.1	24.50	26.0	41.0	0.56(1.0)
92071503	Q=47.5	V=10.08	P=1.27	Tsat=190.54			
	NO.	Vacc(kv)	Iacc(A)	q(MW/m2)	T0(°C)	Tbulk(°C)	t(sec)
1	H43	30.0	3.0	0.77	24.8	25.8	1.0
2	H44		5.2	2.69	26.0	28.0	1.0
3	H45		6.1	4.65	25.0	28.0	1.0
4	H46		6.9	6.96	25.0	29.5	1.0
5	H47		7.8	9.10	24.2	30.2	1.0
6	H48		11.0	12.80	24.5	32.5	1.0
7	H49	34.0	13.8	18.20	24.3	35.3	1.0
8	H50	38.0	16.8	24.50	25.3	40.3	1.0
9	H51	40.0	18.4	28.10	25.2	42.2	1.0
10	H52	41.0	19.0	30.00	25.3	43.3	1.0
11	H53	42.0	19.0	32.10	25.6	44.6	0.61(1.0)
92071504	Q=40.75	V=8.65	P=1.28	Tsat=190.9			
	NO.	Vacc(kv)	Iacc(A)	q(MW/m2)	T0(°C)	Tbulk(°C)	t(sec)
1	H54	30.0	2.9	0.77	25.0	26.0	1.0
2	H55		5.2	2.69	24.2	26.2	1.0
3	H56		5.9	4.15	24.0	27.0	1.0
4	H57		6.9	6.96	24.3	29.8	1.0
5	H58		8.0	9.50	25.0	31.0	1.0
6	H59		11.1	12.80	24.3	32.3	1.0
7	H60	34.0	13.9	18.20	25.0	36.0	1.0
8	H61	38.0	16.9	24.50	25.3	40.3	1.0
9	H62	40.0	18.2	28.10	25.0	42.0	1.0
10	H63	41.0	19.3	30.00	25.4	43.4	0.96(1.0)

Continue (Table 4-2.)

92071601	Q=30.0	V=6.37	P=1.27	Tsat=190.36			
	NO.	Vacc(kv)	Iacc(A)	q(MW/m2)	T0(°C)	Tbulk(°C)	t(sec)
1	I64	30.0	3.2	0.77	23.5	24.5	1.0
2	I01		5.0	2.35	23.5	25.5	1.0
3	I02		5.9	4.15	23.5	26.5	1.0
4	I03		7.1	7.55	23.7	28.2	1.0
5	I04		7.8	9.10	23.7	29.7	1.0
6	I05		11.0	12.80	23.5	31.5	1.0
7	I06	34.0	13.8	18.20	25.2	36.2	1.0
8	I07	36.0	15.0	21.20	25.0	38.0	1.0
9	I08	38.0	16.8	24.50	25.2	40.2	1.0
10	I09	39.0	17.3	26.20	24.5	40.5	1.0
11	I10	40.0	17.7	28.10	25.0	42.0	0.52(1.0)
92071602	Q=20.0	V=4.2	P=1.28	Tsat=190.82			
	NO.	Vacc(kv)	Iacc(A)	q(MW/m2)	T0(°C)	Tbulk(°C)	t(sec)
1	I11	30.0	3.2	0.77	25.3	26.3	1.0
2	I12		5.0	2.35	25.3	27.3	1.0
3	I13		5.8	3.92	24.0	27.0	1.0
4	I14		6.8	6.65	25.3	29.3	1.0
5	I15		7.9	9.31	25.5	31.0	1.0
6	I16		11.4	12.80	25.3	32.8	1.0
7	I17	34.0	13.8	18.20	25.4	35.4	1.0
8	I18	35.0	14.2	19.70	25.2	37.2	1.0
9	I19	36.0	15.1	21.20	23.5	36.5	1.0
10	I20	37.0	15.4	22.80	24.8	38.0	0.6(1.0)
92071603	Q=40.25	V=8.45	P=0.981	Tsat=179.05			
	NO.	Vacc(kv)	Iacc(A)	q(MW/m2)	T0(°C)	Tbulk(°C)	t(sec)
1	I21	30.0	3.0	0.77	25.0	26.0	1.0
2	I22		5.0	2.35	27.2	29.2	1.0
3	I23		6.1	4.65	24.0	27.0	1.0
4	I24		7.3	8.02	23.9	28.4	1.0
5	I25		8.1	9.69	23.5	29.5	1.0
6	I26		11.4	12.80	24.5	32.5	1.0
7	I27	34.0	13.7	18.20	23.6	34.6	1.0
8	I28	38.0	16.8	24.50	23.9	38.9	1.0
9	I29	40.0	18.5	28.10	24.0	41.0	1.0
10	I30	41.0	19.4	30.00	25.0	43.0	0.98(1.0)
92071604	Q=30.38	V=6.45	P=1.43	Tsat=196.1			
	NO.	Vacc(kv)	Iacc(A)	q(MW/m2)	T0(°C)	Tbulk(°C)	t(sec)
1	I31	30.0	3.0	0.77	24.0	25.0	1.0
2	I32		5.0	2.35	23.0	25.0	1.0
3	I33		6.1	4.65	23.6	26.6	1.0
4	I34		7.0	7.30	23.4	27.9	1.0
5	I35		8.1	9.69	24.4	30.4	1.0
6	I36		11.3	12.80	24.2	32.2	1.0
7	I37	34.0	14.0	18.20	23.7	34.7	1.0
8	I38	36.0	15.2	21.20	24.3	37.3	1.0
9	I39	38.0	16.6	24.50	24.3	39.3	1.0
10	I40	39.0	17.4	26.20	23.9	39.9	1.0
11	I41	40.0	17.4	28.10	23.9	40.9	0.45(1.0)
92071605	Q=20.25	V=4.3	P1=15.6	P2=14.3	P=14.95	1.47MPa	
	NO.	Vacc(kv)	Iacc(A)	q(MW/m2)	T0(°C)	Tbulk(°C)	t(sec)
1	I42	30.0	3.1	0.77	23.9	24.9	1.0
2	I43		5.0	2.35	24.2	26.2	1.0
3	I44		6.1	4.65	25.1	28.1	1.0
4	I45		7.1	7.30	23.5	28.0	1.0
5	I46		8.2	9.69	24.0	30.0	1.0
6	I47		11.4	12.80	24.6	32.6	1.0
7	I48	34.0	14.0	18.20	23.7	34.7	1.0
8	I49	35.0	14.6	21.20			1.0
9	I50	36.0	15.3	24.50	24.9	37.9	1.0
10	I51	37.0	15.7	26.20	37.2	37.2	0.64(1.00

Continue (Table 4-2.)

920717

92071701	Q=60.0	V=12.74	P=0.78	Tsat=169.37			
	NO.	Vacc(kv)	Iacc(A)	q(MW/m2)	T0(°C)	Tbulk(°C)	t(sec)
1	I52	30.0	3.2	0.77	25.0	26.0	1.0
2	I53		5.1	2.51	23.5	25.5	1.0
3	I54		6.1	6.65	23.5	26.5	1.0
4	I55		7.0	7.30	24.3	28.8	1.0
5	I56		8.1	9.69	25.0	31.0	1.0
6	I57		11.3	12.80	24.2	32.2	1.0
7	I58	34.0	14.0	18.20	23.7	34.7	1.0
8	I59	38.0	16.4	24.50	24.8	39.8	1.0
9	I60	40.0	18.2	28.10	24.2	41.2	1.0
10	I61	42.0	19.7	32.10	24.0	43.0	1.0
11	I62	43.0	20.6	34.30	23.5	43.5	1.0
12	I63	44.0	21.5	36.60	24.8	45.8	0.6(1.0)

920722

92072201	Q=47.25	V=10.03	P=0.79	Tsat=169.89			
	NO.	Vacc(kv)	Iacc(A)	q(MW/m2)	T0(°C)	Tbulk(°C)	t(sec)
1	H01	30.0	3.0	0.77	30.6	31.4	1.0
2	H02		5.2	2.69	30.0	31.6	1.0
3	H03		6.3	5.18	30.6	33.0	1.0
4	H04		7.1	7.55	30.0	33.5	1.0
5	H05		8.1	9.69	31.0	35.3	1.0
6	H06		11.4	12.80	31.0	36.5	1.0
7	H07	34.0	17.0	18.20	31.0	38.5	1.0
8	H08	38.0	18.3	24.50	30.0	40.0	1.0
9	H09	40.0	19.2	28.10	31.0	42.1	1.0
10	H10	41.0	20.0	30.00	31.0	44.5	1.0
11	H11	42.0	20.0	32.10	30.1	44.1	1.0
12	H12	43.0	20.7	34.30	23.7	38.2	1.0
13	H13	44.0	21.2	36.60	30.9	45.4	0.84(1.0)
92072202	Q=40.5	V=8.59	P=0.785	Tsat=169.63			
	NO.	Vacc(kv)	Iacc(A)	q(MW/m2)	T0(°C)	Tbulk(°C)	t(sec)
1	H14	30.0	2.9	0.77	30.1	30.9	1.0
2	H15		4.9	2.19	30.6	31.7	1.0
3	H16		6.0	4.40	30.1	32.6	1.0
4	H17		7.1	7.55	29.9	33.1	1.0
5	H18		8.0	9.50	29.8	33.6	1.0
6	H19		11.2	12.80	30.9	36.4	1.0
7	H20	34.0	13.8	18.20	30.4	38.6	1.0
8	H21	38.0	16.7	24.50	30.9	41.9	1.0
9	H22	40.0	18.0	28.10	29.9	43.4	1.0
10	H23	41.0	18.8	30.00	30.1	44.1	1.0
11	H24	42.0	19.8	32.10	29.9	44.4	0.88(1.0)

ITER TASK/JB-DPI-3/JAPAN

Continue (Table 4-2.)

920723

92072301	Q=30	V=6.37	P=0.785	Tsat=169.63			
	NO.	Vacc(kv)	Iacc(A)	q(MW/m2)	T0(°C)	Tbulk(°C)	t(sec)
1	H25	30.0	3.1	0.77	29.9	30.8	1.0
2	H26		5.0	2.35	28.7	31.0	1.0
3	H27		5.8	3.92	29.9	32.4	1.0
4	H28		7.1	7.55	29.9	33.9	1.0
5	H29		7.8	9.10	29.0	34.2	1.0
6	H30		11.0	12.80	29.9	37.8	1.0
7	H31	34.0	14.0	18.20	29.4	40.4	1.0
8	H32	36.0	15.0	21.20	30.1	43.4	1.0
9	H33	38.0	16.5	24.50	30.3	45.3	1.0
10	H34	39.0	17.5	26.20	29.4	44.9	1.0
11	H35	40.0	17.8	28.10	29.7	45.7	0.6(1.0)
92072302	Q=20.0	V=4.11	P=0.795	Tsat=170.15			
	NO.	Vacc(kv)	Iacc(A)	q(MW/m2)	T0(°C)	Tbulk(°C)	t(sec)
1	H36	30.0	3.1	0.77	30.0	31.0	1.0
2	H37		5.2	2.69	29.0	31.2	1.0
3	H38		6.3	5.18	29.4	31.9	1.0
4	H39		6.8	6.65	30.3	35.0	1.0
5	H40		8.0	9.50	29.4	36.9	1.0
6	H41		11.4	12.80	30.4	41.9	1.0
7	H42	34.0	13.7	18.20	29.4	46.4	1.0
8	H43	36.0	15.2	21.20	30.1	49.1	1.0
9	H44	37.0	15.8	22.80	29.7	49.7	1.0

ITER TASK/JB-DPI-3/JAPAN

Continue (Table 4-2.)

070901

ch	H20	H21	H22	H23	H24	H25	H26	H27	H28	H29	H30
TP1	39.4	76.1	136.4	233.7	252.2	269.3	284.3	303.1	312	321.2	326.3
TP2	40.6	85	171.8	262.4	281.3	296.1	313.9	339.8	351.1	362.5	379.6
TP3	41.2	92.1	199.8	269.7	289	303.3	320.5	348.1	359.2	371.9	401.8
TP4-1	32.1	50.9	88.3	121.9	131	138.7	147.1	159.8	163.5	168.8	172.1
TP4-2	35.8	67.8	129.8	188.6	205.3	218.2	233.4	253.3	261.2	268.9	278.3
TP4-3	0	0	0	0	0	0	0	0	0	0	0
TP4-4	0	0	0	0	0	0	0	0	0	0	0
TP4	42.4	87.6	175.3	257.5	274.2	289.2	305.2	327.3	337.3	348.5	372.2
TP4-5	40.6	88.6	182.1	278.8	302.7	322.8	346.5	377.3	389.5	404.5	429.2
TP4-6	37	69.6	132.8	199.6	214.5	233.3	248.6	269.1	277.6	285.1	292.6
TP4-7	32.7	55.7	100	148	163.1	174.2	189.9	206.7	214.7	221.3	227.7
TP4-8	30.3	43.6	69.8	97.5	104.9	112	120.2	130.9	135	138.3	141.5
TP4-9	28.5	36.9	52.9	71.5	75.8	78.8	83.5	91.1	93.4	96.2	97.1
TP4-10	28.4	32.6	43.9	55.2	57.9	60.9	64	69.7	71.5	73.1	73.9
TP4-11	27.8	31.9	40.2	52.1	53.5	55.3	57.8	63	64.2	67.1	68.6
TP4-12	27.2	31.4	40.2	50.2	52.4	54.7	58.4	62.4	64.3	65.3	68
TP5	40.6	81.4	155.9	246.6	263.9	278.4	293.2	313.2	322.7	333.7	348.2

070902

ch	H32	H33	H34	H35	H36	H37	H38	H39	H40	H41	H42	H43
TP1	42.2	78	147.3	110.5	245.6	217	259.4	272.3	287.7	304.3	311.8	317.5
TP2	41.6	85.8	184.2	130.6	264.5	256.8	283	297.8	317.3	346.3	355	397.2
TP3	42.2	92.3	212.2	146.6	266.9	262.2	286.6	303.2	325.6	360.4	369.5	654.3
TP4-1	33.1	53.4	96.1	73.6	127.5	124.6	139.1	146.8	156.9	168.4	170.6	197.2
TP4-2	36.8	69.2	140.2	101.6	193.1	186.6	211.9	226	242.2	260.5	265.3	374.6
TP4-3	0	0	0	0	0	0	0	0	0	0	0	0
TP4-4	0	0	0	0	0	0	0	0	0	0	0	0
TP4	42.9	88.8	186.6	132.4	258.3	248.7	277.7	291.3	310.8	337.5	347.3	618
TP4-5	43.4	90	193.2	136.4	281.3	267.7	305.6	328.1	353.8	386	397.5	590.3
TP4-6	38	71	141.9	103.9	206.5	195.1	226.5	241.2	257	275.2	280.9	365.2
TP4-7	33.7	57.6	108.5	81.3	155.4	146.6	171.6	185	201.4	217.2	221.2	237
TP4-8	31.8	45.5	76.5	59.8	104.8	98.5	114.2	120.2	129.6	139.6	142.5	142.2
TP4-9	29.5	39.5	58.7	47.7	76.4	73.1	82.2	86.4	92.2	99.4	101.6	98.9
TP4-10	28.2	34.5	48.3	41.5	60.2	58	64.4	66.2	72.1	76.9	79	76.4
TP4-11	28.7	32.8	45.8	39.7	55.9	53.7	58.9	60	65.4	69.6	72.4	69.3
TP4-12	28.2	33.9	45.9	39.1	54	54.4	59.5	59.4	65.5	69.7	71.9	68.7
TP5	41	82.8	165.9	120.5	246.8	234.1	265.6	279.5	295.9	320.9	330.8	497.6

ITER TASK/JB-DPI-3/JAPAN

Continue (Table 4-2.)

070903.

ch	H44	H45	H46	H47	H48	H49	H50	H51	H52	H53	H54
TP1	44	88.4	128	167.8	213.4	251.1	264.9	279	286.1	305.6	308
TP2	44.1	96.7	152.3	210.5	246.4	272.5	287.6	305.6	318.5	344.7	391.4
TP3	44.1	106.1	174.1	233.6	253.7	276.1	291.8	312.2	329.1	362.2	666.4
TP4-1	34.8	60.2	88.1	113.4	127	143	151.5	160.7	164.1	172.2	206.4
TP4-2	38.6	79.5	121.4	161.7	184.2	209.1	224	237.6	244.2	259.4	381.5
TP4-3	0	0	0	0	0	0	0	0	0	0	0
TP4-4	0	0	0	0	0	0	0	0	0	0	0
TP4	43.4	99.1	157	213.5	242.8	268.9	284.1	298.5	313.3	341.7	615.6
TP4-5	44.6	100.8	160	218.4	257.4	294	313.7	335.9	353.6	383.6	584.5
TP4-6	39.8	80.1	122.6	163.5	192.7	223.7	238.7	251	258.7	274.1	358.2
TP4-7	35.4	65.2	97.1	127.2	149	174.8	188.5	202.2	208	219.7	235.1
TP4-8	32.4	51.2	70.9	89.1	103.2	120.3	128.9	136.2	141.4	149.4	145.2
TP4-9	30.7	42.2	57.7	69.6	78.9	90.2	96.3	100.8	104.7	110.7	105.5
TP4-10	29.5	37.3	48.5	57.4	62.8	71.1	75.5	79.3	83.3	88.2	81.7
TP4-11	29.3	36.6	45.5	53.2	58.7	65.8	69.7	73.4	76.2	82.3	75.7
TP4-12	29.3	36.6	45.6	53.3	58.7	64.6	68.5	72.3	75	81.7	74.7
TP5	43.3	93.7	141.5	188.5	225.6	256.7	272.2	287.3	303	325.7	493

071001

ch	H55	H56	H57	H58	H59	H60	H61	H62	H63	H64
TP1	44.9	101.8	193.5	127.9	259.2	271.8	281.7	296.3	305.8	314.2
TP2	45.4	112.4	228.8	149.1	279.8	296.2	311.8	332.5	344.2	361.9
TP3	46.1	123.7	238.1	169.6	283.9	306.2	326	350.9	369.4	557.1
TP4-1	35.1	72.2	129.1	94	162.3	170.5	177.4	183.5	185.9	196.3
TP4-2	41.8	94	175.7	124.8	225.6	238.8	249.4	264	271.9	300.5
TP4-3	0	0	0	0	0	0	0	0	0	0
TP4-4	0	0	0	0	0	0	0	0	0	0
TP4	48.7	119.3	228.3	156.9	276.3	292	310.6	333.7	354.8	390.1
TP4-5	48.1	119.9	238.7	157.5	302.3	323.4	344.9	371.8	389.7	415
TP4-6	42.4	97.1	187.9	125.4	240.4	251	259.6	272.6	280.8	292.7
TP4-7	37	76.9	149.8	100.5	198.9	211.4	220.1	228.6	232.2	241.4
TP4-8	33.3	60.1	110	75.6	144.4	152.4	158.5	162.8	165.1	170.1
TP4-9	30.8	51.1	85.6	62.4	112.8	117.9	124.7	127	128	132.9
TP4-10	29.1	44.4	71.4	54.5	91.5	96	101.6	106.9	106.2	108.6
TP4-11	28.5	42.6	66.1	51.6	85.1	88.9	93.8	97.4	100.3	101.5
TP4-12	29.7	42	65.6	51.5	82.1	87.1	92.1	96.8	97.3	100.4
TP5	46.1	109.5	212.4	142	266	278.9	301.1	318.9	332.9	353.8

071002.

ch	H65	H66	HH67	H68	H69	H70	H71	H72	H73	H74	H75	H76	H77
TP1	38.4	73.5	146.1	113.9	239.2	183.1	251.7	266.4	281.5	297.7	306.6	319.4	326.8
TP2	38.9	79.4	181.7	135.2	260.6	225.9	274.3	292.7	312.3	338.5	352.2	367.7	384.2
TP3	38.9	86.5	208.6	152.4	264.9	233.7	279.6	299.8	325.2	353.2	373.4	399	585.2
TP4-1	31.7	50.5	96.9	77.2	132	111.9	139.4	149	157.8	164.7	166.7	173.6	178.8
TP4-2	34.6	65.8	140.2	107.2	198.3	164.2	210.9	225.4	239	253.2	260.6	272.4	290.6
TP4-3	0	0	0	0	0	0	0	0	0	0	0	0	0
TP4-4	0	0	0	0	0	0	0	0	0	0	0	0	0
TP4	39	81.2	187.4	140	256.9	223.3	268.2	286.1	305.7	332.6	348.8	367.7	397.8
TP4-5	39.7	82.9	192.2	142.4	282.3	233.7	299.8	322.8	347.2	378.8	396.7	415.9	441.5
TP4-6	36.5	66.9	143.2	108.5	211.1	171.5	224.2	239.6	253.6	268.4	275.2	287.9	296.5
TP4-7	32.3	55.4	110	86	164.2	131.4	174.9	188.9	204.1	214.7	219.7	229.8	235.6
TP4-8	29.9	43.9	76.7	64	111.8	89.9	116.9	126.4	134.1	140.8	143.3	149	149.8
TP4-9	29.2	38.4	59.9	49.9	82.2	67.8	84.7	93.1	97.3	102.2	103.5	107.4	105.9
TP4-10	27.4	33.5	49	42.7	64.9	54	67	72.4	75.9	79.7	80.4	80.6	80.4
TP4-11	26.8	32.9	45.4	40.3	58.9	50.6	60.3	66.4	68.8	73.1	73.9	77.8	72
TP4-12	27.4	33.5	46	40.9	58.8	50.3	60.3	64.6	69	72	73.9	77.2	72.1
TP5	38.3	80	164.7	127.6	244.1	204.5	256.6	271.9	290.3	314.2	328	343.7	361.6

Continue (Table 4-2.)

071003.

ch	H78	H79	H80	H81	H82	H83	H84	H85	H86	H87
TP1	44	72.7	113.4	158.1	241.5	254.4	270	283.1	299.1	310.7
TP2	43.4	78.5	132.3	198.4	263.4	278.7	298.6	319.3	343.6	357.9
TP3	44.1	84	148.4	217.9	266.5	285.9	313	334.1	367.8	490.1
TP4-1	34.9	51	77.8	106.5	141.3	148.5	157.8	164.4	169.9	175.1
TP4-2	39.2	65.4	105.6	152.2	205.3	217.7	232.2	245.4	258.3	269.5
TP4-3	0	0	0	0	0	0	0	0	0	0
TP4-4	0	0	0	0	0	0	0	0	0	0
TP4	44.7	82.4	138.4	202.7	258.5	273.3	293.5	313.9	344.3	360.6
TP4-5	44.7	83.6	140.3	206.4	285.1	305.5	330.8	354.1	385.8	404.3
TP4-6	39.8	67.3	108	155.7	218.2	231.2	246.3	258.3	271.8	280.4
TP4-7	34.9	55.2	86.1	121.3	174.4	186.1	199.3	210.7	220.5	228.8
TP4-8	31.9	43.7	62.9	86.3	121.7	127.8	136.4	143.5	148.3	152.7
TP4-9	30.1	38.8	51.3	67.9	90.8	94.4	100.8	107.3	108.9	114.7
TP4-10	28.2	33.3	44.1	55.2	71.9	74.9	79.5	84.8	87.7	89.7
TP4-11	28.2	33.9	41	51.6	66.5	68.4	72.9	79.4	80.6	82.7
TP4-12	28.2	33.3	42.2	50.9	65.3	67.8	72.4	77.7	80.6	80.9
TP5	43.4	78	125.3	178.8	246.3	260.4	279.6	298.5	322.2	337.4

ITER TASK/JB-DPI-3/JAPAN

Continue (Table 4-2.)

071301.

ch	H88	H89	H90	H91	H92	H93	H94	H95	H96	H97
TP1	46.1	98.2	185.4	139.3	245.5	260.1	269.4	284.9	305.1	295.4
TP2	46	110.5	210.3	168.6	265	281.3	296.8	321.5	354.7	337.6
TP3	49.8	121.3	220.2	194.4	268.1	290.1	305.3	344.3	582.6	370.6
TP4-1	37	72	118.8	103.1	153.5	162.5	166.4	172.3	210.8	178.9
TP4-2	41.2	94	161.5	139.9	214.3	227.3	235.9	251	369.9	265.6
TP4-3	0	0	0	0	0	0	0	0	0	0
TP4-4	0	0	0	0	0	0	0	0	0	0
TP4	50.4	117.1	211.6	178.5	260.8	277.7	293	324.9	563.7	348.3
TP4-5	50.4	117.7	220.1	179.7	286.5	307.3	326.7	360.3	506.6	381
TP4-6	43.1	95.2	175.5	141.7	226.5	239.5	248.1	263.3	302.5	271.6
TP4-7	37.6	76.8	141.3	112.6	190.5	202.9	209.7	219.3	242.4	226.5
TP4-8	33.9	60.6	105.1	84.1	139.2	146.4	150.7	155.9	169.9	161.8
TP4-9	31.5	51	83.2	68.1	108.9	116.2	118	122.7	131.6	127.4
TP4-10	29.1	44.9	68.9	56.7	88.8	94.3	95.5	100.8	107.8	105.4
TP4-11	29.1	43	64.1	54.2	81.1	86.5	88.4	94.4	99.6	98.4
TP4-12	29.1	43	63.5	54.8	79.3	84.9	87.2	92.5	98.5	97.2
TP5	47.9	108.3	196.3	156.5	249.7	265.1	280.8	306.8	341.1	323.3

071302.

ch	H98	H99	I01	I02	I03	I04	I05	I06	I07	I08	I09	I10	I11	I12	I13
TP1	34.5	63.3	79.4	111.6	201.6	256.8	288.1	318.3	341	353.8	362.9	373.4	379.6	394	397.4
TP2	35.1	67.5	90.6	135.9	233.4	304.1	332.6	358.9	384.2	399.1	412.3	423.4	435.4	456.9	484.9
TP3	35.2	72.2	98.3	152.6	244.3	316.4	345.1	371.3	398.9	413.3	428.4	445.8	462.3	486.7	591.3
TP4-1	28.5	41.4	49.9	66.5	101.4	125.4	135.4	147.2	158.7	165.3	171.7	176	181.3	188.6	185.4
TP4-2	30.8	54.1	69.8	101.4	164.5	209.9	231.8	254.4	277.6	289.8	300.9	308.6	317.9	332.7	342
TP4-3	0	0	0	0	0	0	0	0	0	0	0	0	0	0	0
TP4-4	0	0	0	0	0	0	0	0	0	0	0	0	0	0	0
TP4	35.2	68	91.2	136.6	228.5	295.8	327.3	353.9	380.4	394.2	404.7	415.8	431.6	451	494.7
TP4-5	35.8	71	95.3	145.6	246.1	321.9	360.9	396.4	432.6	451.9	468	481.8	500.5	522.4	554
TP4-6	32.1	56	72.2	103.8	171	218.5	244.1	269.6	295.4	307.6	319.2	328.7	338.6	352.2	355.5
TP4-7	29.1	46.3	57.9	79.6	128.1	161	178.7	196.9	216.1	227.5	240.7	249.2	256.3	267.9	267.7
TP4-8	27.2	37.2	42.6	54.4	81.2	98.7	108.8	117.6	128.4	133	139.9	144.7	148.6	153.9	151.4
TP4-9	25.3	31.6	36.6	41	57.8	68.3	73	77.7	84.4	87.1	91.1	94.1	95.8	99.3	94.9
TP4-10	25.4	29.3	31.1	35	46.3	50.8	53.8	56.8	62.5	61.7	65.6	67.4	68.4	71.4	65.2
TP4-11	25.4	28.6	29.9	32.5	42.6	47.2	49	51.4	55.2	56.2	59.7	60.8	61.3	63.7	58.1
TP4-12	25.4	29.2	30.5	32.5	42	46.6	48.4	50.2	53.9	55.6	59	60.3	60.6	63.1	58.7
TP5	35.1	66.8	85.8	125.3	219.4	283.4	309.4	334.3	356.8	368.8	379.7	390.2	403.3	419.1	453.8

ITER TASK/JB-DPI-3/JAPAN

Continue (Table 4-2.)

071401.

ch	I14	I15	I16	I17	I18	I19	I20	I21	I22	I23	I24	I25	I26	H01
TP1	36.6	63.7	84.5	111.5	215	136.1	272	303.1	321.9	344	361.3	373.2	384.2	388
TP2	35.5	68.5	96.9	135.9	255.9	167.9	311.8	337.4	360.8	385.9	408.2	427.7	443.4	467.4
TP3	36	71.4	106.5	151.9	266.9	186.8	323.1	347.4	370.8	395.6	429.9	453.2	481.2	608
TP4-1	29.3	41.1	52.7	68.1	111.3	80.2	133	145.5	155	167.3	177.2	185	189.9	187
TP4-2	31.8	54.6	74.4	101.4	180.9	123.7	220.7	242.9	263	284.7	300.4	316.1	327.4	338.2
TP4-3	0	0	0	0	0	0	0	0	0	0	0	0	0	0
TP4-4	0	0	0	0	0	0	0	0	0	0	0	0	0	0
TP4	35.5	69	97.6	135.9	249.2	166.7	307.7	332.7	355.7	378.2	402.6	422.6	442.5	490.6
TP4-5	36	71.4	102.5	143	265.7	174.7	333.1	366.7	397	428.8	459.1	484.5	506.7	540.5
TP4-6	33	55.9	76.8	104.4	187	125.4	231.1	256.9	278.6	302.5	319.4	334.5	345.1	348.9
TP4-7	30.6	46.1	61.2	80.6	139.3	95.7	170.1	189.2	207.3	227.7	244.4	256.8	266	265
TP4-8	28.2	36.9	45.4	56.6	88.7	64.3	106.2	116.6	125.4	137.3	145.9	151.6	156.9	154.8
TP4-9	27.5	31.5	37	44.5	63.3	49.2	73	79.8	85	91.7	97.3	101.1	104.1	99.5
TP4-10	25.7	28.5	31.5	37.2	49.4	40	55.6	59.4	63.1	67.9	71.8	74.4	76.2	71
TP4-11	26.2	27.9	31.5	34.8	46.3	38.2	51.3	54	56.9	60	64	67.8	69	62.7
TP4-12	26.2	27.8	30.3	36	44.4	36.9	50.7	53.2	56.2	59.3	64.6	66.8	68.5	63.3
TP5	36.1	68.5	91.5	124	236.4	152.2	292.2	316.1	336.2	358.6	379.8	395.9	412.1	453.6

071402.

ch	H02	H03	H04	H05	H06	H07	H08	H09	H10	H11
TP1	38.4	67.2	134.3	96.9	237	169.7	292	326.5	350.6	353
TP2	39.6	72.5	164.9	112.9	279.5	214.8	321.1	362.4	395.3	409.4
TP3	39.6	77.9	185	124.3	285.3	232.5	328	371.5	424.1	565.7
TP4-1	31.1	44.8	84.4	61.8	127.4	102.3	147.7	168.7	182	183.4
TP4-2	35.4	58.1	125.5	86.7	200.4	156.3	236.4	274.3	297.3	311.5
TP4-3	0	0	0	0	0	0	0	0	0	0
TP4-4	0	0	0	0	0	0	0	0	0	0
TP4	39.6	75.1	166.1	114.8	272.3	208.8	316.3	355.9	395.7	450.4
TP4-5	39.6	76.8	171	118.4	285.3	216.7	346.5	398.9	446.9	481.6
TP4-6	36	59.4	128.5	89.7	205.9	158.1	251	290.3	313.9	317.4
TP4-7	32.3	49.7	98.1	70.6	154.1	121.2	187.6	223.5	244.9	248.5
TP4-8	29.9	39.3	68.5	52.5	100.2	81.5	120.8	140.6	151.7	153.5
TP4-9	28.7	34.5	52.1	42.4	72.8	61.3	85.9	97.9	104.8	104.8
TP4-10	27.4	30.8	43.1	36.3	57.9	50.2	65.7	73.5	78.2	78.8
TP4-11	27.4	29.6	40.6	35	53	46.1	60.1	66.9	71	70.3
TP4-12	27.4	29.6	41.1	35.1	52.3	46	58.4	65.8	69.2	69.8
TP5	39.6	70.6	151	106.2	259.6	191.7	302.1	338.9	369.9	397.2

ITER TASK/JB-DPI-3/JAPAN

Continue (Table 4-2.)

071403.

ch	H12	H13	H14	H15	H16	H17	H18	H19	H20	H21	H22
TP1	40.9	75.3	108.2	138.5	175	253.8	295.3	320.5	337.3	343.3	334.5
TP2	41.5	80.6	125.3	171	218.5	284	323.8	359.5	383.5	402.8	376.7
TP3	40.9	84.7	137.8	192.9	240.4	291.7	330.2	379.1	465.5	596.5	400.9
TP4-1	32.4	49.4	70.1	89.2	108.1	134.7	156.2	173.7	179.9	180.1	181.2
TP4-2	36.7	65.8	98	130.8	161.1	208.7	244.1	273.7	298.8	319.7	287
TP4-3	0	0	0	0	0	0	0	0	0	0	0
TP4-4	0	0	0	0	0	0	0	0	0	0	0
TP4	40.8	81.8	126.5	172.8	214.8	281.1	317.8	351.3	419.6	496.3	374.8
TP4-5	42	83.6	128.9	177.1	221.5	297.1	347.9	393.1	443.4	498	418.9
TP4-6	37.3	67.6	99.8	132.6	162.3	217.2	258.7	287.9	304.7	312.5	302.4
TP4-7	33.5	55.4	79	102.8	125.3	164.2	198.2	227.2	238	237.4	238.7
TP4-8	31.1	44.5	57.6	72	85.5	109.2	130.2	147	151.4	147.3	153.3
TP4-9	28.8	37.9	46.6	55.9	64.8	79.6	93.4	105	107.5	99.9	108.3
TP4-10	27.5	34.1	39.8	45.5	52.5	62.4	72.1	80.7	81.5	74.4	83.4
TP4-11	27.4	32.9	38	42.4	48.4	56.4	66.1	72.9	74.4	66.6	76.2
TP4-12	26.9	32.9	38	43	48.3	56.2	64.9	71.8	73	66	75.1
TP5	41.4	78.9	118.2	156.2	196.3	267.1	304.3	335.4	370.7	402.2	352.8

071501.

ch	H23	H24	H25	H26	H27	H28	H29	H30	H31	H32
TP1	39.9	82.8	113.3	157.4	197.5	270.9	296.7	306.7	322.3	333.5
TP2	40.6	89.2	129.8	192.8	250.6	291.8	325.7	342.9	362.3	378
TP3	41.2	96.2	143.3	221.5	261.6	297	329.9	360.5	388.3	565.7
TP4-1	32.6	57	77.5	104.5	127	152.8	170.3	178.2	183.8	197.9
TP4-2	35.8	74.4	105.5	149.7	185.4	225.2	257	268.6	281.3	316.9
TP4-3	0	0	0	0	0	0	0	0	0	0
TP4-4	0	0	0	0	0	0	0	0	0	0
TP4	43.1	92.1	134.4	197.7	246.3	289.3	319.8	340.6	364.6	481
TP4-5	43.1	92.6	135.1	201.4	253.7	309.4	353	372.8	401.1	484.4
TP4-6	37.6	75	106.6	153.8	193.3	239.9	270.5	279.4	293.2	318.1
TP4-7	33.3	61.2	85.2	121.1	148.9	187.4	216.2	227	238.1	254.7
TP4-8	30.8	48.4	63.8	87.3	106.2	130.8	147	153.9	160.6	169.3
TP4-9	28.5	40.7	52.4	67.8	80.8	97.6	109.5	114.3	119.7	124.5
TP4-10	27.3	36.3	44.5	56.2	65.2	78.5	85.8	89.4	94.8	97.2
TP4-11	27.8	34.5	43.2	52.7	60.6	72.1	78.7	82.3	88.3	88.8
TP4-12	27.3	35.1	43.1	50.9	61.1	70.9	76.2	81.1	85.2	88.3
TP5	41.2	88.7	121.3	178	225	277	306.1	319.2	344.8	362.9

ITER TASK/JB-DPI-3/JAPAN

Continue (Table 4-2.)

071502.

ch	H33	H34	H35	H36	H37	H38	H39	H40	H41	H42
TP1	44.8	93	139	176.4	240.9	274.4	299.4	304.5	308.2	314.9
TP2	46	102.5	164.9	223.4	264.2	294	328.5	341.2	349.1	364.5
TP3	49.6	111.5	186.2	243.5	273.2	297.4	349.6	370.4	387.1	602.7
TP4-1	36.8	67.5	101.6	127.2	148.5	170.6	183.5	184.6	185.3	200.1
TP4-2	41.7	87.7	136.7	175.2	207.4	239.1	262.9	271.2	279.1	357.5
TP4-3	0	0	0	0	0	0	0	0	0	0
TP4-4	0	0	0	0	0	0	0	0	0	0
TP4	49.5	108.5	171.5	228.9	262.8	289.2	328.4	347.1	363.2	557.8
TP4-5	49.6	107.3	171.5	230.1	275.1	312.8	355.5	374.5	390.5	515.6
TP4-6	41.7	88.3	136.7	180.7	220.9	252.4	276.3	279	283.3	313.7
TP4-7	38.1	72.8	109.9	142.1	177.4	209	228	232.7	235.4	239.1
TP4-8	33.8	58.4	82.8	105.8	130.2	152.5	165.2	167.4	167.1	161.7
TP4-9	32.6	50	67.9	83.9	102.8	119.4	129.6	131.6	131.2	121.3
TP4-10	30.8	43.3	57.1	69.1	83.8	95.6	105.2	109	108.6	97
TP4-11	30.2	41.9	54.5	65.5	77.2	89	97.4	100.6	99.8	89.8
TP4-12	30.2	42.5	55.7	65.5	76.7	88.5	95.2	99.6	99	89.3
TP5	46.6	100.6	152.7	201.3	247.1	280.4	313.6	331.1	350.3	423.2

071503.

ch	H43	H44	H45	H46	H47	H48	H49	H50	H51	H52	H53
TP1	37.6	70.9	96.6	124.5	158.7	234.1	299	338.5	349.1	356.2	356.5
TP2	37.6	77.4	112	151.8	198.4	277.3	329.2	375.4	391.6	405.1	421
TP3	36.4	80.8	123.3	168.1	217.3	288.7	340.6	386.5	418.8	436.3	579.2
TP4-1	30.3	48.5	62.1	78.8	96.3	125.8	149.9	172.6	180.5	183	185.8
TP4-2	33.3	63.1	87.1	116.2	145.7	199.9	241.2	284.6	296.4	304.8	318.1
TP4-3	0	0	0	0	0	0	0	0	0	0	0
TP4-4	0	0	0	0	0	0	0	0	0	0	0
TP4	37	77.9	113.8	152.4	194.1	268.9	325.3	371.5	389.8	406.6	443.2
TP4-5	36.4	79.7	117.4	157.2	201.5	284.6	351.8	414.5	437.4	454.9	483.6
TP4-6	34.5	64.9	89.5	118	148.6	204.2	252.2	299.4	311.8	319.5	323.4
TP4-7	31.5	53.4	71.6	91.3	113.6	153	188.7	229.3	243.2	248.9	252.1
TP4-8	29.1	43.5	53	64.6	77.4	100.8	121.3	143.8	152	154.3	155.9
TP4-9	27.9	37.6	43.3	50.6	58.2	72.9	85.2	99.8	105.1	107.6	106.1
TP4-10	27.9	32.7	36.6	42.7	47.3	56.8	65	76.1	79.6	80.8	79.4
TP4-11	27.2	33.8	35.3	39.6	43.7	51.9	59.5	67.8	71.8	73.7	71.1
TP4-12	27.2	33.2	35.8	40.1	44.2	51.9	59.4	67.3	71.3	73.2	70.5
TP5	38.2	76.2	106.7	139.3	179.5	261.5	309.1	352.2	368.9	384.1	413.6

ITER TASK/JB-DPI-3/JAPAN

Continue (Table 4-2.)

071504.

ch	H54	H55	H56	H57	H58	H59	H60	H61	H62	H63
TP1	37.8	75.1	99	132.7	171.7	250.9	303.3	338	347.2	351.1
TP2	38.4	82.2	114	161.3	214.4	291.3	332.9	371.9	390.8	404.6
TP3	40.8	86.3	124.7	180.1	235.2	299.6	341.6	381.6	422.1	570.9
TP4-1	31.6	50.4	64.2	85.2	106.6	137.4	158.8	179.8	183.8	188
TP4-2	34.7	66.1	89.1	124.4	158.9	212.5	251	286.4	296.8	312.6
TP4-3	0	0	0	0	0	0	0	0	0	0
TP4-4	0	0	0	0	0	0	0	0	0	0
TP4	40.2	83.3	117	161.8	211.3	286	328.1	366	393.1	428.3
TP4-5	41.4	84.5	118.8	166.7	219.8	300.2	357.5	409	437.2	463.7
TP4-6	35.4	67.9	90.8	126.2	161.4	219.9	264.5	301.8	310.4	315.5
TP4-7	31.7	55.7	72.4	97.6	124.4	165	202.2	234.8	245.4	250.1
TP4-8	30.4	44.2	54.4	69.8	85.9	109.5	131	150.8	155.9	159.2
TP4-9	28.7	37.6	44.7	54.7	65.2	79.9	94.8	106.9	110.2	113
TP4-10	27.4	33.9	38.6	45.6	52.9	62.6	72.9	81.4	84.7	85.7
TP4-11	27.9	32.1	36.2	42.6	48.7	57.7	66.3	73.2	77.6	78.5
TP4-12	28	32.6	36.7	42.4	49.9	57	66.3	73.2	77	77.4
TP5	39.5	80.4	108.6	149.8	196	274.7	313.9	349.2	371.1	402.3

071601.

ch	H64	I01	I02	I03	I04	I05	I06	I07	I08	I09	I10
TP1	41.1	79.1	108.8	152.9	186.8	276.8	307.6	321.6	329	337.2	344.8
TP2	41.2	85	124.2	185.1	232	300	337.3	354.1	370.7	381	394.3
TP3	40.4	92.3	137.9	209.5	258.9	307.9	340.6	376.9	397.8	456.1	594.9
TP4-1	31.9	55.1	73	102.4	120.7	152.5	176.2	183.2	186.5	189.5	193
TP4-2	36.9	70.2	100.4	145.1	175.3	229.4	264.7	279	288.6	302.1	319.3
TP4-3	0	0	0	0	0	0	0	0	0	0	0
TP4-4	0	0	0	0	0	0	0	0	0	0	0
TP4	41.1	88.7	129	189.4	231.6	297.2	330.6	349.5	373	404.9	462.5
TP4-5	40.5	89.3	130.8	193.6	237.6	316.7	361.7	386.8	410.7	430.4	471.6
TP4-6	38	73	102.2	148.1	180.2	242.8	279.2	293.8	300.5	304.5	316.3
TP4-7	33.2	59.3	81.3	116	139.7	189.7	221.9	235.7	243.2	248.6	252.2
TP4-8	31.4	46.5	61.1	83.3	98.7	130.7	150.7	158.2	163.9	166.9	163.7
TP4-9	29	40.5	50.3	65.6	75.7	97.4	111.6	116.8	121.1	122.8	116.2
TP4-10	27.2	36.2	43	54.7	62	77.3	87.9	91.2	95	95.5	88.3
TP4-11	27.7	35	41.7	51.7	57.1	70.8	79.5	84.2	86.7	87.1	79.4
TP4-12	27.7	35.6	41.1	51.7	56.4	68.3	79	81.8	86.1	86	78.1
TP5	41	85	118.2	172.2	211.9	283.9	317.7	333.5	353.8	375.8	390.8

ITER TASK/JB-DPI-3/JAPAN

Continue (Table 4-2.)

071602.

ch	I11	I12	I13	I14	I15	I16	I17	I18	I19	I20
TP1	44.1	83.1	112.8	167.1	222.8	282.8	309.6	314.1	314.7	323.7
TP2	44.2	90.4	128.8	205.6	263.8	303.6	338	347.3	353.3	360.4
TP3	44.7	96.7	144.9	234.9	275.9	307.6	387.6	377.1	382.4	587.2
TP4-1	36.1	60.4	81.2	120.5	145.8	175	194	185.9	187.9	190.9
TP4-2	40.5	76.1	106.9	164.7	204	245.9	275.2	275.6	281.6	304.3
TP4-3	0	0	0	0	0	0	0	0	0	0
TP4-4	0	0	0	0	0	0	0	0	0	0
TP4	45.3	95.2	136.6	212.9	262.5	299.8	337.4	346.8	366.3	395.9
TP4-5	45.9	95.1	136.6	214.1	272.9	321.8	365.6	375.3	388.4	406.9
TP4-6	41.6	77.9	108	169	216.1	259.8	287.7	289.9	284.6	291.2
TP4-7	37.4	64.7	87.9	134.8	171.5	213.5	241	234.6	234.9	233.6
TP4-8	33.2	53.2	67.6	100.3	126.7	156.2	173.2	166.4	166.5	161
TP4-9	32	47.1	56.3	31.3	100	122.4	134.4	130.6	130.7	122.5
TP4-10	30.2	40.5	48.3	67.2	82.2	98.7	109.4	108.1	108.1	98.7
TP4-11	30.1	39.3	47	63.6	76.2	92.1	99.4	99.7	99.8	91
TP4-12	30.7	39.8	47.1	63.6	76.3	89.1	98.1	98.6	99.1	89.9
TP5	44.8	89.1	124	188.5	244.2	288.7	321.4	328.3	345.5	366.2

071603.

ch	I21	I22	I23	I24	I25	I26	I27	I28	I29	I30
TP1	37.2	69.2	96.8	145.3	172	254.8	308.9	344.8	350.9	357.1
TP2	37.2	72.7	111.6	178.6	211.7	298	339.8	379.8	398	411.8
TP3	38.3	75.5	93.6	197.4	231.8	305.1	349.5	390.5	429.5	552.9
TP4-1	30.5	47.3	63.4	92.4	103.9	138.7	160.5	182.1	184.8	189.9
TP4-2	34.1	60.7	87.8	135.3	155	215.8	255.8	292.7	301.6	315.7
TP4-3	0	0	0	0	0	0	0	0	0	0
TP4-4	0	0	0	0	0	0	0	0	0	0
TP4	37.8	73.2	112.2	178	205.1	289.2	334	374.7	404.5	429.3
TP4-5	38.3	74.4	115.9	184.1	213.6	302.8	362.9	417.2	446.4	467.1
TP4-6	35.2	61.2	89.1	138.3	158.6	222.4	266.7	308.1	314.7	319.8
TP4-7	32.8	52	71.1	107.3	123.6	168.1	203.3	239.5	249.4	253.4
TP4-8	29.3	42.9	53.7	75.3	84.9	112	133.8	152.9	157.8	161.2
TP4-9	28.1	38.2	44.1	57.9	64.8	81.9	93.4	108.5	111.6	114.4
TP4-10	27.4	34.5	37.4	47	51.4	64.1	72.6	81.2	85.4	87.6
TP4-11	27.4	33.9	35.6	44.5	47.2	59.8	66.7	74.7	77.8	78.1
TP4-12	27.3	35.1	36.7	45.8	47.7	57.9	64.9	71	76.7	78.2
TP5	37.8	72.1	106.7	165.1	194.6	280.3	319.7	357.8	381.7	408.9

ITER TASK/JB-DPI-3/JAPAN

Continue (Table 4-2.)

071604.

ch	I31	I32	I33	I34	I35	I36	I37	I38	I39	I40	I41
TP1	40.4	70.8	109.5	146.6	191.8	283.5	312.6	329.9	338.8	344.9	349.6
TP2	39.8	76.7	125.4	179.3	241.9	305.4	341.7	363.4	381.4	392.1	409
TP3	42.2	81.1	137.3	198.1	257.7	311.2	347.6	367.3	406.4	449.8	601.5
TP4-1	32.5	49.7	74.4	96.8	123.3	156.4	177.1	188.1	187.5	198.6	192
TP4-2	35.6	63.2	99.9	138.2	178.4	233.7	267.4	285.4	292.5	324.7	318.2
TP4-3	0	0	0	0	0	0	0	0	0	0	0
TP4-4	0	0	0	0	0	0	0	0	0	0	0
TP4	42.2	80	127.3	179.8	234.3	301.2	334.7	354.6	381.4	495.6	433.6
TP4-5	42.2	80.6	128.4	183.6	241.3	319.1	366.5	391.8	415.7	487.4	460.3
TP4-6	38	64.8	101.1	141.9	184.6	243.5	280	299	302.5	319.9	317.6
TP4-7	33	54	81.6	112.2	144.1	189.8	221.7	241.2	243.6	252.9	252.9
TP4-8	31.3	44.3	60.6	80.8	101.4	130.3	149.3	163.1	163.7	167.6	162.7
TP4-9	28.8	37	50.3	64.1	78.2	97	110	119.5	120.2	123.3	113.9
TP4-10	28.2	34.5	43.7	52.6	63.9	78	86.3	91.6	95.3	96	87.8
TP4-11	27.6	32.7	41.8	48.9	59.1	70.9	79.9	84	87	87.8	78.9
TP4-12	28.8	33.3	41.2	48.9	59	69.7	78.1	82.9	85.3	87.2	77.2
TP5	40.4	76.8	120.7	163.3	218	290.5	321.5	341.7	362.9	390.9	400.2

071605.

ch	I42	I43	I44	I45	I46	I47	I48	I49	I50	I51
TP1	42.1	127.3	175.5	233	288.6	317.1	322.8		326.9	331.1
TP2	42.7	147.4	215	275.1	309.4	344.4	354.1		361.1	368.7
TP3	42.8	164.8	246.3	284.1	313.5	360.3	419.5		401.7	585.4
TP4-1	34.2	91.1	124	150.3	175.6	196.3	191.8		190.5	196.7
TP4-2	39	121.9	170.6	211.6	249.4	280.3	283.5		284.7	313.2
TP4-3	0	0	0	0	0	0	0	0	0	0
TP4-4	0	0	0	0	0	0	0	0	0	0
TP4	43.4	154.6	219.5	271.6	303.5	337.9	351.5		364.9	416.8
TP4-5	43.4	154.6	223.1	282.5	324.8	370.2	381.2		388.9	422.6
TP4-6	40.9	124.8	177.2	223.9	263.5	291	295.5		296	299.1
TP4-7	35.4	100.5	141.2	177.5	216.4	244.5	244.2		237.5	240.1
TP4-8	31.8	77.4	105	130.7	156.7	175.6	168		169.2	166.3
TP4-9	30.5	63	83.7	101	122.2	135.3	130.8		132.6	125
TP4-10	29.4	54.5	70.6	83.9	98.5	110.5	108.4		109.6	100.1
TP4-11	28.7	50.9	65.2	76.7	90.8	100.4	100.1		102.4	93
TP4-12	28.1	52.2	65.2	76.2	89.1	98.6	98.3		100.7	91.3
TP5	43.3	141.5	199.2	253.8	295.8	324.1	334.6		348.2	367

Continue (Table 4-2.)

071701.

ch	I52	I53	I54	I55	I56	I57	I58	I59	I60	I61	I62	I63
TP1	37.8	60.5	84.4	112.6	141.1	206.9	268.6	319.7	338.7	358.4	365.5	375
TP2	37.7	63.5	95.6	135.5	174.1	244.7	307.9	358.6	378.4	405	420.1	437
TP3	37.8	65.9	102.3	145.8	184.5	247.8	317.6	365.8	385.9	426.4	450.1	607.2
TP4-1	30.5	39.9	52.7	68.6	83	108.2	131.5	155.1	163.6	174.4	178	177.5
TP4-2	34	51.4	73.7	100.6	128	173.4	219.8	263.7	280.5	300.5	310.1	335.1
TP4-3	0	0	0	0	0	0	0	0	0	0	0	0
TP4-4	0	0	0	0	0	0	0	0	0	0	0	0
TP4	37.8	63	94.1	130.9	164.4	230.1	294.4	349.9	367.9	396.8	417.5	523.2
TP4-5	37.8	66.1	98.2	138	176	246.5	319.3	390.5	417.4	453.8	475	537.4
TP4-6	34.7	52.5	76	103	129.9	176.4	223.5	277	296	317.1	325.4	336.8
TP4-7	31.7	44.2	60.5	81.7	100.2	135	168.6	208.1	225.2	245.1	251.9	253.3
TP4-8	28.5	36.3	45.4	57.1	68.7	86.9	106	126.6	136.7	147.2	151.5	149.1
TP4-9	27.9	31.3	36.9	44.9	51.7	62.4	73.2	86.3	91.5	98	101	98.8
TP4-10	27.4	29	33.2	38.3	42.6	49.7	55.8	64.2	67.2	72.4	74.2	72.6
TP4-11	27.4	29	30.8	35.8	40.2	45.5	51.7	59.5	61.2	64.7	65.9	65.5
TP4-12	27.4	29	32	36.4	40.2	46.1	50.4	58.8	60.1	63.5	64.2	63.7
TP5	37.7	64.8	92.1	126.8	160	232.5	290.1	334.5	354.5	381.1	395.2	470.8

072201.

ch	H01	H02	H3	H4	H5	H6	H7	H8	H9	H10	H11	H12	H13
TP1	44.6	80.1	112.1	140.6	174.6	227.8	281.2	317	334	343.5	343.8	343.9	359.8
TP2	44.6	89	132.3	171.2	215.5	260	305.6	347.3	372	383.8	381.7	384.6	426.1
TP3	45.2	92.1	140.2	182.8	224.1	264.3	309.7	348	384.3	397.7	393	397.4	548
TP4-1	36.7	54.4	72.4	87.2	103.8	120.2	141.6	161.4	172.2	176.5	176.2	169.8	181.2
TP4-2	41	71.2	102.1	130	156.5	188.1	225.9	262.7	278.9	286.6	286.3	283.4	322.7
TP4-3	0	0	0	0	0	0	0	0	0	0	0	0	0
TP4-4	0	0	0	0	0	0	0	0	0	0	0	0	0
TP4	44.6	88	129.5	165.7	201.6	247.2	297.9	336.8	358.2	371.5	372.7	375.8	487.6
TP4-5	45.2	90.3	133.6	173	211.3	260.6	320.9	374.9	401.8	418.1	421	425.3	498.5
TP4-6	40.9	72.9	103.2	131.1	157.1	191.7	234.4	274.3	291.9	300.8	301.1	300.6	321.4
TP4-7	37.3	61.6	83.8	102.7	123.2	147.6	178.9	212.1	230.2	236.8	237.2	235.7	247.8
TP4-8	35.5	48.2	61.5	72.9	85.3	99.5	117.9	136.6	146.4	150.5	151.4	147.4	156.3
TP4-9	34.2	42.1	51.2	57.9	66.2	74.6	86.4	97.3	104.8	107.2	106.9	102.3	108.9
TP4-10	33	37.8	43.9	48.8	55.4	60.2	68.1	75.3	80.5	81.7	82	77.3	84.5
TP4-11	32.4	36.6	42.8	46.5	51	55.8	63.2	69.5	73.9	75.9	74.3	70.2	77.4
TP4-12	32.4	37.3	42.1	45.8	51.1	56	62.6	69.5	72.3	74.6	73	68.6	75.8
TP5	43.9	86.1	124.1	157.2	195.4	248.5	287.8	324.3	349.4	361.1	366.6	373.5	477.2

ITER TASK/JB-DPI-3/JAPAN

Continue (Table 4-2.)

072202.

ch	H14	H15	H16	H17	H18	H19	H20	H21	H22	H23	H24
TP1	44.7	80.7	121.3	159.6	191.1	241.7	284.9	315.7	325.8	333.1	341.2
TP2	46.5	87.2	140.1	191.9	229.6	266.7	302	341.6	361.1	370.1	397.8
TP3	46.5	89.6	148.5	202.2	236.3	267.9	303.9	344	373.6	383.1	526.9
TP4-1	36.7	54.9	78	97.9	112.6	128	147.1	166.1	173.6	175.1	182.2
TP4-2	41.6	70.6	108.7	142.9	167.4	195.3	229	263.6	275.4	279.2	323.5
TP4-3	0	0	0	0	0	0	0	0	0	0	0
TP4-4	0	0	0	0	0	0	0	0	0	0	0
TP4	45.3	86.6	137.3	181.5	215	252	295	332.8	356.1	364.5	508.5
TP4-5	45.9	87.7	142	188.9	224.8	266.1	319.3	371.4	396.8	407.5	494.6
TP4-6	41.6	73.7	110.5	144.7	169.2	200.2	240.6	278.8	289	293.4	310.4
TP4-7	38.6	61	89.2	114.5	132.1	154.6	185.7	217.9	229.7	234.1	244.3
TP4-8	34.9	49.4	65.3	80	91.8	106.6	124.4	143.3	150.7	152.6	156.6
TP4-9	33.7	43.3	53.7	63.3	71	80.4	92.4	105.3	108.5	110.4	114.4
TP4-10	32.5	39.7	47.2	54.3	59	64.9	73.5	82.3	83.5	86.1	89
TP4-11	32.5	38.5	44	49.9	53.5	60.1	66.2	74.5	77.8	79.1	78.8
TP4-12	33.2	38.6	44	49.3	52.9	60.1	65.7	72.8	75.2	77.3	77.7
TP5	45.9	86	132	174.9	212	254.4	288.4	323.8	349.5	360.2	461.3

072301.

ch	H25	H26	H27	H28	H29	H30	H31	H32	H33	H34	H35
TP1	46.4	82.5	111	156.6	186.2	262.6	290.4	301.8	311.4	318.3	323.3
TP2	46.4	88.4	124	187.1	225.2	282.1	314.1	327.8	347.5	354.3	377.3
TP3	47.5	93.2	132.2	202.9	240.9	286.2	314.8	345	363.3	380.5	556.2
TP4-1	37.8	57.9	74.7	103.2	119	148.4	165.8	172.6	175.3	145174.4	187.5
TP4-2	42.1	73	99.7	144.8	169	220	249.4	259.2	268.5	276.1	336.9
TP4-3	0	0	0	0	0	0	0	0	0	0	0
TP4-4	0	0	0	0	0	0	0	0	0	0	0
TP4	47.5	90.2	125.1	184.6	216	276.7	307	319.5	342.2	360.1	551
TP4-5	47.5	90.8	126.8	189.4	222.6	295.1	337.3	355	378.5	393.3	515.8
TP4-6	43.3	74.7	102	147.7	172.1	229.8	261.5	273.2	280	283.2	321.5
TP4-7	38.5	61.5	82.5	117.5	136.8	181.5	210.3	220.1	229.5	230.4	236.8
TP4-8	36	50	64	86.7	97	127	144.9	151.5	157.1	157.9	155.2
TP4-9	34.8	44	54.3	69.4	76.9	97.3	108.6	114.1	119	119.3	113.6
TP4-10	33.6	40.9	47.6	58.5	63.7	79	86.7	91	95.3	96.2	88.8
TP4-11	33	39.1	45.1	55.5	58.8	71.8	79.6	83.3	88.2	89.1	81.1
TP4-12	32.4	38.5	44.5	54.3	58.2	70.6	77.2	82.1	86.5	87.3	80.5
TP5	47	87.8	119.8	173	206.3	267.8	298.1	317.3	341	355.5	478.6

ITER TASK/JB-DPI-3/JAPAN

Continue (Table 4-2.)

ch	H36	H37	H38	H39	H40	H41	H42	H43	H44
TP1	49.5	104.1	147.3	181.9	237.8	264.4	286.9	295.9	300.1
TP2	50	114.1	173	222.9	252.3	278.9	306.3	323.1	333.9
TP3	51.9	123.1	192.6	232.5	258.5	281.2	325.4	343.2	472.1
TP4-1	41	73.9	103.9	126.2	144.3	163.1	174.4	178.7	191.7
TP4-2	45.8	95.7	141.2	173.3	201.1	228.3	249.3	264.6	320.3
PT4-3	0	0	0	0	0	0	0	0	0
TP4-4	0	0	0	0	0	0	0	0	0
TP4	51.9	117.8	179.2	222.8	248.7	273.5	314.2	331.3	426.3
TP4-5	51.9	117.8	180.4	225.8	259.1	294.2	334.4	357.3	403.5
TP4-6	47.1	96.9	145.5	180.6	212.1	241.3	259.6	268.3	274
TP4-7	42.8	80.4	117.6	144.6	173.1	200.9	217	225.6	223.9
TP4-8	38.5	63.7	89.1	108.4	128.9	148.8	159.1	165.3	161.8
TP4-9	36.6	55.1	74.3	88.1	102.1	118.5	127	131.3	129
TP4-10	34.9	49.1	62.9	74.5	85	97.8	105.1	110	108.4
TP4-11	34.3	47.3	59.9	69.8	79	89.5	97.4	101.6	100.1
TP4-12	35.5	47.2	59.2	68.6	77.1	87.7	94.9	99.9	98.9
TP5	51.9	112.4	162.1	203.3	236.5	269.3	306.9	337.9	450.7

072302.